

UNIVERSITAT DE
BARCELONA

**Final Degree Project
Biomedical Engineering Degree**

**IMPACT OF ACQUISITION
PARAMETERS ON DIFFUSION
MAGNETIC RESONANCE IMAGING
QUALITY**

Barcelona, 8th June 2022
Author: Marina Gómez Fernández
Director: Saül Pascual-Díaz
Tutor: Alberto Prats Galino

ACKNOWLEDGMENTS

First and foremost, I would like to express all my gratitude to my director, Saül Pascual-Díaz, for guiding and helping me throughout the entire project's development. But most of all, for making me feel, like the (quite comfortable) chair and the computer (which seemed to work in a different dimension where time went by much faster), became not only somehow mine, but also home for those few months. It has truly been a pleasure both working with you and learning from you.

Following the same line, I would also love to thank the entire IDIBAPS' MRI platform team; this TFG could have not been conceived without any of their help and dedication. It has been my first experience working in a biomedical engineering related field and I could not have thought of a more enriching one; many thanks for giving me this opportunity.

Last but not least, I sincerely appreciate all those people who, by placing little grains of sand, made the greatest outcome possible, from my tutor Dr. Alberto Prats-Galino for allowing me to discover what's behind the word neuroimaging; to the MRI technician that was there to pick me up (somehow holding back her laugh) the second I fainted after the scanner.

In an in between, my family and friends for answering each one of all the desperately silly TFG-related questions I have had during those last weeks, and the ones that are yet to come when preparing the oral presentation. My deepest thanks, always.

Each one of you has made this final procedure to obtain the degree something worthwhile going through.

ABSTRACT

Acquisition parameters play a crucial role in Diffusion Tensor Imaging (DTI), having such an impact on white matter (WM) scalar measures values such as Fractional Anisotropy (FA), Signal to Noise Ratio (SNR) or even when it comes to whole brain tractography studies.

Among those acquisitions parameters we find the b-values (e.g. b-value is a factor that reflects the strength and timing of those gradients used to generate Diffusion-Weighted Images; the higher the b-value, the stronger the diffusion effects), voxel size (the smaller the voxel size the higher the quality) and diffusion directions (as the number of directions increases the acquisition time increases as well).

This project, places all of them of the focus of several clinical MRI studies performed on healthy subjects in the IDIBAPS' MRI core facility. Those studies have been grouped into 5 datasets according to different acquisition protocols; in addition, 8 new acquisition proposal are first undergone and analysed.

Results show that as expected those parameters play a crucial role in image quality; however, each one of them has a different weight over those quality measurements. This will be discussed by splitting the results into datasets. Furthermore, the analysis performed on the protocol proposals confirm that they have reached what was their goal, to demonstrate that depending on the purpose of the scanner (emergency MRI, clinical MRI and research MRI) a specifical acquisition sequence can be used.

KEYWORDS:

Magnetic Resonance Imaging; Diffusion Tensor Imaging; Diffusion-Weighted Imaging; Tractography; MRI Acquisition Parameters; Fractional Anisotropy; Signal to Noise Ratio; b-values; voxel size.

LIST OF FIGURES

Figure 1. Methodology flowchart

Figure 2. Only those spins whose Larmor frequency is equivalent to the frequency of the applied RF field will be excited. [11]

Figure 3. In each excitation, and MR signal is acquired as a function of time and recorded as a row of numbers in a data array (k-space). Reiteration of this process with phase-encoding gradients with a later Fourier transform gives the image in the right. [11]

Figure 4. a) MRI T1- weighted image. b) MRI T2- weighted image. c) T1, longitudinal relaxation time. d) T2, transverse relaxation time. [11]

Figure 5. RF pulses transmitted with a flip angle (FA). G_z, G_y and G_x signify the magnetic field gradients in the slice-select, phase-encoding and frequency-encoding directions respectively. [11]

Figure 6. Two RF are applied per TR. Data are acquired after a phase-encoding gradient pulse, in the presence of a frequency-encoding gradient. [11]

Figure 7. DW slices acquired different b-values. Left to right (mm/s²): 0, 1500, 3000. [12]

Figure 8. Anisotropic diffusion, in the ideal case of a coherently oriented tissue. [11]

Figure 9. Three examples of DT to illustrate differences in anisotropy. [11]

Figure 10. Scalar DTI maps of the different measures. [13]

Figure 11. Whole- brain streamline CSD tractography. Colors were assigned automatically according to an atlas-based tractography segmentation method.

Figure 12. FACT representation, the first ROI at voxels 1 and 2 and the second one at voxels 3 and 4, 2 continuous streamlines can be traced. [11]

Figure 13. Examples of complex fibers that can result in very similar FACT-based ellipsoids. [12]

Figure 14. Both tractographies using a DTI or CSD approach and voxels showing their behaviour in complex fiber regions. [14]

Figure 15. Pie chart showing the global MRI market share, by application, 2020 (%)

Figure 16. Histogram showing Brain MRI related articles per year

Figure 17. Magnetic gradients distortion (dataset: ALBUCAT)

Figure 18. BIDS structure for dataset BIOMARCADORS

Figure 19. Step 1, brain extraction (ANTs).

Figure 20. Step 2, DWI registration (ANTs). [23]

Figure 21. Step 3, corrections (MRtrix3).[30]

Figure 22. Brain tractography. ROI: language region (CSD, Dataset: LAB_IMATGE)

Figure 23. SNR CC

Figure 24. FA map difference with the standard DTI and free water DTI

Figure 25. Atlas labels registered into the EPILENG dataset

Figure 26. SNR per each b-value interval and voxel size

Figure 27. WM atlas labels mean FA value per dataset

Figure 28. FA per each mask and dataset (2mm)

Figure 29. FA per each mask and dataset (1.5mm)

Figure 30. NOS per each algorithm, dataset and voxel size

Figure 31. Number of streamlines in accordance to length (CSD, DTI, 1.5mm and 2mm)

Figure 32. Number of streamlines in accordance to length (CSD, DTI, 1.5mm and 2mm). Zoomed in version

Figure 33. WBS

Figure 34. PERT chart

Figure 35. Pie chart, cost divided per specific activity.

LIST OF TABLES

Table 1. Solutions studied per each step developed throughout the project

Table 2. Acquisition sequence parameters per dataset

Table 3. PERT matrix

Table 4. GANTT chart

Table 5. SWOT

Table 6. Economic analysis

LIST OF ABBREVIATIONS

AD	Axial Diffusivity
CSD	Constrained Spherical Deconvolution
CSF	Cerebrospinal Fluid
CC	Corpus Callosum
CT	Computerized Tomography
dMRI	Diffusion Magnetic Resonance Imaging
DTI	Diffusion Tensor Imaging
DWI	Diffusion-Weighted Imaging
FA	Fractional Anisotropy
FACT	Fiber Assignment Through Continuous Tracking
fODF	fiber Orientation Distribution Function
GM	Grey Matter
HARDI	High Angular Resolution Diffusion Imaging
MD	Mean Diffusivity
MRI	Magnetic Resonance Imaging
NMR	Nuclear Magnetic Resonance
NOS	Number of Streamlines
RD	Radial Diffusivity
SNR	Signal to Noise Ratio
STD	Standard Deviation
WM	White Matter

TABLE OF CONTENTS

Acknowledgments	1
Abstract.....	2
List of figures	3
List of tables	4
List of abbreviations	5
1. INTRODUCTION.....	8
A) MOTIVATION.....	8
B) OBJECTIVES.....	8
C) METHODOLOGY	9
D) SCOPE AND SPAN.....	9
E) REGULATIONS AND LEGAL ASPECTS.....	10
2. THEORETICAL BACKGROUND	11
a) STATE OF THE ART.....	11
3. MARKET ANALYSIS	21
a) TARGET SECTORS.....	21
b) HISTORICAL EVOLUTION.....	22
c) FUTURE PERSPECTIVES	23
4. CONCEPTION ENGINEERING	24
4.1. DATA POST-PROCESSING.....	24
4.2. PROGRAMMING ENVIRONMENT.....	26
5. DETAILED ENGINEERING.....	27
5.1. DATA ACQUISITION	27
5.2. DATA POST-PROCESSING	29
5.3. PARAMETERS' EXTRACTION.....	31
5.4. STATISTICAL ANALYSIS	34
5.5. RESULTS	35
6. EXECUTION SCHEDULE	41
a) WORK BREAKDOWN STRUCTURE (WBS).....	41
b) DESCRIPTION OF THE TASKS	41
c) PROGRAM EVOLUTION AND REVIEW TECHNIQUES (PERT)	42
d) GANTT CHART	43
7. TECHNICAL AND ECONOMICAL FEASIBILITY	44
a) TECHNICAL.....	44
b) ECONOMICAL.....	45

8. CONCLUSIONS AND FUTURE PERSPECTIVES	48
9. REFERENCES	49
10. ANNEXES	51

1. INTRODUCTION

a) MOTIVATION

A brain MRI can help doctors look for conditions such as bleeding, swelling, problems with the way brain developed, tumors, infections, inflammation, damage from an injury or a stroke among many others [1]

However, not all MRI scanners are performed in the same way, several acquisition sequences are available depending on both the reason and purpose. The reason why this is done is very simple, if a patient suffering from a possible stroke arrives and needs to be diagnosed what we want to do is a fast acquisition able to diagnose him; a quite similar situation happens for patients that cannot undergo longer scanner times (e.g. they suffer from a neurological disorder, children...) [2]. On the other hand, if the MRI scanner is scheduled for clinical purposes such as tumour diagnosis those acquisition parameters will be different, which will result in images with better quality and less noisy. The opposite case of the stroke patient happens for clinical research, cases where what we want to do is a diffusion study with a whole brain tractography. In here we will need the best acquisition parameters, which will result in a longer scanner.

What is expected up to the completion of this study is to propose several acquisition protocols, each one in accordance with the situations mentioned above, which will be first undergone by controls, analysed and once proven its effectiveness implemented in Hospital Clínic.

The implementation of those sequences gives us as well a major future advance, if in 10 years a specifical study wants to be conducted, it will be necessary that all acquisitions are done following the same parameters. Otherwise we would not know for sure if those changes are due the subjects or the acquisition parameters themselves.

b) OBJECTIVES

The main objective of the following final degree project is to compare the most used MRI acquisition sequences during the last 5 years by performing a statistical analysis on several relevant parameters regarding image quality. Furthermore, eight sequences being developed in IDIBAPS will also be analysed.

The sentence above can be split down into more specifical secondary objectives:

- I. To establish a relationship between the Signal to Noise Ratio (SNR) and b-value's acquisition, is there any optimal b-value?
- II. To establish a relationship between the SNR and voxel's size acquisition.
- III. To determine how the Fraction Anisotropy (FA) changes depending on the brain area (white matter, grey matter and cerebrospinal fluid). Does this value change when the acquisition's sequence is different? Does this value change when the voxel size is different?

IV. To compare two tractography algorithms by displaying streamline's length of the same tractogram. Does this length change when the acquisition's sequence is different?

c) METHODOLOGY

The entire project has been developed under the framework of the Institut D'Investigacions Biomèdiques Agust Pi i Sunyer (IDIBAPS) (<https://idibaps.org>) at Hospital Clínic. It is considered the leading biomedical research center in Spain that strives for excellence in biomedical research to improve people's health and ensure translational research. Its research is broken down into six different platforms, among them is found the magnetic resonance imaging platform. It works under the coordination of Emma Muñoz-Moreno and is the place in which I had a computer assigned and did the TFG under the supervision, guidance and help of my tutor, Saül Pascual- Díaz (Imaging scientist). In addition, the platform is equipped with an MRI scanner, the Siemens MAGNETOM Prisma 3T scanner for human clinical investigation.

On the other hand, it has been divided into four different stages in order to have a practical structure and successfully achieve the main goal of the project. The flowchart of the followed methodology is shown in Figure 1.

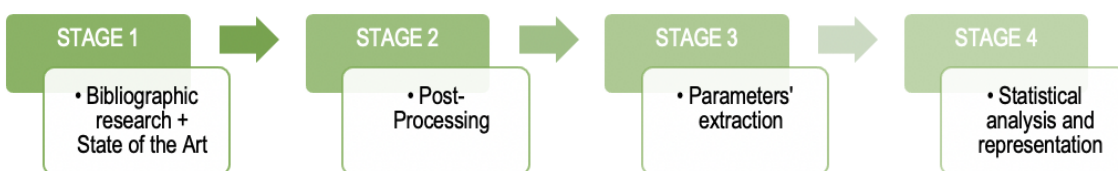


Figure 1. Methodology flowchart

d) SCOPE AND SPAN

First of all, it has to be stated that this is a bachelor's final degree project with one main drawback above all, time. The duration is established deadlines, set for June 2022. This implies only being able to focus on particular aspects of the MRI post-processing such as parameters' extraction done by matrixial operations and their posterior statistical analysis. Since trying to encompass the entire post-processing would be way more complex and time-consuming than the span allows us, it has been left out of the scope of the actual TFG. However, given the relevance it has not only for the project understanding but also for its development it will be briefly explained in Section 5.

With this being said, the scope is in accordance with the accomplishment of its objectives and included in the following breakdown:

- I. Bibliographic search for previous studies related to address a base-knowledge of the project's main technical issues such as dMRI acquisitions.
- II. Performing MRI synthetic acquisitions by using the nowadays most used sequences.
- III. Implementation of different algorithms and post-processing methods of the images acquired to establish which acquisition allows a better description of the synthetic model.

- IV. Implementation of both the previous results and algorithms in MRI acquisitions.
- V. Statistical analysis, comparison and discussion of the results obtained with previous studies.

The entire span of the project has been from March 2022 up to June 2022. Further details will be given in Section 6.

e) REGULATIONS AND LEGAL ASPECTS

This project (including data acquisition and posterior analysis) has been developed in the IDIBAPS' MRI core facility. Meaning that all the legal requirements have to be in accordance with the Spanish regulations.

All data that has been analysed is from MRI core facility acquisitions, and has been anonymised, i.e. there is no feasible way to obtain personal information about the subject, following the *Ley Orgánica 3/2018, de 5 de diciembre, de Protección de Datos Personales y garantía de los derechos digitales*; this is more specifically stated in the health data treatment section in *Disposición adicional decimoseptima* [3].

MRI is both a medical device and a radiation-emitting electronic product. Following the World Health Organization, a medical device is: “Any instrument, apparatus, implement, machine, appliance, implant, reagent for in vitro use, software, material or another similar or related article, intended by the manufacturer to be used, alone or in combination for a medical purpose.” [4]. All medical device regulations are stated in the European Commission Council Directive 93/42/EEC legislation, [5] there are four classes, ranging from low to high risk, MRI lie in Class II (moderate risk). This implies that several certifications need to be followed, such as ISO-13485 and ISO-14971, for quality management throughout its life cycle, and principles and processes for risk management respectively. [6]

On the other hand, regarding the radiation-emitting electronic products they are defined by the FDA as: ‘Any electrically-powered product that can emit any form of radiation on the electromagnetic spectrum. These include a variety of medical and non-medical products’. [7] Regulations related to those products are stated by the European Commission Council Directive 2017/745/EC legislation. [5]. This implies the following standard, ISO 14630 for patients’ whom wearing an active implantable device safety [8].

Furthermore, during MRI diagnostic both individuals being scanned and those in the immediate vicinity of the equipment can be exposed to a static magnetic field, a time-varying magnetic field gradients and radiofrequency. This implies that they must not possess any conductive, metallic nor magnetic material when under the influence. Furthermore, those gradient fields produce quite an important amount of acoustic noise, reaching an unacceptable and even dangerous level when it comes to prolonged exposition. [9] All those latter aspects have to be both explicitly warned by hospital’s signs and professionals’ indications.

2. THEORETICAL BACKGROUND

a) STATE OF THE ART

1. MAGNETIC RESONANCE IMAGING [10]

MRI is a non-invasive technology that uses non-ionizing electromagnetic radiation to generate cross-sectional images of interior structures to provide extensive, multi-parametric information on brain anatomy, function, and metabolism. MRI typically exploits Nuclear Magnetic Resonance (NMR), a phenomenon in which atomic nuclei subjected to a strong magnetic field absorb and reemit electromagnetic waves at a characteristic 'resonant frequency', which falls into the radiofrequency range.

Given the amount of information contained in the signal, several techniques have been tailored to augment factors of interest providing images of particular structures; including white matter (WM) tracts, lesions and arteries. Clinical applications of MRI are vast, encompassing neurological, psychiatric, cardiac, abdominal, musculoskeletal and vascular applications, making MRI one of the most powerful and flexible imaging tools.

1.1. MRI Image Acquisition: [11]

1.1.1. Image Formation: (resumir les fases de baix en una)

When nuclei in a certain slice or slab of tissue are excited, they generate a signal in which each point's contribution must be identified. This is accomplished by encoding spatial information into the signal's phase and frequency, which is accomplished through the use of magnetic field gradients.

1.1.1.1. Slice- Selective Excitation:

By stimulating nuclear magnetisation just in the slice of interest, imaging of specific slices of tissue can be obtained. This is accomplished by applying an RF pulse in the presence of a magnetic field gradient, causing the Larmor frequency to vary spatially. Only those spins whose Larmor frequency is equal to the applied RF field's frequency will be activated. The amplitude of the gradient and the bandwidth of the RF pulse determine the slice thickness.

1.1.1.2 Spatial Encoding:

A frequency encoding in one direction and a phase encoding in the perpendicular one is used to determine the position of the spins inside the imaging plane, as shown in Figure 2. During signal capture for frequency encoding, a magnetic field gradient is applied, which provides information about the position of the spins along the gradient's direction. Prior to image acquisition, a magnetic field gradient is introduced as a short pulse, forcing a phase shift among the spins that is imprinted on their signals during phase encoding. The entire process must be repeated numerous times to obtain position information from the phase.

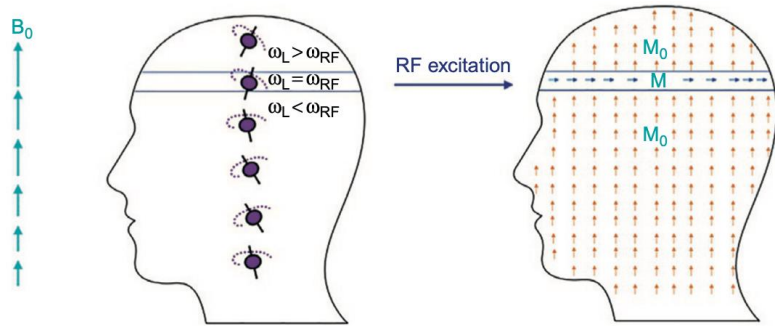


Figure 2. Only those spins whose Larmor frequency is equivalent to the frequency of the applied RF field will be excited.

1.1.1.3. Image Reconstruction:

A combination of frequency and phase encoding is required to generate a 2D image. To do so, the same slice of tissue must be excited multiple times, with the signal sampled as a function of time after each stimulation. The amplitude of the frequency-encoding gradient remains constant with each iteration, whereas the amplitude of the phase-encoding gradient increases with each repetition. The output is collected in a 2D array, and the signal's spatial distribution is recovered using the Fourier transform (Fig 3).

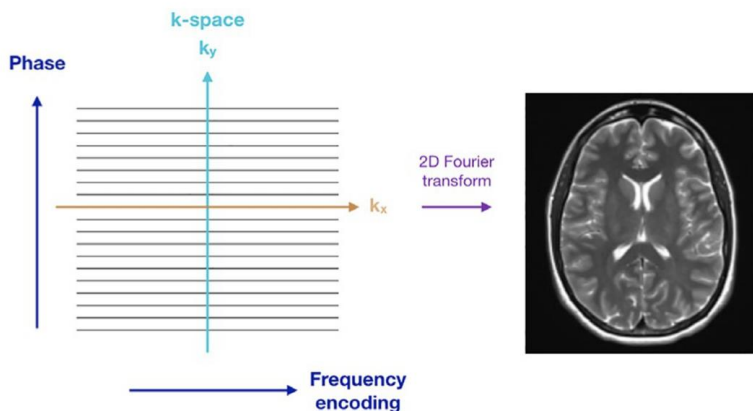


Figure 3. In each excitation, an MR signal is acquired as a function of time and recorded as a row of numbers in a data array (k -space). Reiteration of this process with phase-encoding gradients with a later Fourier transform gives the image in the right.

1.1.2. Image Contrast (resumir en 1 frase)

The relative signal appearance of particular tissues is determined by the sequence type, sequence parameters and tissue properties. Decay and recovery of the MR signal are depicted by several relaxation constants. The longitudinal relaxation time, T₁, signifies the rate at which magnetization return to its equilibrium value, M₀, following RF excitation. The value of T₁ differs depending on the tissue type; tissues with longer T₁ appear hypointense on a T₁-weighted image. The transverse relaxation time, T₂, refers to the rate of signal decay following RF excitation; tissues with longer T₂ appear hyperintense on T₂-weighted images. (Fig 4)

Furthermore, TR and TE are also critical factors, with the first referring to the time between subsequent RF excitations and the second to the time between those RF excitations and signal capture. The relative contrast weighting of different tissues can be calculated by combining TE and TR; acquisitions with long TR and short TE produce proton-density-weighted images, in which the image signal is mostly dictated by the voxel hydrogen concentration.

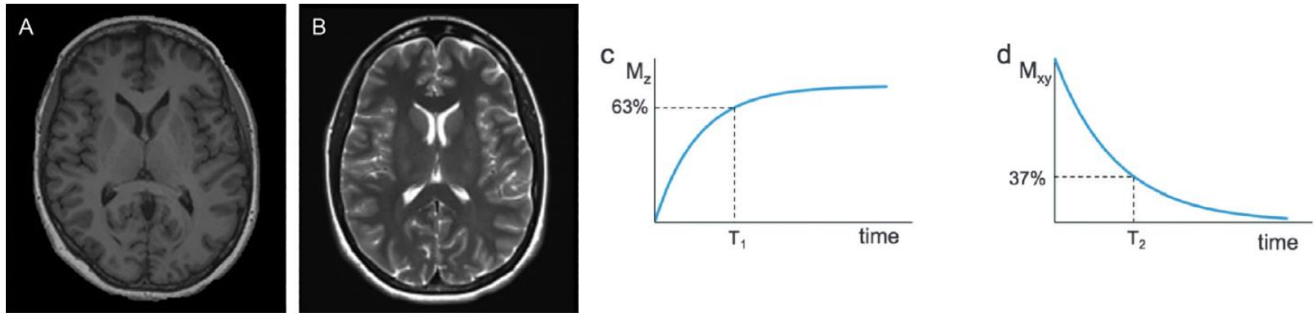


Figure 4. a) MRI T1- weighted image. b) MRI T2- weighted image. c) T1, longitudinal relaxation time. d) T2, transverse relaxation time.

1.1.3. Pulse Sequences: (resumir molt)

For explicit applications, the acquisition of an MR image necessitates optimal MR sequences. Sequences are a set of well-defined repetitive RF pulses and signal acquisition that must be coordinated with magnetic field gradients. The most frequent ones are known as gradient-echo and spin-echo sequences. This procedure is known as pulse sequence and can be changed to offer best signal contrast for a certain application.

1.1.3.1. Gradient-Echo Sequences:

During one of them, a single RF pulse is administered to each TR period individually (Fig 5). TE denotes the time between RF excitation and the gradient's echo center in this context. Short TR values are frequently used in gradient-echo sequences, resulting in T1-weighing. This image is also affected by the flip angle, with the highest value indicating more saturation; the value generally ranges from 10° to 40°. Tissues having a shorter T1 tend to be more hyperintense than those with a longer T1.

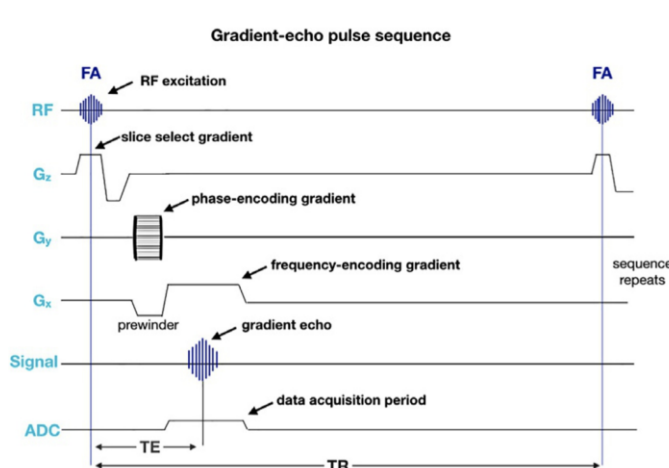


Figure 5. RF pulses transmitted with a flip angle (FA). G_z, G_y and G_x signify the magnetic field gradients in the slice-select, phase-encoding and frequency-encoding directions respectively.

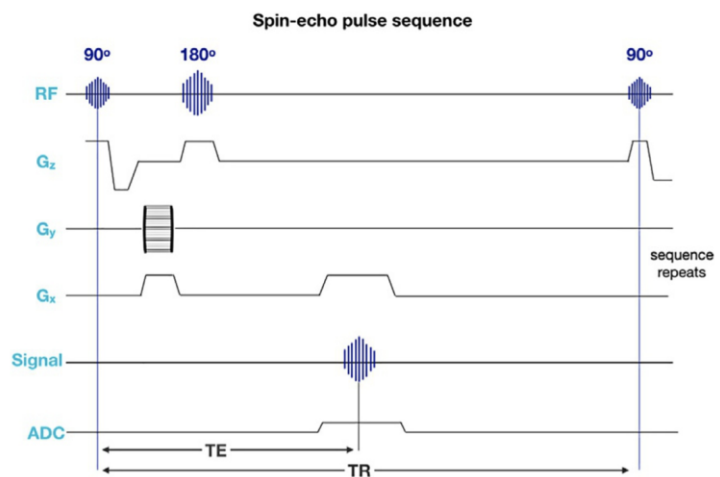


Figure 6. Two RF are applied per TR. Data are acquired after a phase-encoding gradient pulse, in the presence of a frequency-encoding gradient.

1.1.3.2. Spin-Echo Sequences:

Employs two RF pulses per TR period, while the initial excitation pulse has a flip angle of 90° the second one is of 180° (which required long TRs) (Fig 6). Data are collected during the spin echo once the spins have refocused. As T2 relaxation affects the amplitude of the spin echo, the resulting images are T2-weighted. The degree of the T2-weighing is dictated by the TE value.

1.1.4. Imaging Parameters:

There are a range of factors that enable the diversity of MR imaging for every particular pulse sequence, and these are the ones that investigators take advantage of. The flip angle and timing parameters (TR, TE) affect signal contrast, image resolution by spatial parameters, and total SNR by the number of signal averages. The size of the matrix and the number of pixels in the image establish the raw data dimensions. Each pixel represents a voxel, and the size of each voxel indicates the image's resolution. The flip angle, acquisition spatial resolution, and timing parameters can all affect image SNR. Despite SNR can also be influenced independently of these parameters by altering the number of excitations or signal averages it increases the scan time. The scan time is proportional to the number of excitations, phase-encoding steps, and TR; by using a gradient-echo sequence with a short TR, this can be kept within reasonable limits.

2. DIFFUSION-WEIGHTED IMAGING

The Brownian motion of molecules coupled with their thermal energy is referred to as diffusion. Diffusion is constrained by the presence of cell membranes when tissue is intact; consequently, an increase in diffusivity indicates membrane disruption and is frequently used to detect lesions and degenerative processes.

Diffusion Weighted Imaging (DWI) is an MRI imaging technique that allows for the estimation of water molecules diffusivity inside tissue, providing information about the architecture of the brain's WM and the direction of its fiber tracts. Molecular diffusion is a term that refers to the Brownian motion of particles caused by the thermal energy they carry, and can be described as follows: [10]

$$\langle r^2 \rangle = 6Dt \text{ (Eq 1).}$$

where $\langle r^2 \rangle$ is the mean squared displacement, t the diffusion time and D de diffusion constant, which can be described as: [10]

$$D = \mu K_B T \text{ (Eq 2).}$$

For homogeneous materials, D is the same in every direction, although for highly structured materials and some biological tissues as WM, it becomes anisotropic and thus has different D coefficients along different directions. Because of the linkages discovered between a variety of neurological and neurosurgical disorders and WM alterations in recent years, this approach has sparked the scientific community's interest.

2.1. DWI Acquisition Sequence

To obtain DWI acquisitions from an MRI machine it is needed to measure the spin-echo signal after applying a set of diffusion pulse gradients; the spin-echo signal of the particles that lost energy will be reduced during this procedure. As a result of having a degree of freedom in the gradient direction, the voxels with higher isotropy display higher intensity in the final volume.

Furthermore, those particles must diffuse for a given amount of time in order to characterize the diffusion of water in a medium. This quantity is known as the b-value in diffusion sequences, and it represents the time that passes per each mm². The strength of the observed signal for each voxel is determined not only by the diffusion restriction for that voxel, but also by the b-value chosen. However, despite obtaining a greater diffusion contrast with higher b-values we would be also obtaining a drop in the signal as can be seen in Figure 7.

The most used b-value is 1000 s/mm², as it offers a good signal/ contrast relation. [12]

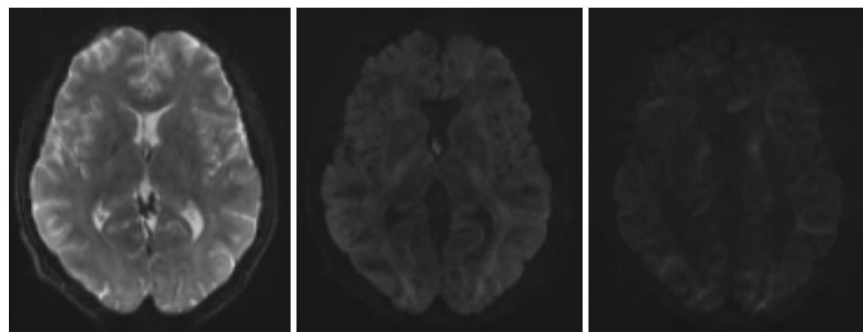


Figure 7. DW slices acquired different b-values. Left to right (mm/s²): 0, 1500, 3000.

While DWI refers to the contrast of the acquired images, Diffusion Tensor Imaging (DTI) is characterised by the application of the Diffusion Tensor (DT) model, which enables the indirect quantification of the degree of anisotropy and structural orientation.

3. DIFFUSION TENSOR IMAGING [11]

The most popular diffusion profile model is based on the Gaussian assumption, which allows the diffusion to be modelled with a single covariance matrix. This is known as diffusion tensor imaging (DTI); which is a sensitive probe of cellular structure that works by measuring the diffusion of water molecules.

What is being quantified is the diffusion coefficient (a proportionally constant that relates diffusive flux to a concentration gradient) in mm²/ s. When measuring diffusion through tissue, unlike in a glass of pure water, which is isotropic (all in the same direction), the directions fluctuate, making it anisotropic. This anisotropy is mostly created by cellular membranes in the WM of the brain, with some contributions from myelination and axon packing. Anisotropic diffusion can reveal the underlying tissue orientation, as shown in Figure 8, with the quickest diffusion measured parallel to the axons in a WM fiber tract. As a result of DTI analysis, interferences concerning features including diffusion directional preference (fractional anisotropy, mean diffusivity), diffusion rate along the primary axis, and transverse direction can be established within each voxel.

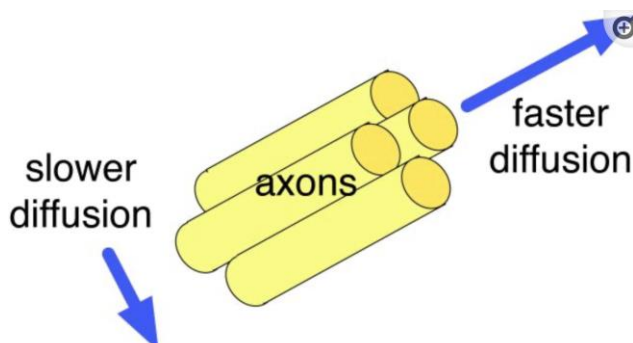


Figure 8. Anisotropic diffusion, in the ideal case of a coherently oriented tissue.

3.1. Diffusion Tensor image analysis

Magnetic field gradients are used to create an image that is sensitized to diffusion in a certain direction, which is then used to assess diffusion using MRI. A 3D diffusion model can be estimated by repeating the diffusion weighting process in several directions. As a result, extra gradient pulses are introduced, whose effect balances out for stationary water molecules, generating a random phase shift for diffusing molecules; this random phase causes a loss of signal from the diffusing molecules, resulting in darker voxels. This means that in the DWI for that direction, WM fiber tracts parallel to the gradient direction will appear darker.

The diffusion tensor (D) is then calculated by solving the Stejskal-Tanner equation (Eq 3) to compare the decreased signal (S_k) to the original signal (S_0), which depicts how the signal intensity at each voxel drops in the presence of Gaussian diffusion.

$$S_k = S_0 e^{-b g_k D g_k} \quad (\text{Eq 3})$$

The product $g_k D$ represents the diffusion coefficient (diffusivity) in the g_k direction. This leaves us with an equations' system that is solved for D , the diffusion tensor (Eq 4).

$$D = \begin{bmatrix} D_{xx} & D_{xy} & D_{xz} \\ D_{yx} & D_{yy} & D_{yz} \\ D_{zx} & D_{zy} & D_{zz} \end{bmatrix} \quad (\text{Eq 4})$$

DTI is usually displayed taking into account that the information contained in the tensor is usually condensed into a scalar number, or into four numbers equivalent to the R (red, x-axis, right to left), G (green, y-axis, anterior to posterior), B (blue, z-axis, head to feet) color, and a brightness value; and viewed by estimating the course of WM tracts through the brain via a process called tractography.

3.2. Diffusion Tensor Model

Peter Basser proposed the diffusion tensor (DT) for use in magnetic resonance imaging (MRI) in 1994. It was essential in proving the efficacy of diffusion MRI in describing the microstructure of white matter tissue and its biophysical properties.

DT is proportional to the covariance matrix of a three-dimensional Gaussian distribution that models the displacements of the molecules and describes the diffusion of water molecules using a Gaussian model. As a result, we're talking about a 3x3 positive-definite matrix with three orthogonal and mutually perpendicular eigenvectors ($\epsilon_1, \epsilon_2, \epsilon_3$) and three positive eigenvalues ($\lambda_1, \lambda_2, \lambda_3$) (Eq 5). The major DT's eigenvector points towards the principal diffusion direction (i.e. the direction of the fastest diffusion); while the eigenvalues give the diffusivity in the direction of each eigenvector. Together, eigenvectors and eigenvalues define an ellipsoid that represents an isosurface of diffusion probability, the higher the anisotropy the more ellipsoid the shape gets as can be seen in Figure 9.

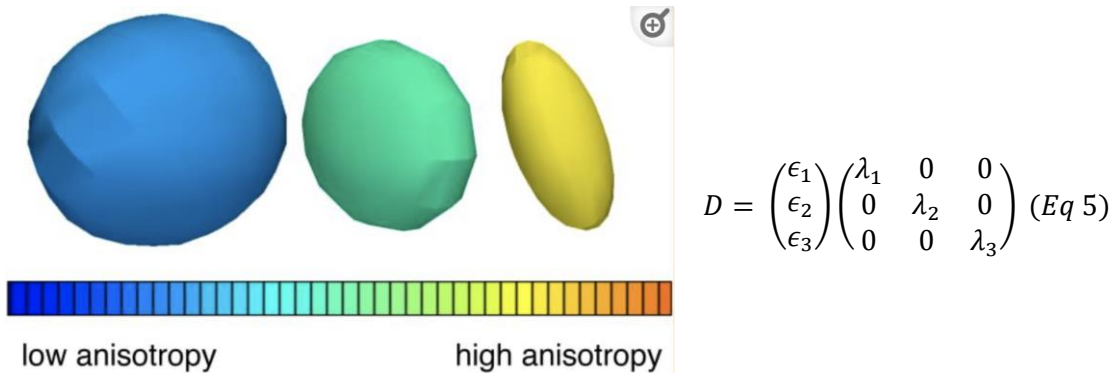


Figure 9. Three examples of DT to illustrate differences in anisotropy.

The fundamental disadvantage of DT is that there is only one main diffusion direction. As a result, in areas of the brain containing multiple fiber crossing each other, the tensor model may show that the primary diffusion direction is intermediate to these directions, causing inaccuracies in track definition. Other reconstruction approaches can, fortunately, be utilised to represent diffusion and fiber orientation in certain areas.

3.3.1. Diffusion Tensor measures [13]

In DTI, several quantitative measures can be defined from the eigenvalues of the tensor. The Axial Diffusivity (Eq 6) is defined as the diffusion coefficient along the principal direction of the fastest diffusion of the tensor; while the Radial Diffusivity (Eq 7) is defined as the average diffusivity perpendicularly to the principal diffusion direction. On the other hand, the Mean Diffusivity (Eq 8) is a quantitative map that describes the average amount of diffusion in a voxel, which is obtained by averaging the eigenvalues. (Fig 10)

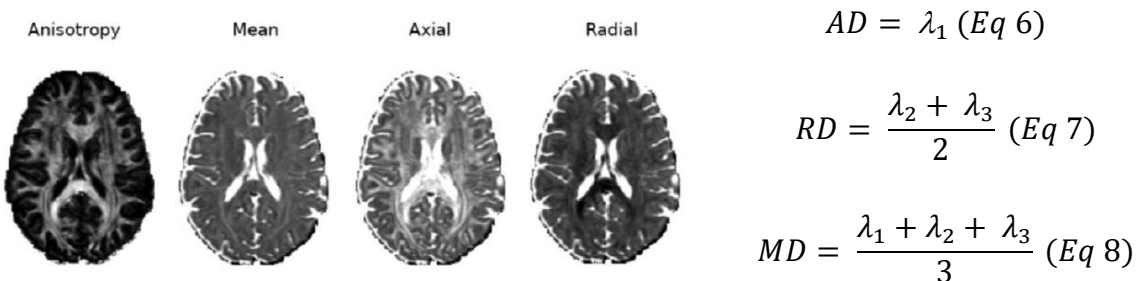


Figure 10. Scalar DTI maps of the different measures.

3.3.3.1.1. Fractional Anisotropy

The FA, which is used to quantify the degree to which the diffusion distribution in a voxel is directed, can be calculated using the DT's eigenvalues. That is, whether there is relatively unrestricted diffusion in one particular direction; it is also normalised and ranges from 0 (isotropic) to 1 (anisotropic). Furthermore, it is the most extensively used anisotropy measure, with the name attributed to the fact that it measures the anisotropic fraction of diffusion, which can be thought of as the difference between the form of the tensor ellipsoid and that of a perfect sphere (Eq 9).

$$FA = \sqrt{\frac{1}{2} \sqrt{\frac{(\lambda_1 - \lambda_2)^2 + (\lambda_1 - \lambda_3)^2 + (\lambda_2 - \lambda_3)^2}{\lambda_1^2 + \lambda_2^2 + \lambda_3^2}}} \quad (Eq\ 9)$$

Nonetheless, while FA is frequently used to assess WM integrity, it should be interpreted with caution since, while it can indicate the density of fiber packing in a voxel and the quantity of myelin enveloping these axons, it is not always a measure of 'tissue integrity.' In other words, FA may be reduced in areas where white matter fibers are fanning out or where more than one population of white matter fibers crosses.

Alternatively, more complex models have been developed, such as the High Angular Resolution Diffusion Imaging (HARDI) model, which is capable of acquiring a larger number of DWI and thus better modelling of more convoluted fiber topologies.

4. TRACTOGRAPHY

The information obtained by the measures seen above allows us to obtain a set of diffusion-derived parameters very much useful in the development of microstructural biomarkers in the WM. However, those maps are not a direct representation of structural connectivity in the brain. That is when tractography takes the lead, which uses the diffusion information to achieve a representation of the neural pathway. Nonetheless, fibers are not by any means a representation of the axons, but a representation of regions in which water diffusion is favored.

The streamline tractography method is the most common approach; it creates discrete curves or trajectories, also known as tracts or fibers, as an output. And operates by successively stepping in the direction of the primary eigenvector (direction of the fastest diffusion). As a result, the eigenvectors are tangent to the generated trajectory. Each streamline shows the connectivity between two areas via the WM (or voxels), based on the path along which water molecules can diffuse more easily. They do not, however, include information regarding the connection's orientation (i.e. it is not known if it goes from A to B, or B to A). (See Figure 11).

Expert knowledge or an automatic method are required to process DTI data to display fiber tracts of interest. After performing streamline tractography, the fiber trajectories of interest can be interactively selected using 'virtual dissection,' which involves defining inclusion/exclusion zones and using them to pick trajectories. There have also been created automated algorithms for atlas-based tractography segmentation that employ prior knowledge to determine trajectories. [10]

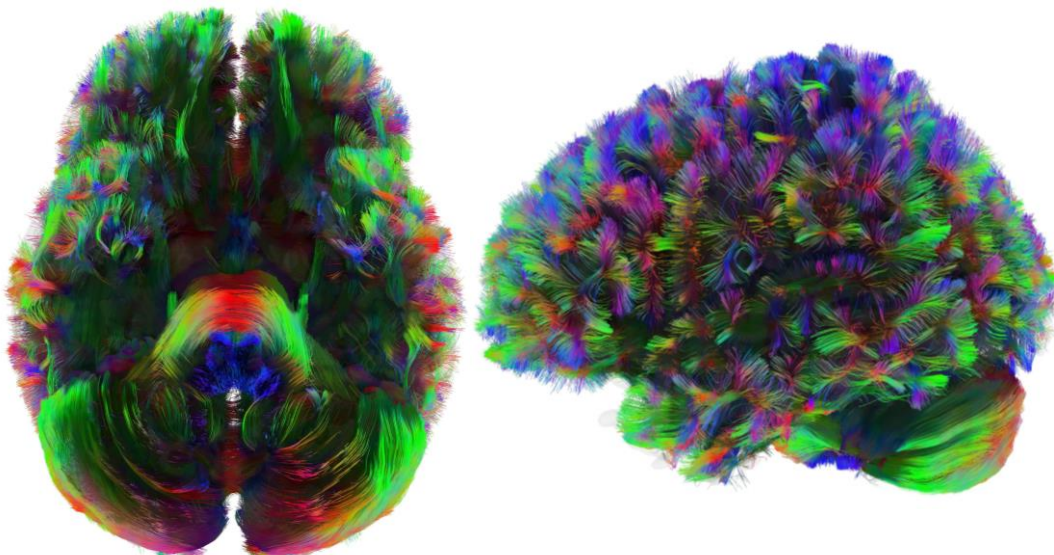


Figure 11. Whole-brain streamline CSD tractography. Colors were assigned automatically according to an atlas-based tractography segmentation method (Dataset: LAB_IMATGE).

4.1. DTI tractography

One of the simplest tractography reconstruction methods is the Fiber Assignment Through Continuous Tracking (FACT) algorithm; which consists of connecting adjacent voxels through the direction obtained in turn from the first eigenvector (ϵ_1).

The procedure is broken down into three stages: seeding, propagation, and termination. Seeding entails defining regions of interest and inserting one or more seeds in each of their voxels; the placement can be random or defined, and it commonly begins with a voxel located in the WM. Propagation (Fig 12) is where the fiber tracts are gradually generated, which can be performed with several algorithms besides FACT; finally, termination of the fiber tracking procedure is based on the termination criteria, which goal is to avoid propagation of the fibers in voxels where robustness of the vectorial field is not guaranteed. Common termination criteria include a minimum threshold for FA (ranging 0.1- 0.3, which usually indicates that the fiber has propagated into the GM or cerebrospinal fluid) and turning angle threshold (ranging 40- 70°). [11]

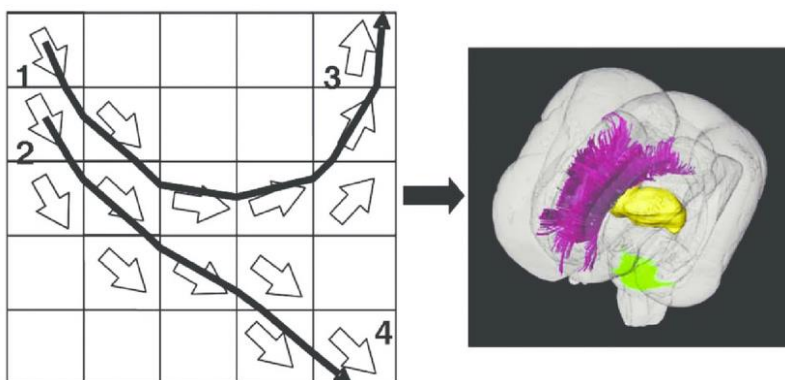


Figure 12. FACT representation, the first ROI at voxels 1 and 2 and the second one at voxels 3 and 4, 2 continuous streamlines can be traced.

The tensor model, on the other hand, can only represent one primary fiber orientation in a voxel, which causes a difficulty in tractography when we reach a region of crossing fibers, as shown in Figure 13. And because those locations correspond to a large number of WM voxels in the brain with various fiber bundles oriented in different directions, the tensor model is unreliable for crossing, 'kissing,' and 'fanning' fiber bundles. Ambiguous configurations also cause a decline in the FA, forcing the reconstruction algorithm to stop propagating the streamline; in these instances, DTI reconstructions will be missing those specific structures.

This can be partially solved by using higher-order models, which have been proposed to address regions with complex fiber configurations, such as Constrained Spherical Deconvolution (CSD).

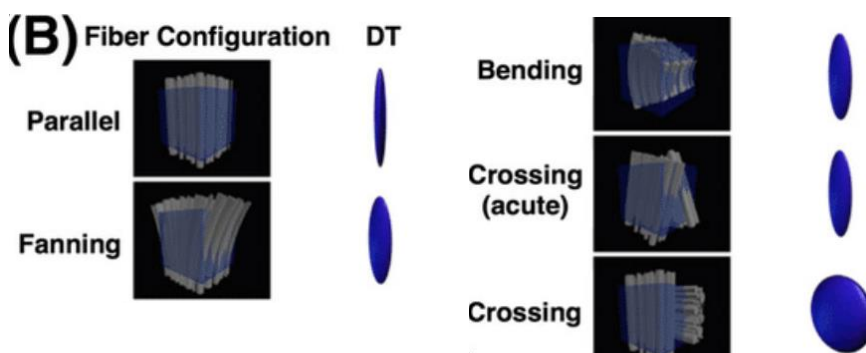


Figure 13. Examples of complex fibers that can result in very similar FACT-based ellipsoids.

4.2. Constrained Spherical Deconvolution tractography

The CSD estimates the WM fiber Orientation Distribution Function (fODF) based on an estimate of the signal expected for a single-fiber WM population. This is used as the kernel in a deconvolution operation to extract a WM fODF from dMRI final measured within each voxel. In other words, it exploits the dependencies of the different macroscopic tissue types with the unique b-values to obtain a tissue-specific fODF.

To reconstruct anatomically constrained tractograms that better represents the structure of the WM in complex fiber configurations, CSD tractography algorithms use information calculated using spherical deconvolution methods in combination with anatomical information provided by a T1 sequence and different b-values.

Despite the advancements compared to the FACT algorithm, CSD has its own set of constraints. The first is that when it comes to fiber configurations, the number of diffusion gradient directions required grows exponentially with the complexity of the model, making it not feasible to collect sufficient information in all clinical circumstances. Figure 14 shows the difference when using DTI or CSD on the same voxel. [14]

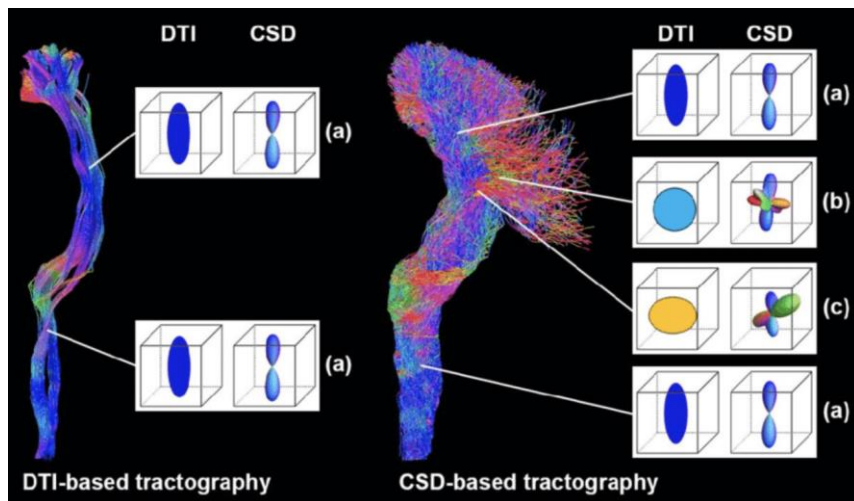


Figure 14. Both tractographies using a DTI or CSD approach and voxels showing their behaviour in complex fiber regions.

3. MARKET ANALYSIS

The market sector contemplated in this project is the one related to MRI. Therefore, a deep analysis will be carried out throughout the following section.

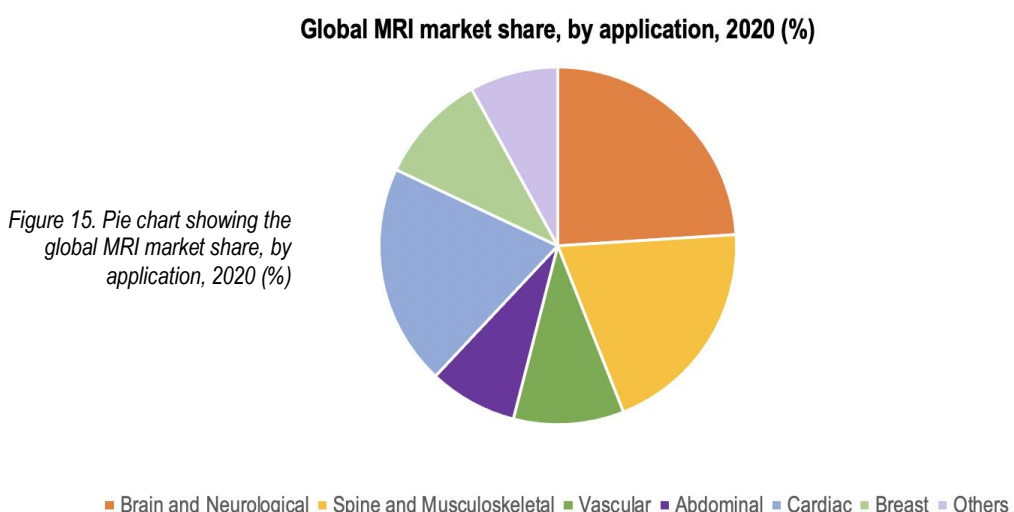
a) TARGET SECTORS

The global MRI market size was valued at \$6.7 billion in 2021 and expected to reach \$11 billion by 2030, at a compound annual growth rate of 6.5%. It also accounted for the largest market share with 75.78% in 2020. Within those numbers, it has to be taken into account that the Covid-19 pandemic has had a negative impact in the MRI market, reporting an 87% reduction in outpatient imaging services over 2020 and early-mid 2021; this being equivalent to a decline of 6% in 2020 as compared to 2019. [15]

Main reason for the expected growth relies over the fact that MRI is an efficient diagnostic machine to identify diseases related to areas concerning blood vessels and brain; diseases that are not only increasing their prevalence (e.g. breast cancer, cardiovascular and neurological disorders), but also where early detection is critical and decisive of treatment procedure and life expectancy (e.g. osteoporosis, spinal infection and tumors). According to GLOBOCAN2020, 19.3M cases of cancer and 10M cancer deaths were estimated in 2020; this data compares to just over 17M cases and 9.5M deaths in 2018.

This is also supported by the advances in diagnostic techniques such as open MRI, visualization software and superconducting magnets; however, most of them are focused on the software, enabling faster contrast scans and simplifying imaging workflow as well.

In Figure 15 it is depicted each MRI application's market share, and even though brain and neurological MRI hold almost 25% of the share (attributed to factors such as superior quality as compared to CT imaging), the spine and musculoskeletal one is rapidly increasing. This is because, unlike other imaging techniques, MRI's spin-echo technique provides a detailed analysis on internal injuries on soft tissue and spinal cord, which is very much needed for emergency and trauma care units. [16]



On the other hand, when it comes to the key companies in the MRI machine development sector, the market reflects a classical monopolistic scenario, where the established companies have a robust revenue position. We find the following key players leading the market:

- GE Healthcare
- Hitachi Medical Systems America AG.
- Siemens AG
- Toshiba Corporation
- Aurora Imaging Technologies, Inc.
- Koninklijke Philips N.V.
- Esaote SPA
- Sanrad Medical Systems Pvt. Ltd.

b) HISTORICAL EVOLUTION

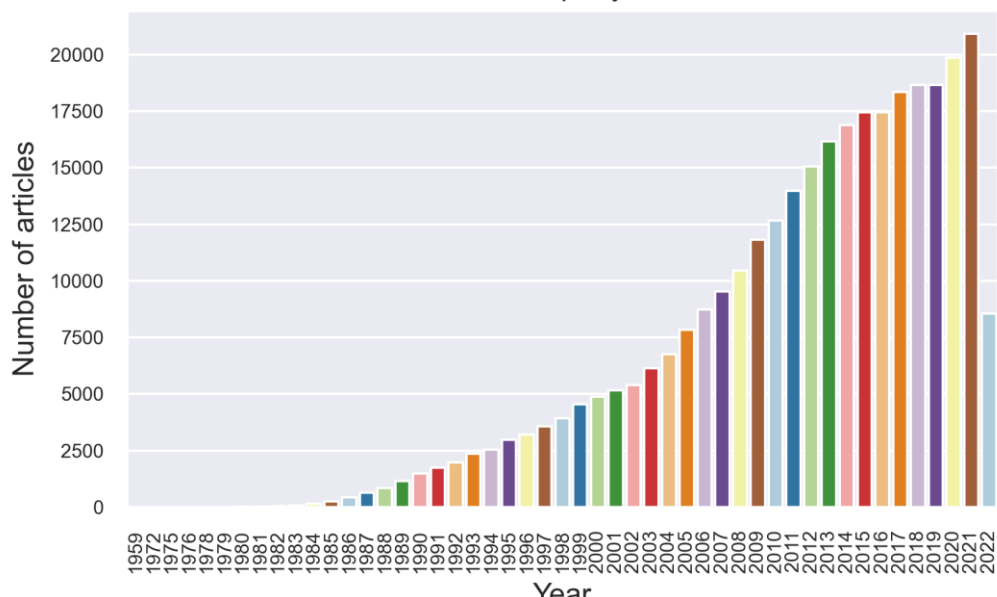
In 1970, Raymond Damadian, discovered that abnormal cancer cells had longer relaxation time lengths than normal cells, this led him to realise the possibility of diagnosing diseases with a human-sized scanner. He called this imaging process ‘field-focused NMR’ and founded FONAR in 1978. [17] Other neuroimaging techniques like computerized tomography (CT) was first applied in 1961, and its discovery led to the invention of the X-ray CT scanner, which received the Nobel Prize for medicine in 1979.

MRI was first approved by the FDA in 1984, we are therefore talking about a field that has not been that long out in the market. Additionally, it did not grow until the early 1990s; until then there were less than 10 scanners per 1M Americans, since it was found not worth it and very expensive. This number spiked up to 27 by 2004 and 39 in 2015, where nearly \$50 billion are spent per year [18].

All this data can be easily corroborated when searching ‘brain MRI’ in PubMed [19]. There are no articles until 1959, and it is not until 1982 when the exponential growth, and therefore the research starts. Figure 16 depicts all previous information.

Figure 16. Histogram showing Brain MRI related articles per year

Brain MRI related articles per year. Source: PubMed



As previously shortly stated, Covid-19 has had a negative impact in this market. The emergence of the pandemic forced all key players operating in the market to decrease their production of MRI equipment due to relocation of healthcare resources, declining patient visits, disruptions in supply chains among others. All those factors impacted highly on the sales, especially for the first half of 2020. However, MRI has been used as the first approach when it comes to detect Covid-19 infection, which triggered as well, an increase in their demand. For instance, GE Healthcare registered a decline of 13.8% in the total revenues generated in 2020 as compared to 2019. [15] Fortunately, as restrictions became more flexible (mid-end 2021) a significant increase in patient visits was seen, which resulted in a higher demand for equipment; this put the market back to the growth where it was right before the outbreak.

c) FUTURE PERSPECTIVES

It has clearly been seen all along the previous subsections that the MRI market is experiencing a growth that will only increase, and one of the main reasons why is because it is a young field in which loads of advances are still to be done. Among all the future perspectives that the market can experience we are going to go through the following ones:

-High magnetic frequency MRI systems: several universities are conducting research/studies on these systems. For instance, in University of Minnesota human MRI scanners have been performed using a 10.5 Tesla MRI. The MAGNETOM 10.5T was manufactured by Siemens and costed \$15M but is expected to open new avenues in diagnosis of a wide range of diseases (e.g. Alzheimer, diabetes, cancer). Machines like that have more advantages associated than just the improvement in image clarity, such as integration with Artificial Intelligence. Further information can be found in the following article [20].

-Open MRIs: Loads of patients feel claustrophobic and disturbed inside an MRI scanner due to its loud noise and small space; these problems sometimes result in inaccurate results. That is why some of the market players are focusing on developing open MRI systems (which are also suitable for oversized patients). As an example, GE Healthcare's Adventure MRI Series is specifically designed for pediatric imaging, this includes themed imaging rooms, lush visuals and hand-on activities to improve the experience. [21] Additionally, FONAR has developed the Upright MRI, which besides being suitable for claustrophobic and large patients it also allows to scan them in any position (sitting, standing, bending or lying down). This brings up few innovations, being able to image them in the positions in which they are experiencing their problems, and a more accurate diagnosis since the body is going to be imaged with their normal weight on the spine and other joints [22].

Despite close MRI still being the preferred one by radiologists, various clinical trials are being conducted to check the efficiency of the open one for the diagnosis of neonates' diseases. In the following years, it is expected that those ongoing clinical trials and product approval of open MRI systems by organisms as the FDA increases.

However, this is all restrained by one big factor, the high cost associated with the acquisition, installation and proper care of these systems; which often requires complex infrastructure and associated costs that cannot be undertaken by many medical institutions.

4. CONCEPTION ENGINEERING

This section goes along the approaches that will be implemented in the TFG to achieve its objectives. All the solutions studied in order to compute the final data frames and posterior statistical analysis have been included in Table 1 (those in bold are the approaches finally taken). This will be described into further detail in the following sub-sections.

	T1W's brain extraction software	DWI registration software	dMRI correction software	Tractography software	Programming environment
SOLUTIONS STUDIED	ANTs BET2 FreeSurfer SPM12	ANTs FLIRT SPM12	Eddy MRtrix3 SMP12	MRtrix3 DTI Studio DSI Studio	Python Spyder MATLAB Octave RStudio

Table 1. Solutions studied per each step developed throughout the project

4.1. DATA POST-PROCESSING

Debating about why those acquisitions are done with one or another value regarding several parameters such as acquisition time, b-values, T1 or T2, goes beyond the scope of the TFG itself, therefore we are not going to take it into account for this Section. So, once images are downloaded from the MRI scanner, a post-process has to be done, the post-process done in question went through the following stages, for each stage a different software was used.

a) STUDY OF SOLUTIONS

4.2.1. T1-WMRI's BRAIN EXTRACTION:

Advanced Normalization Tools (ANTs) is a software package for normalizing data to a template. It includes a Neuroimaging Multimodality that computes high-dimensional mappings to capture the statistics of brain structure and function. Free and open source software. [23]

BET 2 (Brain Extraction Tool) is included inside the FSL software, a comprehensive library of analysis tools for MRI data. BET deletes non-brain tissue from a T1, T2 image of the whole head. Free and open source. [24]

FreeSurfer is a neuroimaging software for processing, analysing and visualisation of MR images. This includes skull stripping, B1 bias field correction, GM and WM segmentation, reconstruction of cortical surface models, labeling of regions on the cortical surface, nonlinear registration of the cortical surface and diffusion tractography toolboxes among many others. Free and open source software. [25]

SPM12 (Statistical Parametric Mapping) is a software package that has been designed for the analysis of brain imaging data sequences. It is designed to work with MATLAB. MATLAB's student license is of \$99/year. [26]

4.2.2. DWI REGISTRATION:

FLIRT (fMRI's Linear Image Registration Tool) is a fully automated robust and accurate tool for linear (affine) intra and inter modal brain image registration. Based around a multi-start, multi-resolution global optimization method. [27] [28]

ANTS (explained in Section 4.2.1.)

SPM 12 (explained in Section 4.2.1.)

4.2.3. dMRI CORRECTION:

Eddy is a tool to correct for eddy current-induced distortions and signal dropouts. It also performs outlier detection to identify slices where signal has been lost as a consequence of subject movement during the diffusion encoding. It is included inside the FSL software; free and open source software. [29]

SPM 12 (explained in Section 4.2.1.)

MRtrix 3 provides a large suite of tools for image processing, analysis and visualisation, with a focus on the analysis of WM using DW MRI. Features include the estimation of fiber orientation distributions using CSD, a probabilistic streamlines algorithm for fiber tractography of WM and a comprehensive visualisation tools in mrview among many others. Free and open source software. [30]

4.2.4. TRACTOGRAPHY:

DSI Studio is a tractography software tool that maps brain connections and correlates findings with neuropsychological disorders. It is a collective implementation of several diffusion MRI methods, including DTI, diffusion MRI connectometry, and generalized deterministic fiber tracking. Free software. [31]

DTI Studio is a diffusion tensor image processing program running under Windows. It is suitable for such tasks as tensor calculation, color mapping, fiber tracking, and 3D visualization. Free software. [32]

MRtrix 3 (explained in Section 4.2.3)

b) PROPOSED SOLUTION

Once all software/ toolboxes have been thoroughly reviewed by comparing all their characteristics and applying them to the objectives of this study, the following solutions have been selected.

For T1-WMRI's brain extraction the software selected has been ANTs. The selection has been partially based on the computational time, while BET2 is the fastest option, it is also quite imprecise on several aspects; the opposite happens with FreeSurfer (it can take up to 7 hours). ANTs stands in the middle, taking a reasonable time and giving us enough precision regarding our needs. SPM 12 is taken out of the options since a MATLAB license is required.

For DWI registration the case is quite similar as above, SPM12 requires a license and FLIRT directly does not work as well as ANTs does, this latter one being a way more developed and documented.

For dMRI correction, the toolbox selected has been MRtrix3 when working with the dMRI correction, since it allows the removal of several aspects as motion, SNR or Gibbs ringing artefacts. For the

Eddy current-induced distortions Eddy FSL (note the redundancy) is the best tool. Once again SPM12 requires a license.

Ultimately, for tractography MRtrix3 is the software being selected, since it includes the tckgen command, this being the best way regarding our objectives to calculate each tractogram for different tractography algorithms.

4.2. PROGRAMMING ENVIRONMENT

In order to group all processed data, perform mathematical operations to obtain new data, extract relevant parameters, collect them into a data frame to later on perform an analysis different software can be used.

a) STUDY OF SOLUTIONS

MATLAB is a programming platform, with a matrix-based language designed specifically for engineers and scientists to analyse and design systems and products. It presents different toolboxes allowing the analysis of data, image processing, visualization and many others. The Student license is \$99/year. [33]

Python is an interpreted, object-oriented, high-level programming language with dynamic semantics for a general purpose and with a flexible environment, that is that makes it one of the most popular programming languages. Furthermore, it includes modules and packages such as *NumPy*, *Matplotlib* or *SciPy*. Free and open source software. [34]

Spyder is a scientific environment written in Python, for Python. It features a unique combination of the advanced editing, analysis, debugging, and profiling functionality allowing data exploration, interactive execution, deep inspection and humongous visualization capabilities. Free and open source software. [35]

RStudio uses the programming environment of R, which is specially focused on the data science environment, its statistical analysis and graphical representation. It includes a big number of R packages for data science, machine intelligence and interoperability between Python and R among others. Free and open source software. [36]

b) PROPOSED SOLUTION

MATLAB offers several image processing toolboxes that can be used for image data segmentation, extraction and analysis and are seen to work faster than Python ones, and that the price is not an impediment at all since UB owns a license. However, the packages/ tools needed to perform those operations (e.g. *DIPY*, *pandas*, *nibabel*) have been developed for Python, and even though DIPY allows to read/ save in MATLAB to later perform the statistical analysis, the quite reasonable approach to develop the entire script in the same programming environment was taken. The statistical and graphical representation pro that RStudio has, is covered by using the *seaborn* library. This being a Python data visualization library based on *matplotlib* yet more comfortable in handling Pandas data frames (which will be highly used throughout the project's development). Finally, between Python and **Spyder** we are sticking to this latter one. Main reasons being the fact that you can work with several consoles at the same time, allowing code to run in one, different scripts without mixing variables among others.

5. DETAILED ENGINEERING

All along this section, as the name says by itself, a detailed explanation of the projects, the different steps, as well as their methodology will be conducted. As is foreseeable, this section will follow the course that the TFG's development did by itself.

As mentioned beforehand (Section 1), this project comprises the comparison of some of the most used MRI acquisition sentences by performing a statistical analysis regarding several parameters that we have considered to be relevant when it comes to image quality. Into this comparison two sequences (meant to be way superior both in image quality and acquisition time) that are being developed by researchers working for the MRI platform IDIBAPS are as well included.

The methodology followed has used a population of 114 controls (a total of 135 acquisitions), classified into 6 datasets. All of them have undergone an MRI scanner at the Hospital Clínic up to May 2022.

Previously to the MRI scanner a protocol has to be designed in order to establish how the acquisitions will be done, how long each one will last etc. Once the images are downloaded into the IDIBAPS computers they have to undergo all the post-processing, this consisting on the brain extraction (brain, WM, GM, and CSF mask) atlas registration into the DWI, posterior correction on several aspects (e.g. subject motion, Eddy induced-currents, SNR, Gibbs or Gibbs ringing artifacts), and tractography. This being done, it will result in several files containing all corrected information.

Once all the files are ready, it is time to upload them into the programming environment, Spyder, by first creating a dataframe in order to group all files into several lists, by performing iterations on those lists all calculations (DIPY, MRtrix3...) will be done. Relevant parameters' values will then be extracted and stored into another dataframe, which will be saved as a csv file. Finally, those csv will be uploaded into another script in which the statistical analysis and representations are performed.

5.1. DATA ACQUISITION

As previously stated, data has been separated into 6 different groups depending on which project they were acquired for, among them we find:

- I. **EPILENG** (Epilèpsia i Llenguatge): comprises 21 subjects.
- II. **EOP**: comprises 80 subjects.
- III. **ALBUCAT**: comprises 2 subjects. For each subject two acquisitions were done, named *AP* (anteroposterior) and *PA* (posteroanterior), a total of 4 subjects. This is done to cancel out the distortion seen in Figure 17, which appears when the magnetic gradients first enter in contact with the skull. And by acquiring those images when emitting gradients both front-to-back and back-to-front, to later superpose them, we end up with a 'neutral' image.
- IV. **BBHSA**: comprises 5 subjects. As for ALBUCAT two acquisitions are done for subject; therefore, we are going to consider it as if we had 10 subjects.
- V. **BIOMARCADORES**: comprises 4 subjects.

VI. **LAB_IMATGE**: Comprises 2 subjects. This dataset is the last one that has been developed for IDIBAPS; this means two things. First, it is a brand new protocol proposal, designed to obtain as much information as possible without considering the acquisition time (which went up to 1.30h); and second, as this TFG had to be delivered by June 8th only two acquisitions were done and processed by then (Saül's one and mine). As just said, for each subject 8 acquisitions were done; repeating each proposal twice (a total of 4) but changing the voxel size. Therefore, a total of 16 of 'subjects' were considered.

Furthermore, given the amount of data we will work with, it is highly needed to establish a consensus on how to organise and share data obtained. Lack of consensus leads to misunderstandings and wasted time on renaming data or rewriting scripts. Therefore, all files have been named in accordance with Brain Imaging Data Structure (**BIDS**) [37], each subject has their own folder; inside the folder two other ones are found *anat* and *dwi*. Being the latter one the one we are going to use throughout all project's development, and where the corrected files are going to be saved into. For a better understanding, Figure 18 shows a screenshot of the files.

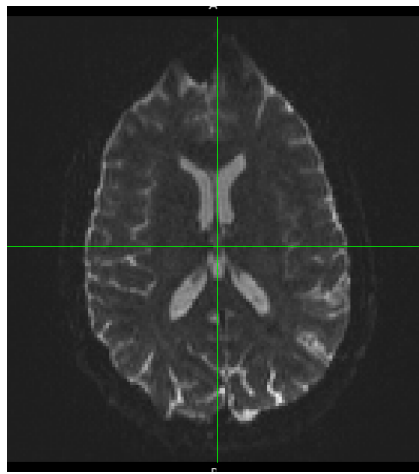


Figure 17. Magnetic gradients distortion (dataset: ALBUCAT)

The MRI scanner used for all acquisitions is the MAGNETOM Prisma fit 3T developed by Siemens Healthineers for clinical imaging and includes the following features: [38]

- XR gradient system: (80/200), with E11c software
- Head/neck coil 20 channels 440 mm × 330 mm × 370 mm
- Cap coil 32 channels 300 mm × 390 mm × 315 mm
- Head/neck coil 64 channels 435 mm × 395 mm × 350 mm
- Body coil 18 channels
- Column coil 32 channels
- VisuaStimDigital
- Presentation® licensed visual and auditory stimuli presentation system
- Screen to project visual stimuli for the 32-channel head coil
- Remote control to respond to fMRI studies

Each acquisition sequence has been done in accordance with the following parameters (Table 2)

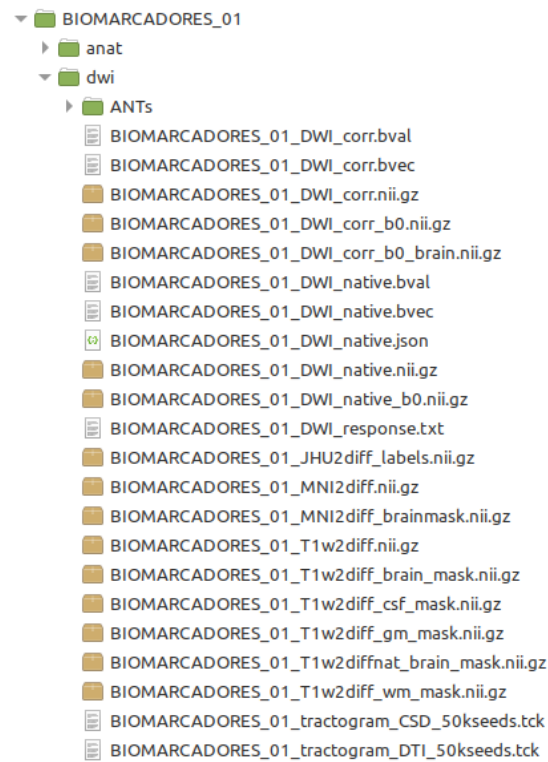


Figure 18. BIDS structure for dataset BIOMARCADORES

DATASET	Voxel size (isometric)	Field of View (FOV)	Diffusion directions	b-values (s/mm ²)
BIOMARCADORES	2 mm	122 x 122 x 60	31	0 (x3) 1000 (x6)
EOP	2 mm	128 x 128 x 60	31	0 (x1) 800 (x30)
EPILENG	1.5 mm	140 x 140 x 92	100	0 (x7) 1500 (x47) 3000 (x46)
ALBUCAT	1.5 mm	140 x 140 x 92	100	0 (x7) 1500 (x47) 3000 (x46)
BBHSA	1.5 mm	150 x 150 x100	47	0 (x3) 1000 (x6) 2000 (x12) 3000 (x26)
Proposal 1 <i>(fastnfurios)</i>	1.5 mm	150 x 150 x100	78	500 (x6) 1000 (x64)
	2 mm	150 x 150 x100	78	500 (x6) 1000 (x64)
Proposal 2 <i>(mortalkombat)</i>	1.5 mm	112 x 112 x 76	165	0 (x17) 500 (x6) 1000 (x32) 1500 (x48) 2000 (x68)
	2 mm	112 x 112 x 76	165	0 (x17) 500 (x6) 1000 (x32) 1500 (x48)
Proposal 3 <i>(diehard)</i>	1.5 mm	150 x 150 x100	149	500 (x6) 1000 (x64) 2000 (x64)
	2 mm	150 x 150 x100	149	500 (x6) 1000 (x64) 2000 (x64)
Proposal 4 <i>(sharknado)</i>	1.5 mm	150 x 150 x100	165	0 (x17) 500 (x6) 1000 (x32) 2000 (x48) 3000 (x64)
	2 mm	150 x 150 x100	165	0 (x17) 500 (x6) 1000 (x32) 2000 (x48) 3000 (x64)

Table 2. Acquisition sequence parameters per dataset

5.2. DATA POST-PROCESSING

5.2.1. T1-WMRI's BRAIN EXTRACTION:

First step includes the skull-stripping of the anatomical image (i.e. the structural acquisition, T1-W) to extract the brain itself, this is done by applying extraction masks; those masks allow to segment the input data into CSF, WM and GM by using reference atlas. Among the outputs generated, we find the tissue segmented, and the brain extraction mask (excluding cerebellum and brainstem). The brain mask provides a reference for matching other modalities, in our case DWI (Figure 19). This has been done with the ANTs software [23].

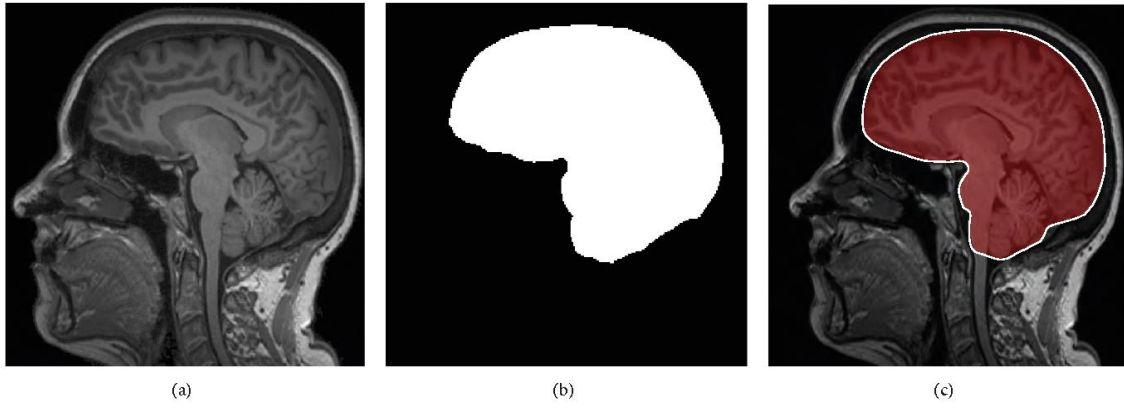


Figure 19. Step 1, brain extraction (ANTs). (a) shows the original T1 -W MRI. (b) depicts the estimated brain mask. (c) presents an overlap of the brain mask and original MR image.

5.2.2. DWI REGISTRATION:

T1w and atlas are registered into the DWI in order to have both a structure and reference of where specific regions are located (this allows us to later extract particular regions). Exemplified in Figure 20. Done with the ANTs software [23].

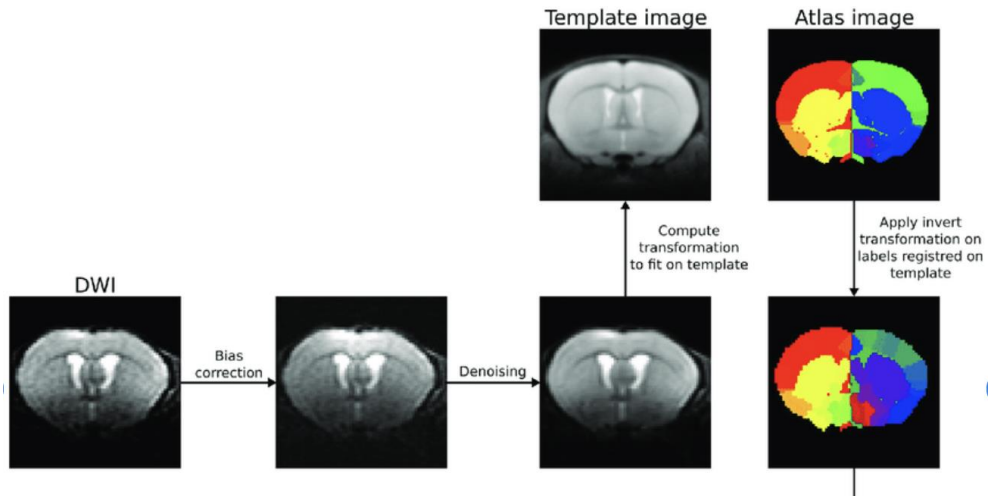


Figure 20. Step 2, DWI registration (ANTs).

5.2.3. dMRI CORRECTION:

This is done with several functions inside the MRtrix 3 package. *mrdegibbs* function, which results in an image where the Gibbs ringing artifacts are removed (Figure 21), and *dwidenoise*, which does a noise level estimation (caused by motion, SNR...) and returns a denoised image. Last one used is *dwibiascorrect*, and as the name says, it performs a field inhomogeneity correction for a DWI volume series and removes the estimated bias field. [30]

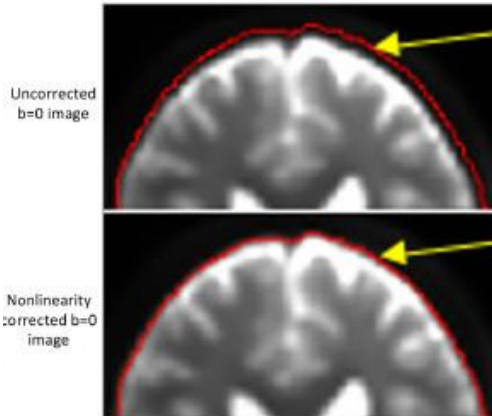


Figure 21. Step 3, corrections (MRtrix3).

5.2.4. TRACTOGRAPHY

Last step inside the post-processing stage is to compute the tractograms with both algorithms, DTI and CSD. The software MRtrix 3 has the *tckgen*, where the number of tracts generated has to be specified (50.000) and the tracking algorithm that is going to be used. [30] Once tractograms are computed, the whole brain tractography can be visualized (an in Figure 11); moreover, by applying the atlas specific regions can be extracted, Figure 22 shows the language region with the CSD algorithm.

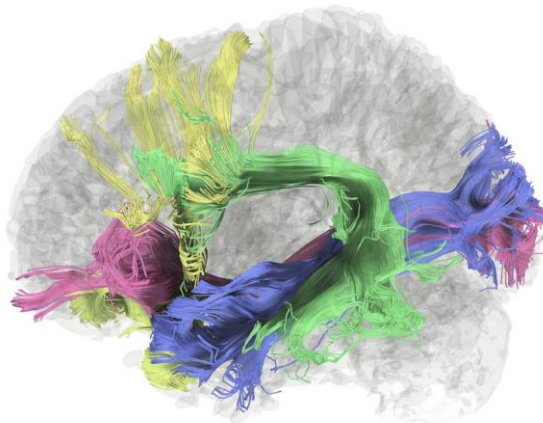


Figure 22. Brain tractography.
ROI: language region (CSD,
Dataset: LAB_IMATGE)

5.3. PARAMETERS' EXTRACTION

At this point of the project, all needed files have already been acquired by performing the post-processing. Three Spyder scripts were created for developing this subsection:

5.3.1. SNR:

Computing the Signal-to-Noise-Ratio (SNR) of DW images is still an open question, as it depends on the WM structure as well as the gradient direction corresponding to each DWI. SNR is defined as the ratio of the signal's mean to the underlying Gaussian noise's standard deviation. [$\text{SNR} = \text{mean}(\text{signal}) / \text{std}(\text{noise})$, Eq 10]. Where $\text{std}(\text{noise})$ is computed from the background of any DW image. To compute $\text{mean}(\text{signal})$, we are using the 'worst-case' approach following the DIPY documentation [39]. Where several WM structures such as the corpus callosum (CC) can be

easily identified from the colored-FA map; since they are mainly oriented in one direction, for the CC specifical case it would appear in red (left-right direction).

First step is to compute the DT model in the brain mask. This brain mask does not need to be post-processed, so we are going to directly upload the brain mask done on the T2- weighted images (T1W2.). In a mathematical view, the brain mask is a matrix of 0s and 1s, 1 meaning that we are in an area where there is a brain. The DT model is computed by doing a gradient table containing both b-values and b-vectors (they give information about which way the diffusion gradients were pointing at). By using the *tenmodel.fit* function we end up with the DT fitted into the brain mask.

Next, a threshold is set to isolate the red voxels of the colored-FA map, meaning we are only obtaining information about the CC registered into the brain mask with the DT already fitted into it. The CC can be seen in Figure 23.

Once we have isolated the voxels in which the CC is, the **mean (signal)** in the region is estimated. **Std (noise)** is then calculated by inverting the brain mask and saving only the 0s (are outside the brain). Finally [Eq 10] is applied for the b-values intervals we had previously established.

The inputs of this first script have been:

- i. DWI native b-values (*file.bval*)
- ii. DWI native b-vectors (*file.bvec*)
- iii. T1W2 native brain mask (*file_T1w2diffnat_brain_mask.nii.gz*)

Corpus callosum (CC)

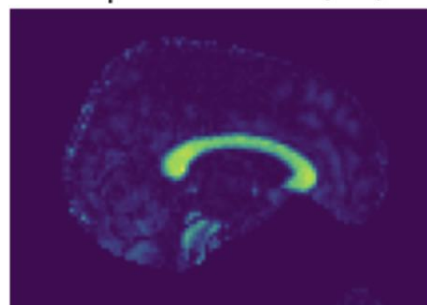


Figure 23. SNR CC

The output of this script has been:

- i. Dataframe containing the SNR ratio for each interval of b-values per each MRI acquisition. Moreover, the voxel size has also been added for posterior purposes.

Both script and dataframe can be found in Section 11 (Annex), named as *01_SNR.py* and *01_SNRs.csv* respectively.

5.3.2. FA:

As seen throughout Section 1 (point 3.3.3.1) the DT model is a simple way to characterize diffusion anisotropy. Nonetheless, regions near the cerebral ventricle and parenchyma can be underestimated by partial volume effects of the CSF causing a free water contamination; which can particularly affect DTI analysis for different subjects (and therefore a different brain morphology) [40]. If this were to happen, a statistical analysis of the FA for all 135 acquisitions grouped by datasets would not be accurate enough. This difference can be seen in Figure 24.

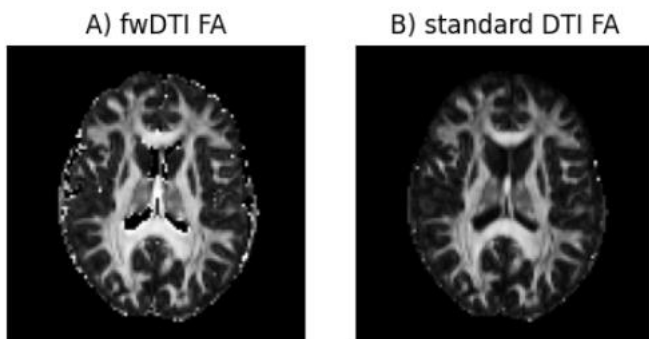


Figure 24. FA map difference with the standard DTI and free water DTI

To remove this free water contamination, the DTI model can be expanded [Eq 11] to take into account an extra compartment representing the contributions of free water diffusion.

$$S(g, b) = S_0(1 - f) e^{-bg*Dg} + S_0 f e^{-bD_{iso}} \quad [Eq\ 11]$$

Where g and b are diffusion gradient directed and weighted, $S(g, b)$ is the DW signal measured, S_0 the signal in a measurement with no DW, D the diffusion tensor, f the volume fraction of the free water component, and D_{iso} the isotropic value of the free water diffusion.

Once explained the approach taken by the DIPY library, it is time to upload all needed files, as for SNR b-values and b-vectors are needed (native file, no post-process is done), to compute the gradient table and eventually the DT model. The case is not the same for the brain mask, since it is better to use the already corrected one in order to make all maps more comparable among themselves. As before the next step is to compute the tensor fit model with the `tenmodel.fit` function. Once done it is possible to extract the FA from it. FA is a matrix the same shape as the brain mask where numbers go from 0 to 1 in accordance with anisotropy.

Upcoming step is to multiply the FA by the WM, GM and CSF brain mask in order to obtain the specific FA for each brain area. As for the normal brain mask the WM, GM and CSF ones are a matrix of same dimensions compounded by 0s and 1s. For each one of them the mean value and standard deviation (std, in order to measure the values' spread) are computed.

Finally, the *JHU WM labels atlas* [41] is uploaded, in there 50 WM tract labels were created by hand segmentation of a standard-space average of diffusion MRI tensor maps. Figure 25 shows the atlas correlated into one of our acquisitions. All 50 labels have been entered into a Spyder dictionary (`atlas_labels`); by registering the file were each label is registered into a certain brain voxel into the FA matrix, we obtain the FA value for a certain number of voxels, which likewise correspond to a specific WM region defined in `atlas_labels`. As for the masks, both `mean` and `std` a computer and stored into the dataframe.

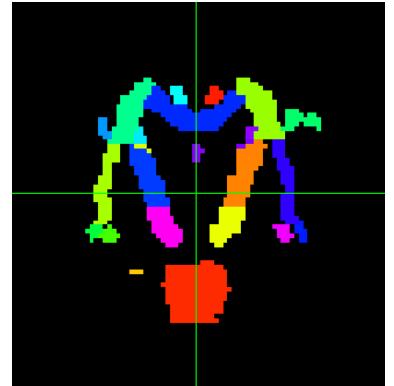


Figure 25. Atlas labels registered into the EPILENG dataset

The inputs of the second script have been:

- i. DWI native b-values (`file.bval`)
- ii. DWI native b-vectors (`file.bvec`)
- iii. T1W2 corrected brain mask (`file_MNI2diff_brainmask.nii.gz`)
- iv. WM brain mask (`file_T1w2diff_wm_mask.nii.gz`)
- v. GM brain mask (`file_T1w2diff_gm_mask.nii.gz`)
- vi. CSF brain mask (`file_T1w2diff_csf_mask.nii.gz`)
- vii. Atlas data (`file_JHU2diff_labels.nii.gz`)

The output of this script has been:

- ii. Dataframe containing the FA value (`mean` and `std`) for each kind of brain mask (simple, GM, WM, and CSF), and atlas label per each MRI acquisition. Moreover, the voxel size has also been added for posterior purposes.

Both script and dataframe can be found in Section 11 (Annex), named as `02_FA.py` and `02_FAmaps.csv` respectively.

5.3.3. TRACTOGRAPHY:

Local fiber tracking is an approach used to model WM by creating streamlines from local directional information. Following the DIPY documentation [42], if the local directionality of a tract segment is known, one can integrate along those directions to build a complete representation of that structure. At this point, local fiber tracking has already been performed (subsection 5.2.4) using two of the algorithms explained in Section 1 (4.1 and 4.2), DTI and CSD; tractograms are then directly uploaded into the script. For each tractogram streamlines are going to be selected and stored into a new variable. Next step is to retrieve the length of each streamline by using the *dipy.tracking.streamline function*; this will be stored into two arrays depending on which algorithm is used (DTI or CSD) next to the total number of measures inside each of the arrays.

The inputs of the third script have been:

- i. Tractogram using DTI algorithm (*file_tractogram_DTI_50kseeds.tck*)
- ii. Tractogram using CSD algorithm (*file_tractogram_CSD_50kseeds.tck*)

The output of this script has been:

- i. Dataframe containing two arrays giving the length of each streamline computed in the tractogram (one per algorithm) and the length of both arrays per acquisition (which corresponds to the number of streamlines).

Both script and dataframe can be found in Section 11 (Annex), named as *03_tractogram.py* and *03_tractogram_data.pkl* respectively.

5.4. STATISTICAL ANALYSIS

Once all the relevant parameters have already been extracted and stored into three different dataframes; the statistical analysis needs to be performed. This will be done by creating another Spyder script in which the dataframes are going to be uploaded and plotted as considered.

First step after uploading the dataframes is to group all acquisitions into the 6 datasets established in Section 5.1; so, all plots can be classified into them allowing a better analysis.

For the **SNR dataframe** we will extract the SNR values per each interval established under the voxel size condition. By simply looking at the dataframe it is seen that the voxel size (*xdim*, *ydim* and *zdim*) only takes to values, 1.5 and 2mm and is the same for all the dimensions; therefore, the analysis is going to be based on two boxplots, one per each voxel size.

When it comes to the **FA dataframe** three plots are going to be extracted. First and second one are 6 different sub-boxplots, representing both mean FA value and std FA value for all the masks already mentioned in the FA script: GM, WM and CSG. As for the SNR, the first plot is done for the 1.5mm voxel size and the second one for the 2mm. Each box represents a different dataframe. For a better analysis each pair (std and mean) of subplots have been set into equal y-axis scale, causing some boxes to look flattened.

Third plot represents the mean FA value for all the WM regions established in the atlas labels; as there are 50 regions the best way to visualise it was through a heatmap (i.e. map where values are turned into a color code). It has as many columns as WM regions (x-axis) and rows as datasets (y-axis). Voxel size has not been taken into consideration.

Finally, the **tractography streamlines length analysis** has been done by creating a set of histograms for each dataset (one color per dataset). Four histograms are displayed, one per algorithm approach followed (DTI and CSD) per each voxel size (1.5 and 2mm). In addition, a boxplot correlating the Number of Streamlines (NOS) per each algorithm, dataset and voxel size has also been created.

The inputs of the fourth and last script have been:

- i. 01_SNRs.csv
- ii. 02_FAmaps.csv
- iii. 03_tractogram_data.pkl

The outputs of this script have been:

- i. Fig 26 (SNR)
- ii. Fig 27 (FA, 1.5mm)
- iii. Fig 28 (FA, 2.5 mm)
- iv. Fig 29 (FA, heatmap)
- v. Fig 31 (Histogram streamlines length)
- vi. Fig 32 (Streamlines length zoomed in)
- vii. Fig 30 (NOS)

Script can be found in Section 11 (Annex), named as *04_statistics.py* and figures are deployed in Section 5.5.

5.5. RESULTS

The results accomplished are presented in this section, along with their corresponding discussion.

5.5.1. SNR:

In Figure 26, it is seen the SNR value of the DWI per each b-value, left plot for a voxel size of 1.5mm and right plot for 2mm.

The b-value interval has been chosen in accordance with the b-values used for each acquisition; in a way in which each dataset had as much representation as possible inside one interval. Main reason to do so, is because each dataset has different acquisition parameters (as seen in Section 5.1); therefore, there is no way to know for sure if the difference is due the b-value or the parameters themselves.

For visualisation purposes each interval comprises a range of 400 values (the first one is not included). The obtained results suggested that as the b-value [s/mm²] increases the SNR decreases, decreasing as well the power to obtain a better specification coming from the useful information (the signal). This decrease in the overall SNR is also seen when decreasing the voxel size (a smaller voxel size corresponds to a higher resolution).

At this point what is essential is to find a balance between the b-values and SNR; since taking only short b-values means that we are not letting enough time for the diffusion to happen, which at itself reduces quality. As mentioned in Section 1 the b-value that has been find to give best performance is around 1000 s/mm², however this should not always be generalized, but applied for each particular case; meaning that if we are in a situation where the patient is critical we will try to perform the shortest possible acquisition (increasing voxel size and considering short b-values).

Nonetheless, SNR does not hold that much value for itself as it does to consider other aspects as FA. So, we cannot just conclude that the bigger the voxel size the better because this will have a significant impact on the FA, as will be seen in the analysis performed below.

SNR per each b-value interval and voxel size

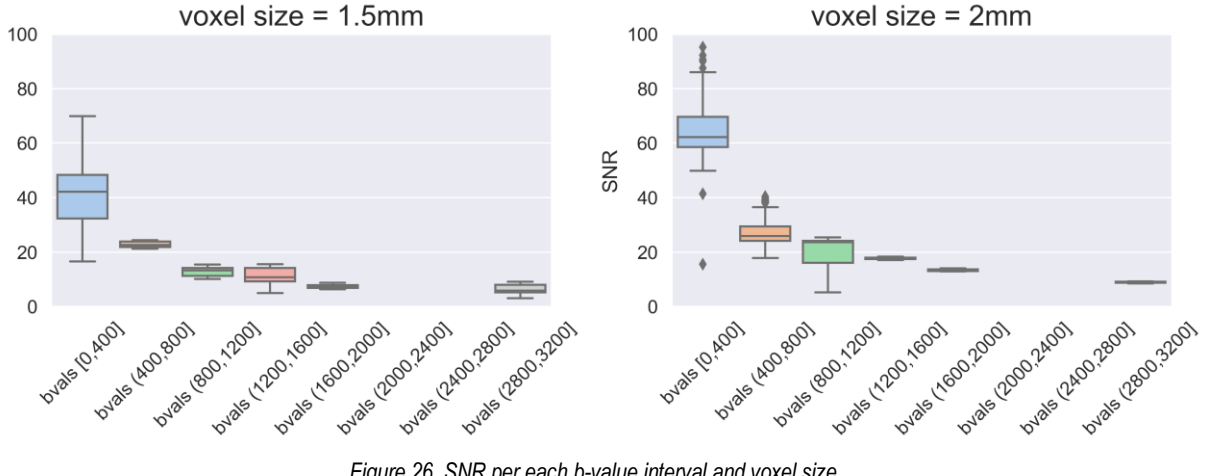


Figure 26. SNR per each b-value interval and voxel size

5.5.2. FA:

Figure 27 shows a heatmap, y axis represents each dataset and x axis specific WM brain areas. First view it can clearly be seen the difference among the old datasets and the new acquisition protocol designed by IDIBAPS; this latter one shows highest FA values, reflecting WM structures will also be better reconstructed, visualised and analysed since the fiber density will be higher.

On the other hand, voxel size does not appear to have a relevant role, this is in fact seen when looking at the slightest color variation among all new acquisitions paired in 1.5 mm and 2 mm voxel size. What appears to have a relevant role, is the number of directions taken in each acquisition (this parameter is displayed in Table 2), since those showing a higher number also have a greater FA value. So, it can be concluded that the best acquisition when it comes to specific structures reconstruction is the one used for *DIEHARD (LAB_IMATGE dataset)*, and the worst one by far *ALBUCAT*.

However, this is a hypothesis and in order to establish a completely accurate conclusion several analyses have to be done for each individual structure.

Figure 29 deploys six sub-boxplots in which the FA value of each individual GM, WM and CSF brain mask is shown per dataset with a 2mm voxel size. Figure 28 shows the same information but for a 1.5 mm voxel size. It is easily seen how for the GM and CSF brain mask the FA values are quite low (i.e. there is almost no diffusivity in those particular regions).

When analysing Figure 28, it is clearly seen that the highest the number of diffusion directions the highest the FA value. Proposal 4 (Sharknado) has the greatest result.

As the voxel size increases, the FA decreases; we are analysing a larger region so it will be more difficult to detect the level of organization or anisotropy of certain structures. For this latter case (voxel size of 2 mm) all acquisitions show a similar FA value, since independently of the number of

directions or b-values the voxel size is enough to reduce FA by itself. A clear result to which discuss the hypothesis stated in Section 5.5.2, where saying that the SNR is higher is not enough to use a 2mm voxel.

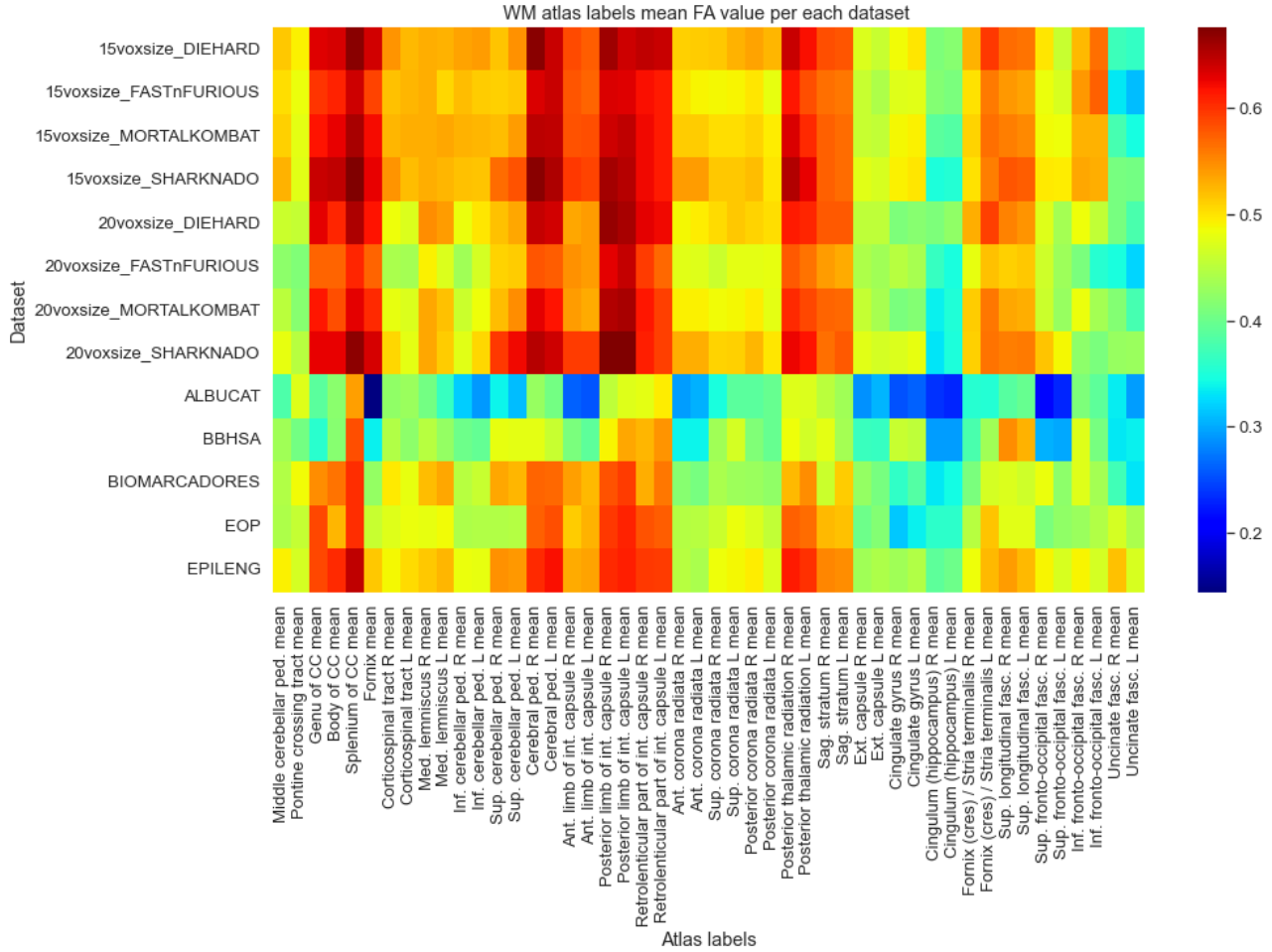


Figure 27. WM atlas labels mean FA value per dataset

FA per each mask and dataset (voxel size = 1.5mm)

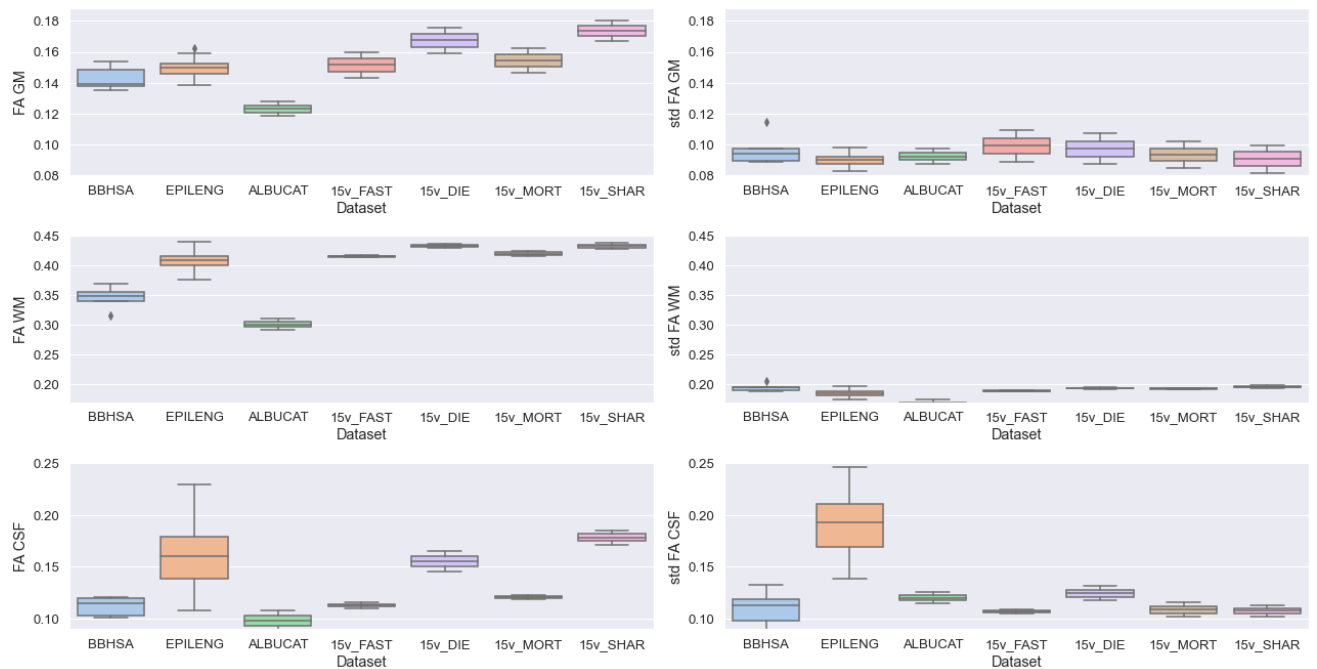


Figure 28. FA per each mask and dataset (1.5mm)

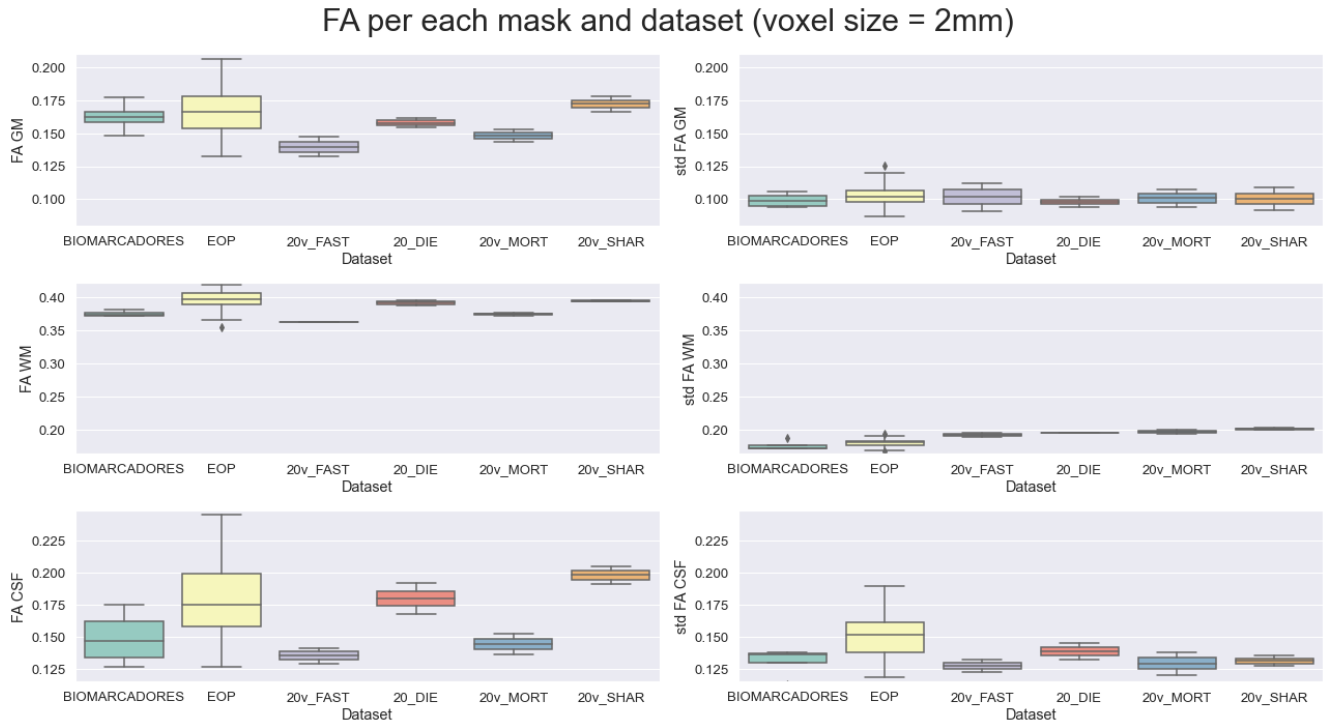


Figure 29. FA per each mask and dataset (1.5mm)

5.5.3. TRACTOGRAPHY

In Figure 30 it is seen the Number of Streamlines (NOS) that each algorithm (DTI and CSD) is capable to reconstruct; once again separated per voxel size and dataset. The NOS value decreases as the voxel size increases; meaning that it is best seen for a smaller voxel if a streamline located in a complex region actually corresponds to several of them. On the other hand,

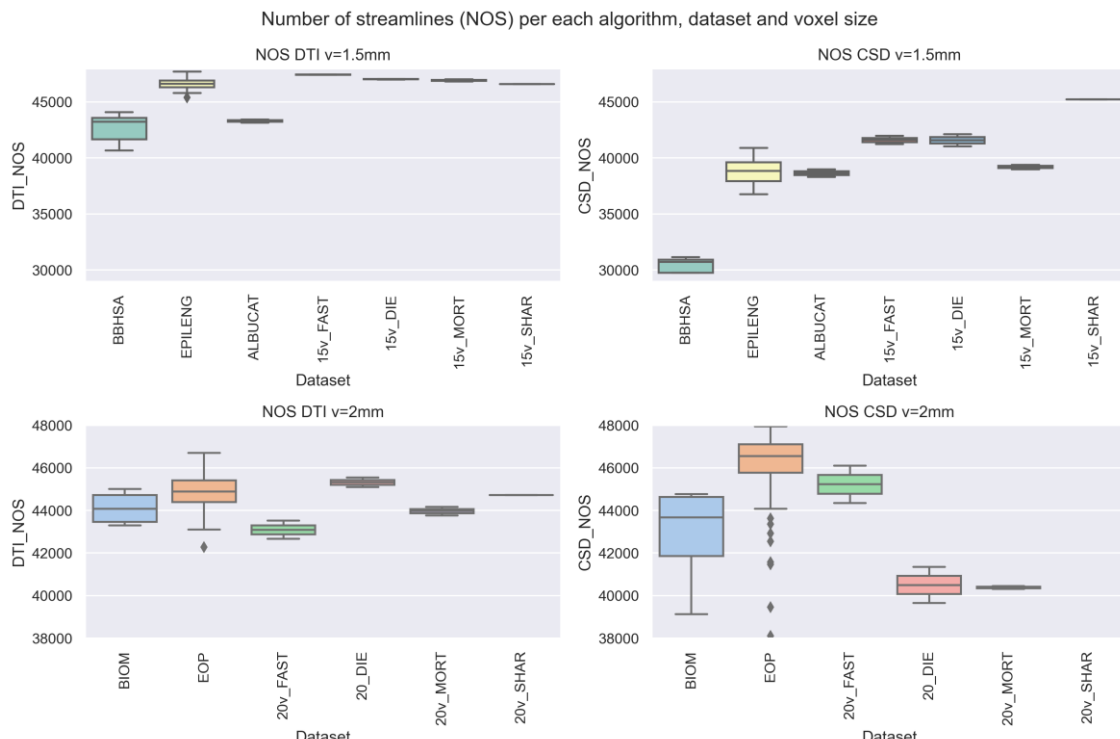


Figure 30. NOS per each algorithm, dataset and voxel size

when it is known that the DTI is the simplest tractography algorithm, makes sense that there is not much NOS difference among the worst and best dataset no matter what the voxel size is.

However, when moving towards a better algorithm as CSD is, results are way different. Once again, the smallest the voxel size the higher the NOS. Considering 1.5mm voxel size as the best approach, Proposal 4 (*Sharknado*) has the best performance.

Nonetheless, the NOS value is such a general concept that can also be affected by many other aspects, results above are just a hypothesis; in order to establish a completely accurate conclusion on why our 1.5 mm proposal works the best in combination with CSD, a whole brain tractography study has to be conducted so the streamlines can be individually analysed. This goes beyond the scope of this TFG.

Last figures (Figure 31) consist of a combination of superposed histograms (one per dataset) deploying on the x axis the length of the streamlines, and y axis the Number of Streamlines that accomplish the latter condition. Different histograms have been done per voxel size and tractography algorithm. By taking a superficial look it is seen that the NOS value per dataset highly differ for short streamlines, this being the main reason why Figure 32 has been done (zoomed in only for streamlines up to 100mm). Once again, the DTI algorithm shows a way more heterogeneous histogram, since its simplicity does not allow him to distinguish between datasets with better parameters.

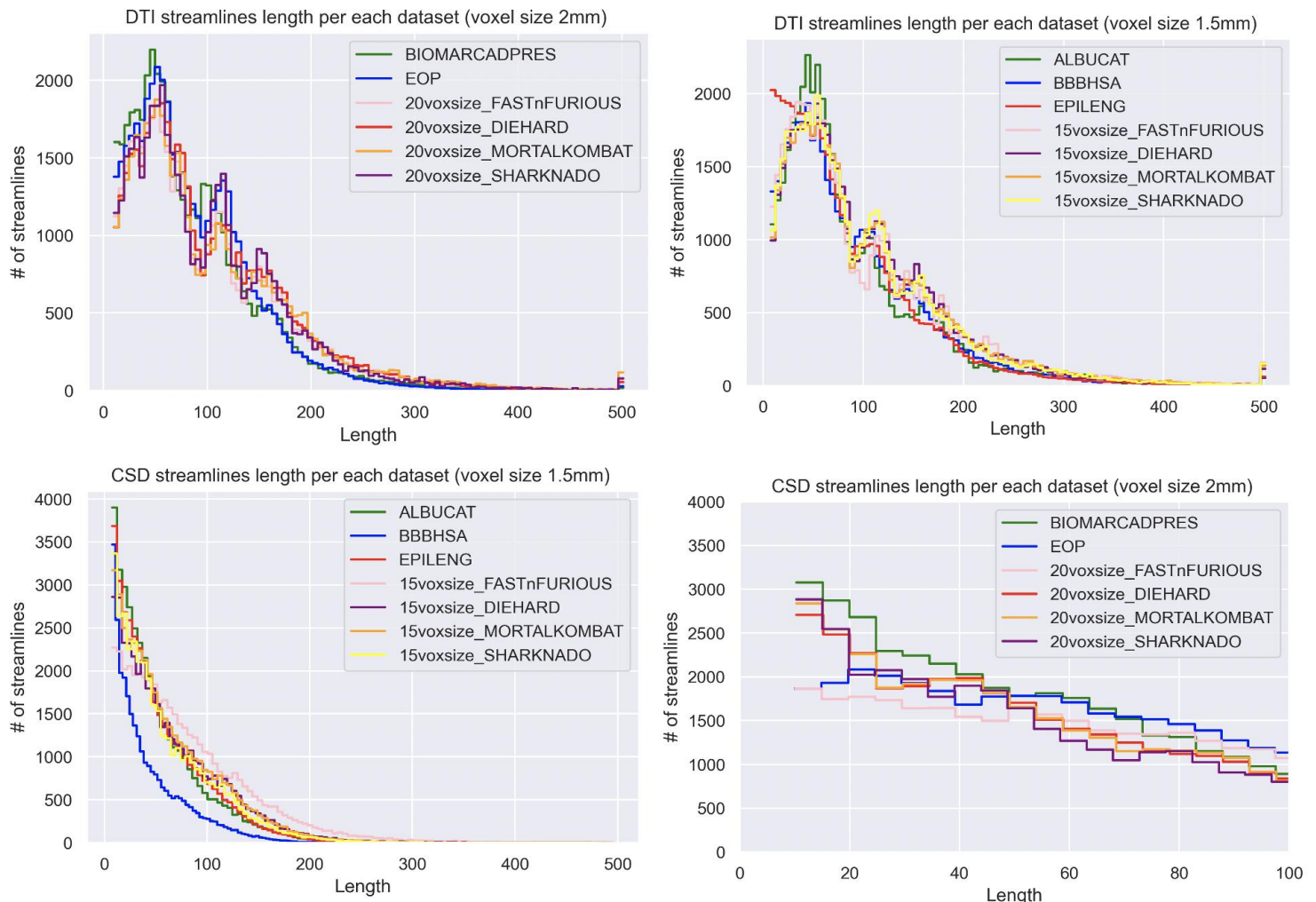


Figure 31. Number of streamlines in accordance to length (CSD, DTI, 1.5mm and 2mm)

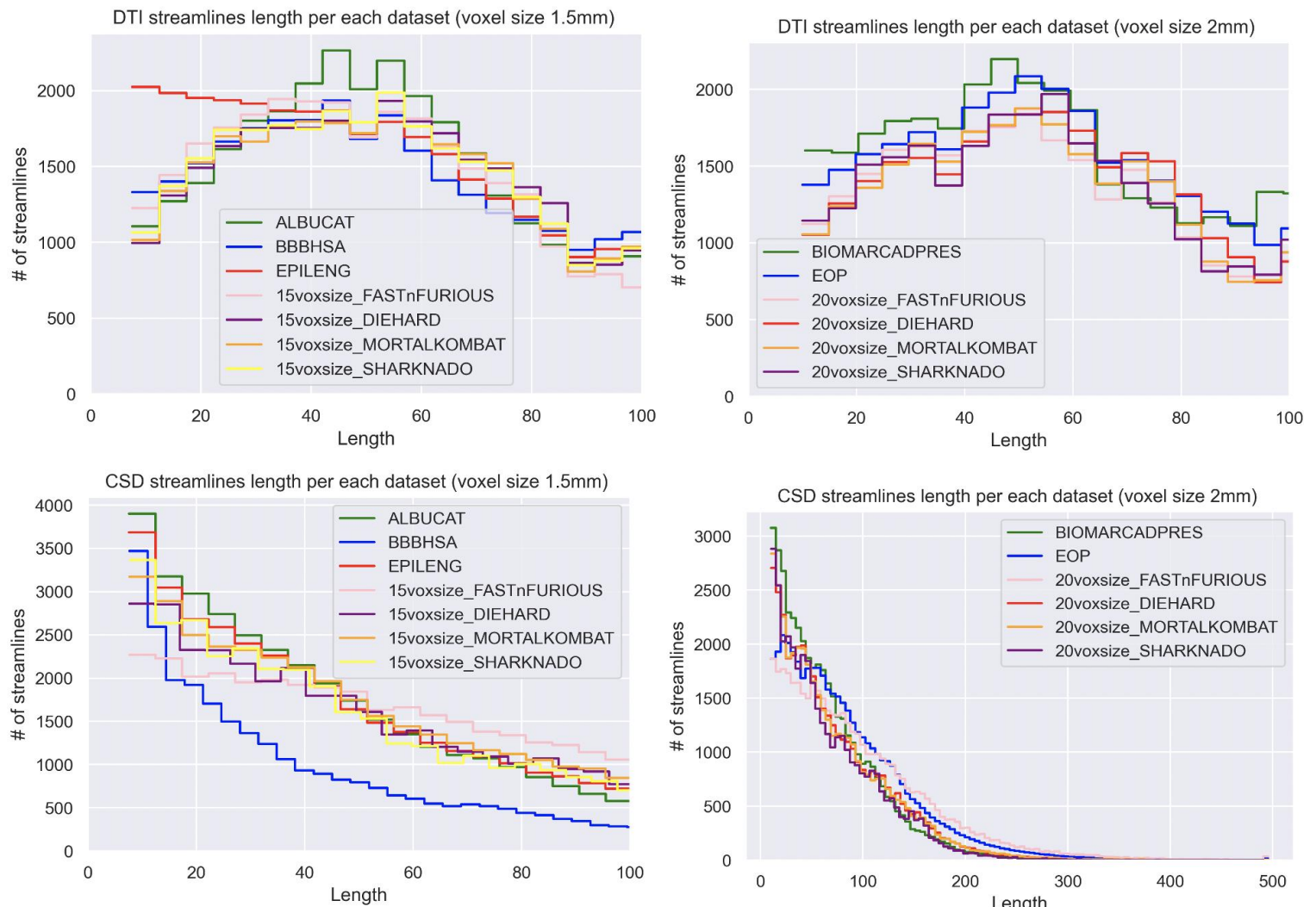


Figure 32. Number of streamlines in accordance to length (CSD, DTI, 1.5mm and 2mm). Zoomed in version

6. EXECUTION SCHEDULE

The following section, as referenced to in the previous ones, includes the phases and milestones that the project has gone through in the course of its development. It includes the timings and the structure followed to achieve the goals in the established timing; additionally, it defines as well the set of activities carried out and the time needed for their implementation.

a) WORK BREAKDOWN STRUCTURE (WBS)

The Work Breakdown Structure (WBS) is a visual, hierarchical and deliverable-oriented deconstruction of a project. It is a very helpful diagram since it allows you to break down the project into its scope and visualize all the tasks required to complete it. [43]

The WBS for this project (Figure 33) is structured into four main tasks: previous study and training, project development, parameters' analysis and project wrap up. In addition, it consists of three levels, the first one enclosing the tasks previously mentioned, the second one

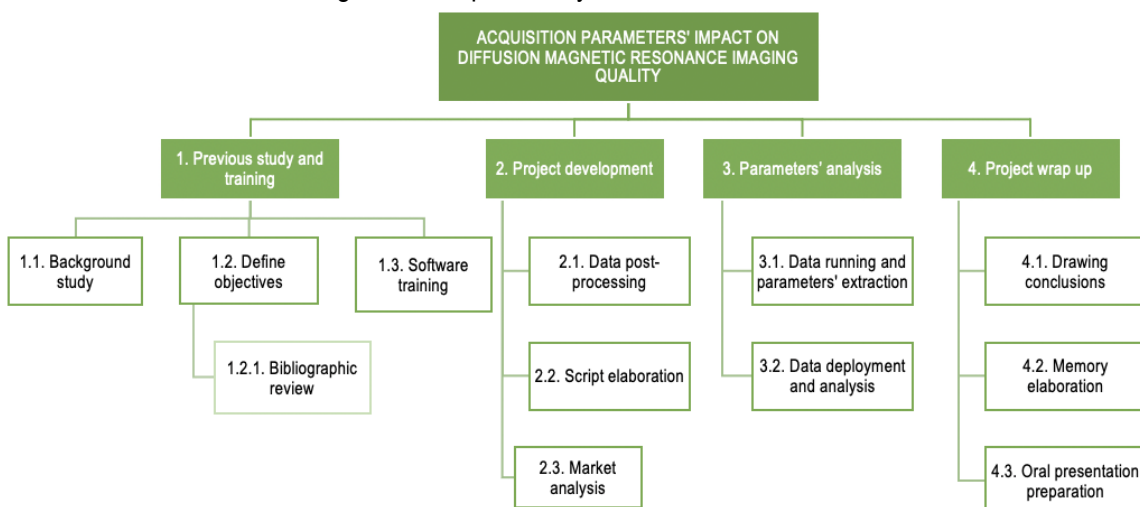


Figure 33. WBS

b) DESCRIPTION OF THE TASKS

Tasks and subtasks from the WBS are briefly defined hereunder.

Task 1 – Previous study and training: firsts readings

1.1. Background study: Analyze previous works related to this field as well as its current situation.

1.2. Define objectives: Establish the aim of the project as well as the most important goals to be achieved by the end of the project.

1.2.1. Bibliographic review: gathering useful information for the project's development.

1.3. Software training: research and practical training on the MRI field's most used libraries for the programming environment used, in the projects' case Spyder, and why it is the best one following our approach.

Task 2 – Project development: steps previous to the results' acquisition.

- 2.1. **Data post-processing:** T1W brain extraction, DWI register, DWI correction and tractography.
- 2.2. **Script elaboration:** Once the images have been processed into data (e.g. matrix) using Spyder, a script needs to be built in order to first load the subject's data, extract the important parameters and values, and turn them into relevant information according to the project's aim.
- 2.3. **Market analysis:** search for information on the sector to which our application is directed as well as its future potential taking into account legal limitations/ regulations when applied.

Task 3 – Parameters' analysis: results' acquisition and statistical analysis.

- 3.1. **Data running and parameters' acquisition:** using the previous scripts we have to run the processed data in order to obtain the data frames we will later work with.
- 3.2. **Data deployment and analysis:** Those data frames need to be read by other scripts that will display the results in the desirable way (e.g. plots) in order to be able to do a statistical analysis.

Task 4 – Project wrap up: Last tasks, closure.

- 4.1. **Drawing conclusions:** Once results have been obtained and analysed we can draw conclusions and determine whether those objectives have been accomplished as initially thought or not.
- 4.2. **Memory elaboration:** State in a document all knowledge acquired during the process as well as procedure, approaches, results and the previous conclusion.
- 4.3. **Oral presentation preparation:** Determine the key points and highlights about the project and consequent bibliographic context to prepare a clear, short and concise presentation. Visual support material was prepared for this task.

c) PROGRAM EVOLUTION AND REVIEW TECHNIQUES (PERT)

A PERT chart is a visual management tool used to map out and track the tasks and timelines. The main advantage it holds over GANTT charts (studied in the next subsection) is that it indicates dependencies, which gives knowledge of how one missed deadline could affect other tasks. [44]

Task	Activity	Description	Predecessor activities	Consequent activities	Expected time (hours)
1.1	A	Background study	-	B, C	5
1.2	B	Define objectives	A	F	3
1.3	C	Software training	A	D, E	10
2.1	D	Data post-processing	C	G	50
2.2	E	Script elaboration	C	G, H	50
2.3	F	Market analysis	B	H, J	5
3.1	G	Data running and parameters' extraction	D, E	H	50
3.2	H	Data deployment and analysis	E, F, G	I, J	50
4.1	I	Drawing conclusions	H	J	10
4.2	J	Memory elaboration	F, H, I	K	60
4.3	K	Oral presentation preparation	I	-	10

Table 3. PERT matrix

The projects' PERT chart has been elaborated from a task matrix (Table 3) where the activities defined in the WBS are assigned a letter, duration and dependencies with previous ones are established. It has to be taken into account, that according to the UB Teaching Plan, the TFG is equivalent to approximately 300h.

From this last table, the PERT chart was built (as Figure 34 shows). In each node, two main values can be found, in the bottom-left the Early time (i.e. the minimum time needed to reach a node) and in the bottom-right the Late Time (i.e. the maximum time the task needs to be completed without delaying the project). In addition, green arrows indicate the Critical Path, this being the minimum necessary time to carry out the project

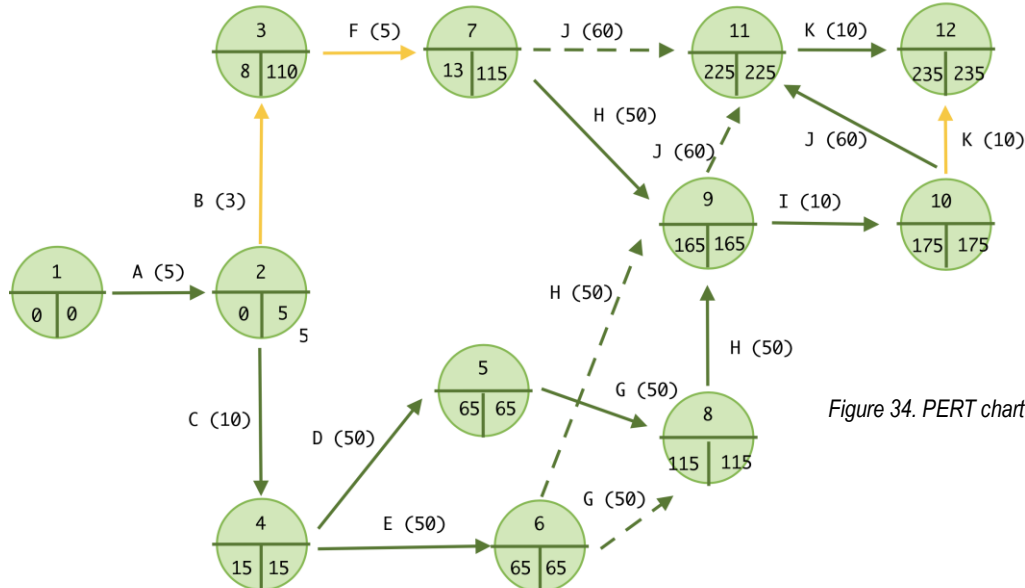


Figure 34. PERT chart

d) GANTT CHART

And last but not least, the Generalized Activity Normalization Time Table (GANTT) displays the tasks against time. On the left of the chart the tasks are shown, and along the top there is a suitable time scale. Each activity is represented by a bar; the position and length of the bar reflects the start date, duration and end date of the tasks (Table 4).

TASK	March (in weeks)				April				May				June			
	1	2	3	4	1	2	3	4	1	2	3	4	1	2	3	4
Background study																
Define objectives																
Software training																
Data post-processing																
Script elaboration																
Market analysis																
Data running and parameters' extraction																
Data deployment and analysis																
Drawing conclusions																
Memory elaboration																
Oral presentation preparation																

Table 4. GANTT chart

7. TECHNICAL AND ECONOMICAL FEASIBILITY

a) TECHNICAL

The technical feasibility corresponds to a SWOT (strengths, weaknesses, opportunities and threats) analysis. A strategic planning technique that studies and detailing both internal (SW) and external (OT) factors that might affect the realization of the project, both in a positive or negative way. Mentioned information is depicted in Table 5.

In order to take as much advantage as possible of the opportunities as well as avoid those threats, the confluence of strengths and opportunities and of weaknesses and threats must be studied. The internal strengths have to be focused into fitting the opportunities.

In between the strengths that have been analysed, we find that the data that has been used corresponds to a temporal period going up to 2022; heterogenous data since new developments have been done and protocols designed. Additionally, it has all been acquired and post-processed in the IDIBAPS' MRI in Hospital Clínic.

There are a variety of opportunities that this project could benefit from, mainly focused on possible improvements in the MRI acquisitions, perfect examples are the new protocols that have been used as proposals. Even more opportunities can come with the introduction of the 7T MRI scanner, and the fact that the market is experiencing an exponential growth causing the same growth on related articles published.

Threats are external and therefore unavoidable. However, this does not mean that strategies can be thought to control them and actuate as soon as possible so their consequences have the smallest impact possible.

Even though the project presents a wide number of strengths, it also has important weaknesses to consider. First of all, computation times related to post-processing take an incredibly high value, limiting even more the available time to perform it. Moreover, as each dataset has their own acquisition parameters it is impossible to know if some variations are due to only those parameters that we are considering, or due to the impact of secondary ones. Finally, the new acquisition proposals only have two samples per each one, making hard to distinguish personal variation from the one caused by acquisition parameters.

Last but not least, the principal threat this project is facing is that with so many technological advances, and the emergence of new technologies, this study could end up being neglected. Two main reasons are, the elevated cost of performing not only the MRI scanner but also the post-processing, and the implementation of the 7T MRI.

	Positive factors	Negative factors
	STRENGTHS	WEAKNESSES
Internal environment	<ul style="list-style-type: none"> - Data are controls acquired in Hospital Clínic by IDIBAPS - High motivation and dynamism - MRI scanner in which to perform acquisitions (3T). - Guidance and support - Possibility to access to data from previous studies done by IDIBAPS 	<ul style="list-style-type: none"> - Slow computation time - Limited time - Only two samples per each acquisition proposal - Different acquisition parameters make it hard to compare them
External environment	<ul style="list-style-type: none"> - 7T MRI imaging - Improvements on MRI acquisitions - Exponential growth on both market size and related articles 	<ul style="list-style-type: none"> - Cost MRI - Implementation of 7T can leave this study neglected

Table 5. SWOT

b) ECONOMICAL

The following subsections comprises all theoretical costs of this project and consequent study. The cost of the project has been divided into two main sections, while the first one comprises the cost of what has been the TFG by itself; the second one comprises several studies performed by the platform from which I was able to take the data and apply it into my project. This division is somehow crucial since the prices' range is so much different. For both cases, IDIBAPS has provided the funds for covering all expenses, this includes human resources, facilities and required equipment (software/ hardware). Overall, it does not take a rocket scientist to realise that the project's entirety was technically feasible by virtue of IDIBAPS. All expenses, together with further details have been listed in Table 6.

Starting with **human resources**, the salary which has been taken into account when it comes to the student is 15 €/hour, an average salary in Spain for junior biomedical engineers. Since the total amount of hours needed to complete the project has been stated to be 300h (Section 6) the cost of that person is 4.500€. This total cost has been specifically divided taking into account two main stages: **educational and developing stage** (e.g. bibliographic research, background's analysis, conduction of the study) which took about 160 h. And **writing and editing stage** (memory elaboration and oral presentation preparation), counting approx. 140h.

Keeping on with the **software**, the ones used only when considering the TFG has been **Spyder**, an open- source cross-platform integrated development environment for scientific programming in the Python language. Additionally, **FSLeyes** was also used for complementary visualization, this

consisted on an open- source image viewer for 3D and 4D data. As both names say by themselves, the cost was of 0 €. Detailed information was given in Section 4.

The **hardware** only consisted of a regular **desktop computer** located in the IDIBAPS' MRI lab, which was estimated to cost approx. 800 € but it is hard to know since it is as well quite old.

Moving on towards the part where the substantial cost weight is, the studies conducted by IDIBAPS and from which all data to develop the project was taken from consisted of 114 subjects (as stated in Section 5). Each of those subjects underwent an **MRI scanner**, the price for each MRI acquisition is stipulated to 153.5 € per hour (including preparation, acquisition, medical report and technical support if needed) since each subject was in there 1h, the total cost goes up to 17,499 €*. Later on, those images need to be **post- processed**, taking into account that this is a Diffusion MRI study in which human brain structural connectomics have to be analysed the price just for setting up the equipment is of 1,485 €*. The post-processing itself is 39.38 € per image analysed, considering all 114 images, the cost is of 4,490.46 € *.

All those prices are of public knowledge in *IDIBAPS Scientific Platform Fees 2022* document [45]; taken into account considering that we are internal workers in IDIBAPS (fees for workers in Campus Clínic or external personal are also included) and with the IVA yet to be applied (*).

The total cost of the study is 28.774,46 €. The cost divided by specific activity is depicted in Figure 16, where it can clearly be seen that the second section is the one that holds the majority of the weight. This being the main reason why Figure 35 shows the costs only taking into account the TFG section. One last consideration has to be taken into account, as the TFG is mandatory and therefore all human resources are tasks that have to be done by the student, no actual cost is associated.

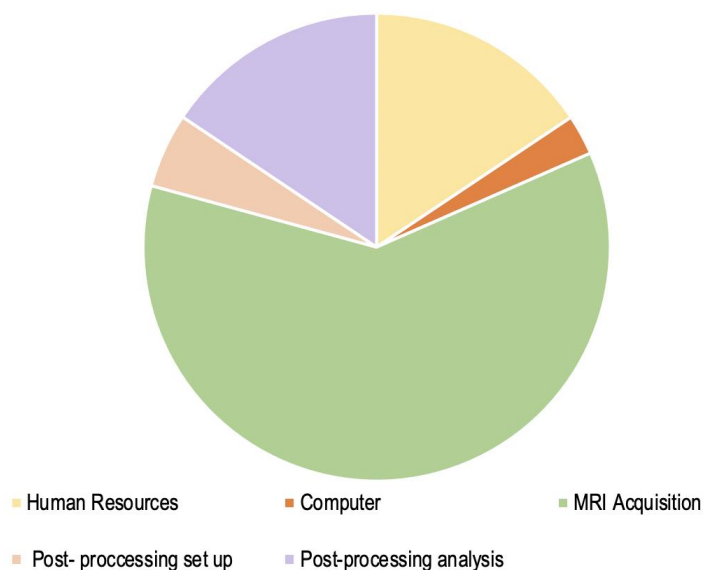


Figure 35. Pie chart, cost divided per specific activity.

	ITEM	COST	
Human Resources	Educational and Developmental Stage	2.400 €	
	Writing Stage	2.100 €	
	Total Cost Student	4.500 €	
Software	Spyder	open source 0€	
	FSLeyes	open source 0€	
Hardware	Desktop computer	800 €	
MRI acquisition	Acquisition 3T: preparation, acquisition, medical report and technical support	153.50 €/ hour 17,499 € *	
Image post-processing and statistical analysis	Diffusion MRI - Set up	1,485€ *	REF: TP560
	Diffusion MRI - Structural Connectomics (human brain fee)	39.38 € (fee per image) 4,490.46 € *	REF: TP561

* IVA not applied

Table 6. Economic analysis

TOTAL COST	28.774,46 €
------------	-------------

8. CONCLUSIONS AND FUTURE PERSPECTIVES

To conclude, this project had the objective of comparing several popular MRI acquisitions designed in the last 5 years by means of different acquisition parameters, among them, and with a new acquisition that has just been designed by IDIBAPS.

To achieve the previous goal a list of previous steps needed to be done, since in order to extract those parameters, both a post-processing stage and several data frames creation was essential. For each post-processing stage, a description of tasks and software/ toolboxes used has been done. Same way, for each data frame created, a description of the Spyder libraries and toolboxes has also been performed, as well as the main steps followed to compute/ extract those parameters.

Taking into account the whole population of the project, there have been 114 control subjects (i.e. healthy), which turned out into a total of 135 acquisitions who had undergone an MRI scanner up to May 2022. All 135 acquisitions have been grouped into 6 datasets according to the acquisition protocol. -

Just by taking a shallow look into the plots it can easily be seen that for each parameter analysed the values undergo such a big variety when split into datasets. Therefore, it can be said that yes, it is possible to not only compare those acquisitions but also to determine which ones have the best performance. And as it has already been done with the new acquisition, use those results to design new proposals which will combine as much of the best acquisition parameters as possible; but most importantly to make further evidence in why those new proposals work way better and should be implemented into the MRI scanners in Hospital Clínic. However, also taking into account up to which step we want to take the diffusion study, we will not use the same protocol with someone who is suffering a stroke or a healthy person undergoing a whole brain tractography study as a control.

With regard to the limitations that have appeared along the development of the project, the major drawback has been time, emphasizing on the fact that this a TFG which has to be handed in before a deadline. Moreover, the computational time limitation could partially be solved by running scripts in a different computer with a bigger capacity; the same approach, was taken when doing the data post-process.

This being said, this project does not end here, several future perspectives have been taken into consideration. In order to obtain substantial evidences on why our protocol proposal is quite a good candidate to be implemented, further control subjects have to undergo it until we reach a substantial number. Scripts should then be re-run to obtain updated dataframes to perform further statistical analyses. To be even way more accurate this new analysis should also include a deepest sight into the FA values for the WM specific structures (i.e. further analysis on Figure 27), and a whole- brain tractography to specifically evaluate the relationship between the CSD and DTI algorithms, voxel size and other acquisition parameters conforming a dataset integrity.

9. REFERENCES

- [1] Resonancia magnética - Mayo Clinic. (n.d.). Retrieved June 8, 2022, from <https://www.mayoclinic.org/es-es/tests-procedures/mri/about/pac-20384768>
- [2] O'Brien, P., Sellar, R. J., & Wardlaw, J. M. (2004). Fogging on T2-weighted MR after acute ischaemic stroke: How often might this occur and what are the implications? *Neuroradiology*, 46(8), 635–641. <https://doi.org/10.1007/S00234-004-1230-2>
- [3] Ministerio de Sanidad y Consumo. «BOE» núm. 294, de 5 de diciembre de 2018. Referencia: BOE-A-2018-16673 Available from: <https://www.boe.es/buscar/pdf/2018/BOE-A-2018-16673-consolidado.pdf>
- [4] Medical devices. (n.d.). Retrieved June 6, 2022, from https://www.who.int/health-topics/medical-devices#tab=tab_1
- [5] EUR-Lex - 31993L0042 - EN - EUR-Lex. (n.d.). Retrieved June 7, 2022, from <https://eur-lex.europa.eu/legal-content/ES/ALL/?uri=celex:31993L0042>
- [6] ISO 13485 Quality Management Systems - A.P. LYON. (n.d.). Retrieved June 7, 2022, from https://www.aplyon.com/iso_13485_quality_management_systems.html?gclid=CjwKCAjwy_aUBhACEiwA2IHHQJxzsBm-E1xtnomK48lf4AX5ulP6jUaLMOf7GuElFK7jomXLZ32iZxoCSg8QAvD_BwE
- [7] Radiation-Emitting Electronic Products | FDA. (n.d.). Retrieved June 7, 2022, from <https://www.fda.gov/industry/regulated-products/radiation-emitting-electronic-products>
- [8] ISO/TS 10974:2018(en), Assessment of the safety of magnetic resonance imaging for patients with an active implantable medical device. (n.d.). Retrieved June 7, 2022, from <https://www.iso.org/obp/ui/#iso:std:iso:ts:10974:ed-2:v1:en>
- [9] Assets: how they work - GOV.UK Developer Documentation. (n.d.). Retrieved June 7, 2022, from <https://docs.publishing.service.gov.uk/manual/assets.html>
- [10] O'Donnell, L. J., & Westin, C. F. (2011). An Introduction to Diffusion Tensor Image Analysis. *Neurosurgery Clinics of North America*, 22(2), 185–196. <https://doi.org/10.1016/J.NEC.2010.12.004>
- [11] Yousaf, T., Dervenoulas, G., & Politis, M. (2018). Advances in MRI Methodology. *International Review of Neurobiology*, 141, 31–76. <https://doi.org/10.1016/BS.IRN.2018.08.008>
- [12] Pascual-Díaz, S., Pineda, J., Serra, L., Varriano, F., & Prats-Galino, A. (2019). Default Mode Network structural alterations in Kocher-Monro trajectory white matter transection: A 3 and 7 tesla simulation modeling approach. *PLOS ONE*, 14(11), e0224598. <https://doi.org/10.1371/JOURNAL.PONE.0224598>
- [13] Martínez-Heras, E., Grussu, F., Prados, F., Solana, E., & Llufriu, S. (2021). Diffusion-Weighted Imaging: Recent Advances and Applications. *Seminars in Ultrasound, CT and MRI*, 42(5), 490–506. <https://doi.org/10.1053/J.SULT.2021.07.006>

- [14] Pascual-Diaz, S., Varriano, F., Pineda, J., & Prats-Galino, A. (2020). Structural characterization of the Extended Frontal Aslant Tract trajectory: A ML-validated laterality study in 3T and 7T. *NeuroImage*, 222. <https://doi.org/10.1016/J.NEUROIMAGE.2020.117260>
- [15] Magnetic Resonance Imaging Equipment Market Forecast, 2029. (n.d.). Retrieved June 7, 2022, from <https://www.fortunebusinessinsights.com/industry-reports/magnetic-resonance-imaging-mri-equipment-market-100087>
- [16] Magnetic Resonance Imaging Market Size, Share Report, 2030. (2022). Retrieved 6 June 2022, from <https://www.grandviewresearch.com/industry-analysis/magnetic-resonance-imaging-market#>
- [17] The Biggest Breakthroughs in MRI History. (n.d.). Retrieved June 7, 2022, from <https://www.uprightmrideerfield.com/the-biggest-breakthroughs-in-mri-history>
- [18] MRI units density by country 2019 | Statista. (2022). Retrieved 6 June 2022, from <https://www.statista.com/statistics/282401/density-of-magnetic-resonance-imaging-units-by-country/>
- [19] brain MRI - Search Results - PubMed. (n.d.). Retrieved June 7, 2022, from <https://pubmed.ncbi.nlm.nih.gov/?term=brain+MRI&timeline=expanded>
- [20] Ertürk, M. A., Wu, X., Eryaman, Y., van de Moortele, P. F., Auerbach, E. J., Lagore, R. L., DelaBarre, L., Vaughan, J. T., Üğurbil, K., Adriany, G., & Metzger, G. J. (2017). Towards imaging the body at 10.5 tesla. *Magnetic Resonance in Medicine*, 77(1), 434. <https://doi.org/10.1002/MRM.26487>
- [21] Adventure Series for CT | GE Healthcare (United States). (n.d.). Retrieved June 7, 2022, from <https://www.gehealthcare.com/products/accessories-and-supplies/adventure-series-for-ct>
- [22] FONAR Upright MRI. (n.d.). Retrieved June 7, 2022, from <http://www.fonar.com/upright-mri.html>
- [23] ANTs by stnav. (n.d.). Retrieved June 7, 2022, from <https://stnav.github.io/ANTs/>
- [24] BET/UserGuide - FslWiki. (2022). Retrieved 6 June 2022, from <https://fsl.fmrib.ox.ac.uk/fsl/fslwiki/BET/UserGuide>
- [25] FreeSurfer. (n.d.). Retrieved June 7, 2022, from <https://surfer.nmr.mgh.harvard.edu/>
- [26] SPM Software - Statistical Parametric Mapping. (n.d.). Retrieved June 7, 2022, from <https://www.fil.ion.ucl.ac.uk/spm/software/>
- [27] FLIRT - FslWiki. (2022). Retrieved 6 June 2022, from https://fsl.fmrib.ox.ac.uk/fsl/fslwiki/FLIRT#Research_Overview
- [28] Jenkinson, M., Bannister, P., Brady, J. M. and Smith, S. M. Improved Optimisation for the Robust and Accurate Linear Registration and Motion Correction of Brain Images. *NeuroImage*, 17(2), 825-841, 2002.
- [29] eddy - FslWiki. (n.d.). Retrieved June 7, 2022, from <https://fsl.fmrib.ox.ac.uk/fsl/fslwiki/eddy>
- [30] MRtrix3. (n.d.). Retrieved June 7, 2022, from <https://www.mrtrix.org/>

- [31] DSI-Studio: A Tractography Software Tool for Diffusion MRI Analysis. (2022). Retrieved 6 June 2022, from <https://dsi-studio.labsolver.org/>
- [32] MRI Studio (2022). Retrieved 6 June 2022, from https://www.mristudio.org › UserManual_v2_10_6
- [33] Mathworks, MATLAB. (2022). Retrieved 6 June 2022, from <https://es.mathworks.com/products/matlab.html>
- [34] What is Python? Executive Summary | Python.org. (n.d.). Retrieved June 7, 2022, from <https://www.python.org/doc/essays/blurb/>
- [35] Team, S. (2022). Home — Spyder IDE. Retrieved 6 June 2022, from <https://www.spyder-ide.org/>
- [36] RStudio | Open source & professional software for data science teams - RStudio. (n.d.). Retrieved June 7, 2022, from <https://www.rstudio.com/>
- [37] Brain Imaging Data Structure. (n.d.). Retrieved June 7, 2022, from <https://bids.neuroimaging.io/index.html>
- [38] SIEMENS Healthineers (2022). Retrieved 6 June 2022, from <https://www.siemens-healthineers.com/es/magnetic-resonance-imaging/3t-mri-scanner/magnetom-prisma>
- [39] DIPY : Docs 1.5.0 - SNR estimation for Diffusion-Weighted Images. (n.d.). Retrieved June 8, 2022, from https://dipy.org/documentation/1.5.0/examples_builtin/snr_in_cc/#example-snr-in-cc
- [40] DIPY : Docs 1.5.0 - Using the free water elimination model to remove DTI free water contamination. (n.d.). Retrieved June 8, 2022, from https://dipy.org/documentation/1.5.0/examples_builtin/reconst_fwdti/#example-reconst-fwdti
- [41] Atlases - FslWiki. (n.d.). Retrieved June 8, 2022, from <https://fsl.fmrib.ox.ac.uk/fsl/fslwiki/Atlases>
- [42] DIPY : Docs 1.5.0 - Introduction to Basic Tracking. (n.d.). Retrieved June 8, 2022, from https://dipy.org/documentation/1.5.0/examples_builtin/tracking_introduction_eudx/#example-tracking-introduction-eudx
- [43] What is a Work Breakdown Structure (WBS) | Project Management. (n.d.). Retrieved June 8, 2022, from <https://www.workbreakdownstructure.com/>
- [44] What is a PERT Chart? | Definition, Examples, and Overview. (n.d.). Retrieved June 8, 2022, from <https://www.productplan.com/glossary/pert-chart/>
- [45] Plataformas | Hospital Clínic Barcelona. (n.d.). Retrieved June 8, 2022, from <https://www.clinicbarcelona.org/idibaps/core-facilities>

10. ANNEXES

```

# -*- coding: utf-8 -*-
"""
Spyder Editor
01_SNR
"""

#%% Loading packages
import os
import pandas as pd
import numpy as np
import nibabel as nib
from dipy.core.gradients import gradient_table
from dipy.io.gradients import read_bvals_bvecs
from scipy.ndimage import binary_dilation
from dipy.segment.mask import bounding_box
import warnings
warnings.simplefilter(action='ignore', category=FutureWarning)

#%%
main_dir="/home/marina/TFG/DATA"
output_file = '/home/marina/TFG/outputs/01_SNRs.csv'

try:
    df = pd.read_csv(output_file)
except:
    df = pd.DataFrame(columns=['SubjID'])

s_list = []
for s in sorted(os.listdir(main_dir)):
    s_wd = f'{main_dir}/{s}'
    if os.path.isfile(f'{s_wd}/dwi/{s}_DWI_native.nii.gz'):
        s_list.append(f'{s_wd}/dwi/{s}_DWI_native.nii.gz')
    elif os.path.isfile(f'{s_wd}/dwi/{s}_DWI_AP_native.nii.gz'):
        s_list.append(f'{s_wd}/dwi/{s}_DWI_AP_native.nii.gz')
        s_list.append(f'{s_wd}/dwi/{s}_DWI_PA_native.nii.gz')

error = []
for f_path in s_list:
    s = os.path.basename(f_path).split(".")[0].split("DWI")[0][-1]
    f_name = os.path.basename(f_path).split(".")[0]
    s_wd = f'{main_dir}/{s}'
    if f_name in df['SubjID'].values: continue

    print(f'{s},{f_name}')

    raw_data = nib.load(f_path)
    data = raw_data.get_fdata()
    affine = raw_data.affine

    bvals, bvecs = read_bvals_bvecs(f'{f_path[:-7]}.bval', f'{f_path[:-7]}.bvec')
    gtab = gradient_table(bvals, bvecs)

    if "_AP_" in f_name: mask_path = f'{s_wd}/dwi/{s}_T1w2diffnat_AP_brain_mask'
    elif "_PA_" in f_name: mask_path = f'{s_wd}/dwi/{s}_T1w2diffnat_PA_brain_ma

```

```

else: mask_path = f'{s_wd}/dwi/{s}_T1w2diffnat_brain_mask.nii.gz'

mask = np.squeeze(nib.load(mask_path).get_fdata())

threshold = (0.6, 1, 0, 0.1, 0, 0.1)
CC_box = np.zeros_like(data[..., 0])

mins, maxs = bounding_box(mask)
mins = np.array(mins)
maxs = np.array(maxs)
diff = (maxs - mins) // 4
bounds_min = mins + diff
bounds_max = maxs - diff

CC_box[bounds_min[0]:bounds_max[0],
       bounds_min[1]:bounds_max[1],
       bounds_min[2]:bounds_max[2]] = 1

mean_signal = np.mean(data[mask > 0], axis=0)
mask_noise = binary_dilation(mask, iterations=10)
mask_noise[..., :mask_noise.shape[-1]//2] = 1
mask_noise = ~mask_noise

noise_std = np.std(data[mask_noise, :])

#bvals
bvals400=mean_signal[np.where(bvals<=400)]/noise_std
bvals800=mean_signal[np.where((bvals>400)&(bvals<=800))]/noise_std
bvals1200=mean_signal[np.where((bvals>800)&(bvals<=1200))]/noise_std
bvals1600=mean_signal[np.where((bvals>1200)&(bvals<=1600))]/noise_std
bvals2000=mean_signal[np.where((bvals>1600)&(bvals<=2000))]/noise_std
bvals2400=mean_signal[np.where((bvals>2000)&(bvals<=2400))]/noise_std
bvals2800=mean_signal[np.where((bvals>2400)&(bvals<=2800))]/noise_std
bvals3200=mean_signal[np.where((bvals>2800)&(bvals<=3200))]/noise_std

s_dict = {'SubjID': f_name,
          'bvals [0,400]': np.mean(bvals400),
          'bvals (400,800)': np.mean(bvals800),
          'bvals (800,1200)': np.mean(bvals1200),
          'bvals (1200,1600)': np.mean(bvals1600),
          'bvals (1600,2000)': np.mean(bvals2000),
          'bvals (2000,2400)': np.mean(bvals2400),
          'bvals (2400,2800)': np.mean(bvals2800),
          'bvals (2800,3200)': np.mean(bvals3200),
          'xdim': raw_data.header.get_zooms()[0],
          'ydim': raw_data.header.get_zooms()[1],
          'zdim': raw_data.header.get_zooms()[2]}

df = df.append(s_dict, ignore_index=True)

df.set_index('SubjID', inplace = True)
df.to_csv(output_file)

```

01_SNRS.csv

SubjID	bvals [1200,1600]	bvals [1600,2000]	bvals [2000,2400]	bvals [2400,2800]	bvals [2800,3200]	bvals [400,800]	bvals [800,1200]	bvals [0,400]	xdim	ydim	zdim
BIOMARCADORES_01_DWI_native							15.420195614328016	51.96732516301598	2.0	2.0	2.0
BIOMARCADORES_02_DWI_native							11.815858564106264	50.90547542017202	2.0	2.0	2.0
BIOMARCADORES_03_DWI_native							16.574770672042423	60.22161236804793	2.0	2.0	2.0
BIOMARCADORES_04_DWI_native							14.912093297874389	49.77668085619136	2.0	2.0	2.0
CTR_HSA_01_DWI_AP_native	6.969034662741811			5.272099832493482			11.494872386714812	37.62907850721266	1.5	1.5	1.5
CTR_HSA_01_DWI_PA_native	6.491886074159544			4.93113703336376			10.637143537992385	34.36156901566207	1.5	1.5	1.5
CTR_HSA_02_DWI_AP_native	6.833276069434743			5.141232467034157			11.74297989772282	44.05207134693453	1.5	1.5	1.5
CTR_HSA_02_DWI_PA_native	7.711107572188735			5.762204511764162			13.151989520710568	48.00390738365197	1.5	1.5	1.5
CTR_HSA_03_DWI_AP_native	6.298098034448074			4.915019815874137			10.11983425832372	32.457009863093106	1.5	1.5	1.5
CTR_HSA_03_DWI_PA_native	6.949635300535198			5.431898271365223			11.138655811942154	35.3481999527511	1.5	1.5	1.5
CTR_HSA_04_DWI_AP_native	7.019493636852315			5.259672961646709			11.89806209723873	44.18168797334005	1.5	1.5	1.5
CTR_HSA_04_DWI_PA_native	7.867969231240818			5.874420290570085			13.376825120733812	48.9350920555768	1.5	1.5	1.5
CTR_HSA_05_DWI_AP_native	6.610130167689274			4.959810994427331			10.906816916346465	36.26847609663918	1.5	1.5	1.5
CTR_HSA_05_DWI_PA_native	6.624785432618995			4.9847611200167785			10.90297664942734	35.95481140021399	1.5	1.5	1.5
EOT_FARA023048_DWI_native					24.16306414160029			62.31428783369943	2.0	2.0	2.0
EOT_FARA025000_DWI_native					25.27538684498613			58.50882378311264	2.0	2.0	2.0
EOT_FARA027048_DWI_native					21.606759613818816			55.25534004612851	2.0	2.0	2.0
EOT_FARA028000_DWI_native					32.56362247818182			95.25158719527803	2.0	2.0	2.0
EOT_FARA029000_DWI_native					22.752341456401066			58.73250114402161	2.0	2.0	2.0
EOT_FARA032000_DWI_native					24.01779980136523			56.58231655063538	2.0	2.0	2.0
EOT_FARA034096_DWI_native					24.060793326228342			61.507669898819096	2.0	2.0	2.0
EOT_FARA036000_DWI_native					23.03131421991909			59.88213282177752	2.0	2.0	2.0
EOT_FARA043048_DWI_native					26.05034654700848			62.0321403317185	2.0	2.0	2.0
EOT_FARA046000_DWI_native					24.1615115202337			59.24486981963304	2.0	2.0	2.0
EOT_FARA048000_DWI_native					24.84066725064396			55.80554606702909	2.0	2.0	2.0
EOT_FARA048024_DWI_native					23.169022292674985			51.72632192044795	2.0	2.0	2.0
EOT_FARA055000_DWI_native					26.43498909378041			67.70715354228989	2.0	2.0	2.0
EOT_FARA057024_DWI_native					29.067961184290954			67.81471593629081	2.0	2.0	2.0
EOT_FARA059000_DWI_native					26.354312426390727			61.35569086338364	2.0	2.0	2.0
EOT_FARA059024_DWI_native					27.353561237641795			65.85982772364518	2.0	2.0	2.0
EOT_FARA060000_DWI_native					28.07341790716251			64.73612836869434	2.0	2.0	2.0
EOT_FARA061000_DWI_native					21.250628486655664			51.67445402243425	2.0	2.0	2.0
EOT_FARA062000_DWI_native					28.237297708912696			68.77401814264981	2.0	2.0	2.0
EOT_FARA065000_DWI_native					25.875453262314583			63.49374768855426	2.0	2.0	2.0
EOT_FARA067000_DWI_native					28.110062093817803			65.04129735035805	2.0	2.0	2.0
EOT_FARA069048_DWI_native					24.22945144395692			57.37358715442253	2.0	2.0	2.0
EOT_FARA074048_DWI_native					24.543171641208183			64.19457507268444	2.0	2.0	2.0
EOT_FARA075000_DWI_native					29.00736535509126			64.80796062500465	2.0	2.0	2.0
EOT_FARA084048_DWI_native					22.37016082191299			61.490875971713656	2.0	2.0	2.0
EOT_FARA085000_DWI_native					26.017537023788083			64.2126990558846	2.0	2.0	2.0
EOT_FARA088048_DWI_native					24.822996793056387			60.42041465915643	2.0	2.0	2.0
EOT_FARA091000_DWI_native					23.37325803005221			57.93244460001328	2.0	2.0	2.0
EOT_FARA092000_DWI_native					21.08782850082861			54.08784679261338	2.0	2.0	2.0
EOT_FARA097096_DWI_native					24.698220550888184			58.59921209871956	2.0	2.0	2.0
EOT_FARA107000_DWI_native					18.588681141353625			51.77662262958047	2.0	2.0	2.0
EOT_FARA115000_DWI_native					5.212718500179788			15.55229455945243	2.0	2.0	2.0
EOT_FARA134000_DWI_native					26.585692365139863			60.44701561285693	2.0	2.0	2.0
EOT_FARA141000_DWI_native					23.60512352074512			57.37880574192582	2.0	2.0	2.0
EOT_FARA144000_DWI_native					29.84531071200441			74.86484466085227	2.0	2.0	2.0
EOT_FARA147000_DWI_native					17.782425275244307			41.32918709328532	2.0	2.0	2.0
EOT_FARA150000_DWI_native					38.09580231310603			87.47977321574125	2.0	2.0	2.0
EOT_FARA151000_DWI_native					23.83305397989873			64.27489308928851	2.0	2.0	2.0
EOT_FAR808408_DWI_native					22.7241988738532			55.6455709396973	2.0	2.0	2.0
EOT_FAR8088048_DWI_native					25.097092558610743			58.66483492686321	2.0	2.0	2.0
EOT_FARB092024_DWI_native					24.10905719779261			63.06616801282452	2.0	2.0	2.0
EOT_FARB097048_DWI_native					38.13596947349086			85.62404423295307	2.0	2.0	2.0
EOT_FARB154000_DWI_native					24.412398548043573			59.50083798808283	2.0	2.0	2.0
EOT_FARC088048_DWI_native					26.262942972413164			64.09231478760883	2.0	2.0	2.0
EOT_FARC148000_DWI_native					38.77797725434673			80.89394874577388	2.0	2.0	2.0
EOT_FARD088000_DWI_native					35.34859818006628			83.04930676219276	2.0	2.0	2.0
EOT_FARE148000_DWI_native					39.27998031091713			86.01469204			

EOT_PRSC031000_DWI_native						24.445567538799544		54.80865345085127	2.0	2.0	2.0
EOT_PRSC033000_DWI_native						26.07409773599277		62.88174946002706	2.0	2.0	2.0
EOT_PRSC034000_DWI_native						22.483279167964167		54.1187289514132	2.0	2.0	2.0
EOT_PRSC035000_DWI_native						24.83778169020201		65.93212757996018	2.0	2.0	2.0
EOT_PRSC039000_DWI_native						25.79705683876555		61.31584220793616	2.0	2.0	2.0
EPILENG_C_0000_DWI_native	13.803703550554031				8.20904472602454			46.025899587159664	1.5	1.5	1.5
EPILENG_C_0001_DWI_native	15.477104560062754				9.11135088745796			55.64998141386248	1.5	1.5	1.5
EPILENG_C_0002_DWI_native	9.335424887304098				5.660633956886147			30.03491277312571	1.5	1.5	1.5
EPILENG_C_0003_DWI_native	10.184727559007596				6.0481642760037735			30.23331428802636	1.5	1.5	1.5
EPILENG_C_0004_DWI_native	14.88435321847253				8.692567941119963			45.8651879542414	1.5	1.5	1.5
EPILENG_C_0005_DWI_native	11.371916107949072				6.994756890870501			45.97867261176096	1.5	1.5	1.5
EPILENG_C_0006_DWI_native	10.234347765113895				6.057349853859779			38.4066066609342	1.5	1.5	1.5
EPILENG_C_0007_DWI_native	9.318302363743456				5.550760596260314			27.98694913010567	1.5	1.5	1.5
EPILENG_C_0008_DWI_native	9.95477930290352				5.988625863785274			33.590231339790094	1.5	1.5	1.5
EPILENG_C_0009_DWI_native	13.039259695095724				7.93162515648094			40.06658636546437	1.5	1.5	1.5
EPILENG_C_0010_DWI_native	9.0886573990222				5.468019068575574			29.92879812226063	1.5	1.5	1.5
EPILENG_C_0011_DWI_native	12.478536380594411				7.33806828328581			41.27946582209336	1.5	1.5	1.5
EPILENG_C_0012_DWI_native	8.04188056415502				4.854151795727477			25.883964003398315	1.5	1.5	1.5
EPILENG_C_0013_DWI_native	8.086008176886336				4.8489914723067065			25.05939460095024	1.5	1.5	1.5
EPILENG_C_0014_DWI_native	14.375028664271278				8.528314963190832			48.5758856632656	1.5	1.5	1.5
EPILENG_C_0015_DWI_native	6.7553535305963175				4.035663312369826			22.52504077738572	1.5	1.5	1.5
EPILENG_C_0016_DWI_native	4.9764947612994375				3.098882178374177			16.525346349582794	1.5	1.5	1.5
EPILENG_C_0017_DWI_native	14.94172636870908				8.513280984189878			46.886987254883294	1.5	1.5	1.5
EPILENG_C_0018_DWI_native	9.04025965673742				5.513589413035636			30.16334898256499	1.5	1.5	1.5
EPILENG_C_0019_DWI_native	7.265853556238358				4.452848588408357			26.032358910134672	1.5	1.5	1.5
EPILENG_C_0021_DWI_native	10.79645538573926				6.420319489099207			32.18544390079053	1.5	1.5	1.5
S14_R209_DWI_AP_native	14.712512774317393				8.592051970014257			57.628326287523294	1.5	1.5	1.5
S14_R209_DWI_PA_native	13.585026933525938				8.265699458970866			55.67545958468448	1.5	1.5	1.5
S15_R106_DWI_AP_native	14.437190038731014				8.727037204827154			67.93147598001924	1.5	1.5	1.5
S15_R106_DWI_PA_native	14.910148699724264				9.041241255198624			69.92223664511991	1.5	1.5	1.5
LABIMATGE_SAUL_15voxsize_FASTnFURIOUS						23.346305686983186	14.794629354941613	48.49888326142496	1.5	1.5	1.5
LABIMATGE_SAUL_20voxsize_FASTnFURIOUS						38.60159952998985	24.653885929489405	78.96967341771328	2.0	2.0	2.0
LABIMATGE_SAUL_15voxsize_MORTALKOMBAT	11.022010731600412	8.607514128073902				23.843353727491422	15.15029671365597	49.308478219397394	1.5	1.5	1.5
LABIMATGE_SAUL_20voxsize_MORTALKOMBAT	18.27518619944205	14.073662516596432				39.73281155459965	25.34911880335853	81.53931539471462	2.0	2.0	2.0
LABIMATGE_SAUL_15voxsize_SHARKNADO		8.708930642155414			6.062472335665055	24.35815697937585	15.372363532514559	50.276484503816	1.5	1.5	1.5
LABIMATGE_SAUL_20voxsize_SHARKNADO		13.722061505081195			9.28496270279235	38.37735401366522	24.552862058552456	78.29088072565969	2.0	2.0	2.0
LABIMATGE_SAUL_15voxsize_DIEHARD		8.652776498904998				23.98392976962147	15.155079422125397	49.543872198804834	1.5	1.5	1.5
LABIMATGE_SAUL_20voxsize_DIEHARD		13.55432665378115				37.98196164590758	24.212449967800374	77.64361612608309	2.0	2.0	2.0
LABIMATGE_MARINA_15voxsize_FASTnFURIOUS						21.862604670497134	14.096445878455341	43.79209743781525	1.5	1.5	1.5
LABIMATGE_MARINA_20voxsize_FASTnFURIOUS						36.32696830194238	23.61272669265659	72.00271917142922	2.0	2.0	2.0
LABIMATGE_MARINA_15voxsize_MORTALKOMBAT	10.087959882706786	7.799854907412628				21.518075376659905	13.814492788257144	42.59814061149045	1.5	1.5	1.5
LABIMATGE_MARINA_20voxsize_MORTALKOMBAT	17.085524489362484	13.0451677873471				36.19983715605259	23.73126578368708	72.21045001247161	2.0	2.0	2.0
LABIMATGE_MARINA_15voxsize_SHARKNADO		7.707943298058974			5.256432613522751	21.19824726996779	13.694987295335697	42.183083028015304	1.5	1.5	1.5
LABIMATGE_MARINA_20voxsize_SHARKNADO		12.881304382157126			8.503112775239188	35.80024903956487	23.361110882884056	70.78667670112299	2.0	2.0	2.0
LABIMATGE_MARINA_15voxsize_DIEHARD		7.9749362456671555				21.93354632449432	14.108979851517464	43.64421766318283	1.5	1.5	1.5
LABIMATGE_MARINA_20voxsize_DIEHARD		13.128492657132288				36.5193967040017	23.774812832623546	72.3014655551367	2.0	2.0	2.0

```

# -*- coding: utf-8 -*-
"""
02_FA
"""

#% Loading packages
import os
import pandas as pd
import numpy as np
import nibabel as nib
from dipy.core.gradients import gradient_table
from dipy.io.gradients import read_bvals_bvecs
from dipy.reconst.dti import TensorModel
import warnings
warnings.simplefilter(action='ignore', category=FutureWarning)

#% Atlas labels

atlas_labels = {1: 'Middle cerebellar ped.'}
atlas_labels[2] = 'Pontine crossing tract'
atlas_labels[3] = 'Genu of CC'
atlas_labels[4] = 'Body of CC'
atlas_labels[5] = 'Splenium of CC'
atlas_labels[6] = 'Fornix'
atlas_labels[7] = 'Corticospinal tract R'
atlas_labels[8] = 'Corticospinal tract L'
atlas_labels[9] = 'Med. lemniscus R'
atlas_labels[10] = 'Med. lemniscus L'
atlas_labels[11] = 'Inf. cerebellar ped. R'
atlas_labels[12] = 'Inf. cerebellar ped. L'
atlas_labels[13] = 'Sup. cerebellar ped. R'
atlas_labels[14] = 'Sup. cerebellar ped. L'
atlas_labels[15] = 'Cerebral ped. R'
atlas_labels[16] = 'Cerebral ped. L'
atlas_labels[17] = 'Ant. limb of int. capsule R'
atlas_labels[18] = 'Ant. limb of int. capsule L'
atlas_labels[19] = 'Posterior limb of int. capsule R'
atlas_labels[20] = 'Posterior limb of int. capsule L'
atlas_labels[21] = 'Retrolenticular part of int. capsule R'
atlas_labels[22] = 'Retrolenticular part of int. capsule L'
atlas_labels[23] = 'Ant. corona radiata R'
atlas_labels[24] = 'Ant. corona radiata L'
atlas_labels[25] = 'Sup. corona radiata R'
atlas_labels[26] = 'Sup. corona radiata L'
atlas_labels[27] = 'Posterior corona radiata R'
atlas_labels[28] = 'Posterior corona radiata L'
atlas_labels[29] = 'Posterior thalamic radiation R'
atlas_labels[30] = 'Posterior thalamic radiation L'
atlas_labels[31] = 'Sag. stratum R'
atlas_labels[32] = 'Sag. stratum L'
atlas_labels[33] = 'Ext. capsule R'
atlas_labels[34] = 'Ext. capsule L'
atlas_labels[35] = 'Cingulate gyrus R'
atlas_labels[36] = 'Cingulate gyrus L'

```

```

atlas_labels[37] = 'Cingulum (hippocampus) R'
atlas_labels[38] = 'Cingulum (hippocampus) L'
atlas_labels[39] = 'Fornix (cres) / Stria terminalis R'
atlas_labels[40] = 'Fornix (cres) / Stria terminalis L'
atlas_labels[41] = 'Sup. longitudinal fasc. R'
atlas_labels[42] = 'Sup. longitudinal fasc. L'
atlas_labels[43] = 'Sup. fronto-occipital fasc. R'
atlas_labels[44] = 'Sup. fronto-occipital fasc. L'
atlas_labels[45] = 'Inf. fronto-occipital fasc. R'
atlas_labels[46] = 'Inf. fronto-occipital fasc. L'
atlas_labels[47] = 'Uncinate fasc. R'
atlas_labels[48] = 'Uncinate fasc. L'
atlas_labels[49] = 'Tapetum R'
atlas_labels[50] = 'Tapetum L'

#%%
main_dir="/home/marina/TFG/DATA"
output_file = '/home/marina/TFG/outputs/02_FAmaps.csv'

try:
    df = pd.read_csv(output_file)
except:
    df = pd.DataFrame(columns = ['SubjID'])

s_list = []
for s in sorted(os.listdir(main_dir)):
    s_wd = f'{main_dir}/{s}'
    if os.path.isfile(f'{s_wd}/dwi/{s}_DWI_corr.nii.gz'):
        s_list.append(f'{s_wd}/dwi/{s}_DWI_corr.nii.gz')

for f_path in s_list:
    s = os.path.basename(f_path).split(".")[0].split("DWI")[0][-1]
    f_name = os.path.basename(f_path).split(".")[0]
    s_wd = f'{main_dir}/{s}'
    s_error=[]
    if s in df['SubjID'].values: continue
    print(f'Adding subject {s}...')

    try:
        raw_data = nib.load(f_path)
        data = raw_data.get_fdata()
        affine = raw_data.affine

        bvals, bvecs = read_bvals_bvecs(f'{f_path[:-7]}.bval', f'{f_path[:-7]}.bvec')
        gtab = gradient_table(bvals, bvecs)
        mask = nib.load(f'{s_wd}/dwi/{s}_MNI2diff_brainmask.nii.gz').get_fdata()
        mask = np.squeeze(mask)

        wm_mask = nib.load(f'{s_wd}/dwi/{s}_T1w2diff_wm_mask.nii.gz').get_fdata()
        wm_mask = np.squeeze(wm_mask)
        gm_mask = nib.load(f'{s_wd}/dwi/{s}_T1w2diff_gm_mask.nii.gz').get_fdata()
        gm_mask = np.squeeze(gm_mask)
        csf_mask = nib.load(f'{s_wd}/dwi/{s}_T1w2diff_csf_mask.nii.gz').get_fdata()
        csf_mask= np.squeeze(csf_mask)
    
```

```

tenmodel = TensorModel(gtab)
tensorfit = tenmodel.fit(data, mask=mask)

fa = tensorfit.fa
fa_wm = fa[fa * wm_mask > 0]
fa_gm = fa[fa * gm_mask > 0]
fa_csf = fa[fa * csf_mask > 0]
fa_m = fa[fa * mask > 0]

s_dict = {'SubjID': s,
          'FA WM': np.mean(fa_wm),
          'FA GM': np.mean(fa_gm),
          'FA CSF': np.mean(fa_csf),
          'FA mask': np.mean(fa_m),
          'std FA WM': np.std(fa_wm),
          'std FA GM': np.std(fa_gm),
          'std FA CSF': np.std(fa_csf),
          'std FA mask': np.std(fa_m)}

atlas_data = nib.load(f'{s_wd}/dwi/{s}_JHU2diff_labels.nii.gz')
atlas_matrix = np.squeeze(atlas_data.get_fdata())

for e in np.unique(atlas_matrix)[np.unique(atlas_matrix) > 0]:
    e_mask = fa[atlas_matrix == e]
    s_dict[f'{atlas_labels[e]} mean'] = np.mean(e_mask)
    s_dict[f'{atlas_labels[e]} std'] = np.std(e_mask)

df = df.append(s_dict, ignore_index=True)
except:
    s_error.append(s)
df.set_index('SubjID', inplace = True)
df.to_csv(output_file)

```

SubjID	Ant. corona radiata L mean	Ant. corona radiata L std	Ant. corona radiata R mean	Ant. corona radiata R std	Ant. corona radiata L int. cap. L mean	Ant. limb of int. cap. L std	Ant. limb of int. cap. R mean	Ant. limb of int. cap. R std	Body of CC mean	Body of CC std	Cerebral ped. L mean
BIOMARCADORES_01	0.414429745218692	0.1185929163149186	0.4012604990840799	0.1068466836849165	0.539496844888964	0.170595475518779	0.5565265737054099	0.1717741949880431	0.552075801207075	0.2294452687221707	0.5691449774676252
BIOMARCADORES_02	0.415635225142412	0.1355326859630862	0.4258199142615245	0.1220585236521055	0.5833689807993871	0.1906746764993771	0.5970397694533454	0.1966409886319247	0.5937703613164947	0.2355561773604071	0.6086822204489215
BIOMARCADORES_03	0.37085581900958	0.09610324490911	0.15789319186057	0.12023793092517405	0.461980820687408	0.1811785056358414	0.18403925160618350	0.5932323303724025	0.222986775563701	0.352654337468882	
BIOMARCADORES_04	0.43120097099397	0.123314670895382	0.437204385053287	0.1188480142353886	0.50486957171671	0.17785156386883	0.5373400921862677	0.1815370403392943	0.5113901511980409	0.235391899255032	0.562695381403854
CTR_HSA_01	0.408130121409417	0.1361366698288244	0.40861003048575874	0.1332393422197238	0.549038645816903	0.175522884102171	0.560743190736428	0.1800669245690403	0.5944976761943568	0.235319899255032	0.520945909029832
CTR_HSA_02	0.3533941923312422	0.132115994121326	0.385018000355114	0.128649650729434	0.347910899475705	0.202032935622482	0.363399187948475	0.2348909057381567	0.5904447785325	0.248481210753915	0.3730267786715078
CTR_HSA_03	0.29424864680789	0.221753847617988	0.38681268545471	0.197057748451555	0.3362862970357153	0.199582544262563	0.48375130479144	0.188602515105265	0.2739344989929867	0.297305647259837	0.363344881319078
CTR_HSA_04	0.23502585862962	0.223327038872087	0.197588433511486	0.192467397880750	0.205806549212847	0.1748963771331516	0.15112846060392	0.15495835826196	0.074583209524	0.0820270110795017	0.1241312591005067
CTR_HSA_05	0.4031968740720373	0.106374916223325	0.417767041421325	0.1121680465396331	0.51568557028266	0.196803002681303	0.521988103495953	0.181903161988432	0.543728642053095	0.263912123685330	0.60343205741471
EOT_FARA023048	0.460284674871929	0.1458160310221289	0.448936527975652	0.1506647499140661	0.5526076706291277	0.17207930798784	0.5189250044471239	0.17472314693891312	0.4835853502711564	0.238576356968245	0.6064179219718301
EOT_FARA025000	0.4744784154341609	0.1504640363711892	0.4630430293922942	0.123518974620882	0.4811164640465313	0.1938996622382940	0.459281075378475	0.19530614441848	0.545972101875874	0.260933781897785	0.182167688325587
EOT_FARA027048	0.489403021238049	0.1288773824968863	0.466914199761655	0.1223335584688282	0.546007559960062	0.196689300442703	0.49407027058212006	0.17155957303170932	0.534667702958473	0.243315131710923	0.588561657140345
EOT_FARA028000	0.4671942271965409	0.1513097438319965	0.52040279979273982	0.148040978650014	0.5699041407086552	0.2193279134084687	0.537464383363277	0.18292891894971	0.57304468888566	0.264265873975897	0.5265986268561333
EOT_FARA029000	0.34717945935567776	0.123598758862116	0.4491086201190200	0.14110743503633	0.495179050713148033	0.17905071131516	0.512839197357035	0.1743830958826196	0.513281937135703	0.2565505051976153	0.65552307090113543
EOT_FARA032000	0.507554647642065	0.132654327270104	0.487410306153055	0.131822747739339	0.5156576944491783	0.15440530033015812	0.51552762695705854	0.156770142170529	0.570589442655816	0.257788288901592	0.5706827743566571
EOT_FARA034096	0.42632616460629	0.129289871568931	0.349095495729891	0.130323294326887	0.5282171687098047	0.198271934166452	0.5006817205275358	0.145274402304946	0.5325905170065339	0.20346186836717177	0.4587470354732359
EOT_FARA036000	0.4651920710493985	0.153664560213094	0.483820130945628	0.136133841549511	0.51496536591815	0.1704717624947205	0.539721825154337	0.181993758011995	0.5777050524928996	0.239031358435980	0.604021568474701
EOT_FARA039048	0.4081102404439045	0.127954704206833	0.4614626842585366	0.1307094972748911	0.5178090654007108	0.1780906504007108	0.4963700453473221	0.187795319261960	0.49830581177798	0.5701130841700061	
EOT_FARA046000	0.50025925989125457	0.148776978807711	0.46212167719596	0.138617897388533	0.5278028071190481	0.20170585035152819	0.52825203178371853	0.188810029888566	0.532455339527569	0.252803178371853	0.154127224583356
EOT_FARA048000	0.438730642018747	0.1301780533833	0.4962703534964	0.1266120305962	0.52093059625602	0.1627230833670254	0.504696956957311	0.151166924604072	0.51451651262004072	0.5066630199624929	0.5837112729419012
EOT_FARA048024	0.43907206851635	0.1243893032299266	0.4468514046872025	0.1197870383706379	0.515678299854962	0.1760556786706714	0.553122413130242	0.153871102334776	0.5708589442655816	0.257881025607144	0.617771150395623
EOT_FARA050000	0.48893240624231049	0.13997298263289	0.503675683163186	0.119883447811482	0.55853405138049	0.1521304720962475	0.5163911881232371	0.171931918449581	0.4847168301781914	0.2425152951200878	0.6054179219718301
EOT_FARA052024	0.50112106611423	0.16291948513182	0.480834463537364	0.1229536384765626	0.49554034345433	0.2130247209624572	0.51871939181171	0.172078077988412	0.4892542663381673	0.2459413116208182	0.562109990709265
EOT_FARA059000	0.4615209710493985	0.153664560213094	0.483820130945628	0.136133841549511	0.51496536591815	0.1704717624947205	0.539721825154337	0.181993758011995	0.5777050524928996	0.239031358435980	0.604021568474701
EOT_FARA059024	0.489403021238049	0.13080023463988	0.4614626842585366	0.1223335584688282	0.504600755996002	0.169905605094714971	0.5169905605094714971	0.17155957303170932	0.534667702958473	0.243315131710923	0.588561657140345
EOT_FARA060000	0.494425232598777	0.141106981497498	0.502774098749884	0.127099999141107	0.55064097130561	0.1764412858169888	0.557987601942902	0.1770987610420902	0.5073644771007151	0.2533901373340781	0.1556464754784568
EOT_FARA061000	0.5271039205933232	0.160936195097357	0.497516114411862	0.1322335584688282	0.502571698899599171	0.17042005712052324	0.516402154240572	0.186402154240572	0.52722687209652	0.2523394173340781	0.1559091158833812
EOT_FARA062000	0.451056337407479	0.160134387481	0.4610141850574	0.127952132635247	0.51465203237207391	0.17780					

Cerebral ped. L std	Cerebral ped. R mean	Cerebral ped. R std	Cingulate gyrus L mean	Cingulate gyrus L std	Cingulate gyrus R mean	Cingulate gyrus R std	Cingulum (hippocampus) L mean	Cingulum (hippocampus) L std	Cingulum (hippocampus) R mean	Cingulum (hippocampus) R std	Corticopial tract L mean	Corticospinal tract std
0.2275672273989206	0.585763128771717	0.22615092197132	0.3784386631378644	0.19874567450545	0.4012205191710468	0.198461432065141	0.357048374362132	0.15346353738531005	0.330404108861161	0.1486625333810033	0.486552246293436	0.174229001161462
0.2374086224704306	0.585520796989049	0.234767637355057	0.44040838972848038	0.210354469862026	0.3896478030877496	0.191991505406278	0.3257755146257154	0.1806509023672764	0.304916852479906	0.22452900388325	0.5222539714084183	0.1822734431361879
0.1963694452042646	0.5435418735560674	0.202295457478333	0.3112853274153785	0.1841065006709609	0.3069782699469084	0.17088301668552	0.36816706975904	0.1593276001437454	0.375178556735703	0.17144561693736	0.5062038217112679	0.191136786928807
0.2061660486204068	0.568993742361247	0.198013342122499	0.41118460951545	0.201285937050288	0.345898243163611	0.194945483769961	0.3233631186992603	0.18158287231656	0.3147867362159589	0.169794347200829	0.4056178897268967	0.148719976858272
0.198488428085617	0.512843175303582	0.203888288609823	0.4480438857778854	0.2150023227981088	0.4047589917796242	0.19184472671327783	0.240022591782283	0.1488742911354689	0.286534072927507	0.1801275293445766	0.3937097632338398	0.1225222224535389
0.134094173003342	0.54864101069962	0.192651927794398	0.39038146158513	0.24003917582530	0.38938048821899	0.21403579386988	0.23703687803239	0.1519605046240312	0.2217069975975556	0.145674283041204691	0.4308656321024691	0.125235081277926
0.1528635911616259	0.4194892153264809	0.179452061017377	0.5931866504022901	0.221298598538256	0.524124896185851	0.2838111469714172	0.328005895744941	0.1546155864345489	0.351874228534969	0.1358603934150233	0.3939842627852	0.1342297451170862
0.183452485362103	0.393809280293961	0.17782552052573	0.3295002322798108	0.3205140547356	0.32889714523675	0.2862887077275812	0.3488805372457507	0.156864049505942	0.1556604049505942	0.1587845804099613	0.1857845804099613	0.1857845804099613
0.18686429269198	0.5027116314649525	0.1954477974502526	0.293908223343997	0.205419040647356	0.338933717380175	0.18153594823878057	0.368050578780057	0.1846888231816867	0.3455778895930367	0.17595848723232	0.422249157809593	0.185042877243606
0.200631872517418	0.5654259927497384	0.2210162348848874	0.3122085440724805	0.16550519305462155	0.421261766778129	0.13655006468314453	0.328982131616347	0.17591123032207074	0.3576823344784091	0.1690585287084489	0.548275733726876	0.183963325347208
0.2079438326526768	0.598067144904262	0.2041720821848009	0.3690755211467122	0.19173987563473	0.463374047602130	0.1743877067801574	0.393144989645987	0.1800084504962484	0.40896736478049	0.146197805221520853	0.1952982115210853	0.1952982115210853
0.20552269153958	0.5367579517003376	0.211557999342947	0.320473520370193	0.1819051131405037	0.3586887234279613	0.1703916101246862	0.317371093412069	0.112332332152861	0.1697748870963875	0.16268861785340975	0.1665825958521925	0.1665825958521925
0.2145543423592755	0.5224625040845688	0.22860022747098	0.327965763168615	0.186082735168512	0.3624607578082113	0.1695291912138046	0.19920705989587	0.1746858712777656	0.149304523533273	0.2112453971369833	0.49337572414812455	0.2112453971369833
0.2156629516155998	0.512895149203936	0.20940860537298961	0.32551605192915998	0.17823106172619397	0.32140322959648	0.17823106172619397	0.3194326980315945	0.1618120726051344	0.394284768049399	0.1900460209141344	0.538007893734948	0.20121206743556
0.19604242693574	0.582592428801000	0.184174432633015	0.4068773317317919	0.2171988427544739	0.4184983885880146	0.191866401821959	0.34937762858359	0.1594528853539449	0.414939880294748	0.1585752791521867	0.5216749215743659	0.166997706418921
0.2272042819153757	0.5297833482432424	0.20926713159390	0.4247833830462112	0.14933594823878053	0.28553299894641711	0.15518465840953901	0.242959696738211	0.1561475753381026	0.2633203325614451	0.153270891604382	0.4721691345396378	0.1822579253163228
0.2117869069670303	0.5082759520072672	0.2054614242981702	0.3926313450462100	0.195177507516704	0.358071807301573	0.153028339204538	0.41411786736178611	0.1655856721111821	0.1655856721111821	0.1655856721111821	0.1918317976690851	0.1918317976690851
0.197615421640925	0.57952972058905	0.2311557999342947	0.320473520370193	0.1660722140309830781	0.32968373652340598	0.16993845069962038	0.4093348345890793	0.1787748870963875	0.170672338402059	0.490510388771901	0.1531971884327442	0.1531971884327442
0.191629951151069	0.558295279553417	0.17823106150673711	0.340703687701872	0.1655205229539197	0.340703687701872	0.14815478112621621	0.35703687701872	0.1545744282892959	0.150322682382959	0.150322682382959	0.1529978162293093	0.1529978162293093
0.205642112488279	0.508264345452311	0.1807693031230918	0.328400678886611	0.1758451832629234	0.368717508229363	0.1748393274393013	0.34760874382618503	0.1629114694841049	0.342871164494841049	0.17767780116632314	0.1694781362639081	0.1694781362639081
0.19604242693574	0.562859151162596	0.180864237025406	0.4071574057162286	0.165505192915998	0.3635007598200113	0.1553302698291113	0.210522974005123423	0.16277780116632314	0.3044915624045623	0.15042303324356119	0.1704230234356119	0.1704230234356119
0.2060610371643103	0.534020511643103	0.1807693016154741	0.40537159614652106	0.16530519301513104	0.3340471717302704	0.1478687171530238	0.343394455769041	0.15116891004376902	0.2633203325614451	0.1532157091720035	0.4532913427005473	0.1822579253163228
0.2198226595075057	0.5070725594265629	0.20390261218162452	0.3065727439857895	0.1728993240631761	0.26950506452173	0.14123530473548184	0.329941494470028914	0.109253442744470062	0.24268874470028914	0.1535507728005259	0.432433101202915	0.183963325347208
0.2049384180533020	0.5174738265204209	0.204688931295317	0.3217215452645813	0.16670722140309871	0.32172154520370193	0.153770191801821	0.27088116449481049	0.153561077228005259	0.177780116632314	0.177780116632314	0.177780116632314	0.177780116632314
0.2170825256514396	0.5616162836010299	0.2214058586335449	0.32946715									

Corticospinal tract R mean	Corticospinal tract R std	Ext. capsule L mean	Ext. capsule L std	Ext. capsule R mean	Ext. capsule R std	FA CSF	FA GM	FA WM	FA mask	Fornix (cres.) / Stria terminalis L mean	Fornix (cres.) / Stria terminalis L std	Fornix (cres.) / Stria terminalis R mean
0.51621561681178	0.1613133403892203	0.396062753768207	0.1654494239686762	0.423750447186084	0.149861051502392	0.1571966538611738	0.163074917958696	0.3719468261022159	0.248872336420217	0.470169433462837	0.1821715285833093	0.4046396623300943
0.5287121128838381	0.194589567085787	0.445089882504743	0.1649495891663818	0.4447436718521962	0.1582158480879305	0.162827332949176	0.1615195774446092	0.3812095384109297	0.2375272349514071	0.42463774778766	0.1908629972990516	0.374813959180152
0.4894203938844102	0.1641837754857787	0.397826533293153	0.147727143939928	0.41285253164031	0.140516101804092	0.175045311474078	0.1777273170982344	0.3722316720291087	0.252918094328090	0.4655309893438807	0.16232069514168005	0.4125194065533039
0.4537711400650841	0.156122267799222	0.413486448974819	0.1385534323910524	0.418446109903831	0.1404335244339808	0.1395956204237397	0.148512521634312	0.3755937557278805	0.2392291715820391	0.474700011565225	0.141509899315352	0.4155145568276938
0.4685370865027814	0.1411777329660614	0.3468724911346977	0.1674594945843229	0.354072467867081	0.1724267501644059	0.1504548109633324	0.13904321023711	0.3556643373598053	0.23628291715820391	0.474700011565225	0.141509899315352	0.4155145568276938
0.4442905424290979	0.154810996020681	0.31819295934149895	0.1651672752545986	0.364259404971701	0.1613909882099866	0.114707970612207	0.137690426752661	0.31498597024692	0.210185153987711	0.34127811820734	0.13675826709870	0.3797368635818797
0.432848596218654	0.1534256089323342	0.329381616448381	0.2265533708548085	0.369432021819673	0.2178775776128315	0.1209550245105138	0.1540424061098957	0.34042041796092751	0.2148046636491098	0.4347172664714468	0.175485206407937	0.3507468768542028
0.40159719485942996	0.153280160539996	0.4291105144510121887	0.38408334178895	0.152079673838299	0.11740799530516985	0.11989530516985	0.1489584728895189	0.2326436851978502	0.17158778457761486	0.14184122423451506	0.3322656510079334	0.408201940348592
0.480195348960623	0.1383479285232683	0.3931984606831877	0.1787656206268322	0.3693265290526151	0.16527064821743	0.103589717184573	0.1351767497974784	0.493232168304717	0.219988358841161	0.495982124061941	0.1378575857521271	0.408817101241956
0.507388696853947	0.1858279250001848	0.4204626361645973	0.1420515107070154	0.1554200622285975	0.17066958832746	0.055395379195988	0.258234576677897	0.554856862645942	0.1566701454323733	0.470738176249585	0.1566701454323733	0.470738176249585
0.42897170549577	0.16991025380600000	0.478412369393932	0.131352460124356	0.428607862497024	0.1613149008809194	0.1823394716674392	0.1823394716674392	0.4793996062667071	0.4599916842680997	0.16244628194754708	0.1479670545474704	0.16244628194754708
0.460801430300063	0.1595881107498457	0.460435732150428	0.1450952130610537	0.4396693072652507	0.157978663219111	0.170213731040349	0.448784476143131	0.2689566727111045	0.2016997515320268	0.4424059280703424	0.2016997515320268	0.4424059280703424
0.509978691496698	0.1596940538627388	0.42865548721756508	0.1876547257061366	0.45324971769838	0.1821491726770333	0.1835721653924867	0.176625489139439	0.4129724930965101	0.21798029739439	0.5257854701226413	0.1890863043680186	0.4432448979827631
0.507789845392161	0.207545969557335	0.153280160539996	0.4291105144510121887	0.38408334178895	0.152079673838299	0.11740799530516985	0.11989530516985	0.1489584728895189	0.2326436851978502	0.1702984937784216	0.480201940348592	0.3322656510079334
0.557825217407826	0.162225493493732	0.4286171253434486	0.1550813351118711	0.424427503112627	0.156730709545978	0.2095154168873612	0.187346693433556	0.4156795191381651	0.2869711830674963	0.5321092237042323	0.16451093327019058	0.46965857468986
0.4483234784561603	0.19804427284043147	0.423384875058877	0.15580222801620342	0.40139885251074051	0.1488569193879988	0.157179051905285	0.1605974689321355	0.24184513331050815	0.503517608943794124	0.1999418096144742	0.36148521069433774	0.408201940348592
0.503333232862246	0.146769745172385	0.46769745172385	0.131352460124356	0.428607862497024	0.1613149008809194	0.1823394716674392	0.1823394716674392	0.4793996062667071	0.4599916842680997	0.16244628194754708	0.1479670545474704	0.16244628194754708
0.503200053359492	0.15497700256471	0.462545138625428	0.1450952130610537	0.4077567330207032	0.1732165245880622	0.1770719056122119	0.170213731040349	0.25370566727111045	0.2689566727111045	0.2016997515320268	0.4424059280703424	0.2016997515320268
0.5993039537285497	0.15945873317892341	0.404926861499894	0.16157544550516985	0.3764239207493765	0.1508669586274247	0.14508669586274247	0.14508669586274247	0.401191906995956	0.4958760992550582	0.13012936549573377	0.4515289769595377	0.1890863043680186
0.482456581151958	0.16226565520321	0.394705816393665	0.147234915853405	0.42865548721756508	0.1518721653924867	0.1835721653924867	0.176625489139439	0.412974930965101	0.20895111221558	0.5257854701226413	0.14953118972351	0.4326943270319058
0.541510259623928	0.191372863040277	0.428955882251205	0.1571710569482895	0.439520552747558	0.1440664912986535	0.21763423637401	0.168322847078491	0.390632081252591	0.27001902448164	0.5270600445991719	0.16667044794955904	0.4607895045130993
0.469382409484487	0.1606279311789234	0.403750861309353	0.152051662340804	0.403750861309353	0.152051662340804	0.152051662340804	0.152051662340804	0.403750861309353	0.152051662340804	0.403750861309353	0.152051662340804	0.403750861309353
0.350955986302301	0.156044238477312	0.381600515598904	0.1617175574511205	0.319338461154598	0.141715178058857	0.190831390588345	0.18704577202104907	0.25179887231589	0.19115485857211117	0.3637805197884485	0.19115485857211117	0.3637805197884485
0.4365605086444992	0.1505052323430795	0.4095674011118388	0.1611834028118318	0.419706395174442	0.151982425383225	0.230004787050658	0.180391610626829	0.4038744844725058	0.251179887231589	0.448373697464883	0.1422717191056197	0.4422717191056197
0.4626045385944594	0.1719139169459426	0.404926861499894	0.1617571905459842	0.3438112339398374								

Fornix (res) / Stria terminalis R std	Fornix mean	Fornix std	Geno of CC mean	Geno of CC std	Inf. cerebellar ped. L mean	Inf. cerebellar ped. L std	Inf. cerebellar ped. R mean	Inf. cerebellar ped. R std	Inf. fronto-occipital fasc. L mean	Inf. fronto-occipital fasc. L std	Inf. fronto-occipital fasc. R mean	Inf. fronto-occipital fasc. R std
0.1711713957272174	0.477478198883514	0.207280652932567	0.588062827159262	0.176604826680886	0.4550715160866648	0.197090500925985	0.4502967850044415	0.1967895303629892	0.314363900279892	0.1424785371482481	0.403203466792635	0.1673405110838345
0.2016443737169246	0.361649227271871	0.223733079456041	0.5214079206186043	0.23520218793012	0.419093701433877	0.2202031335192137	0.4375998506323738	0.2205784271117497	0.086495204287895	0.1586293687045334	0.461098880295561	0.195982540472537
0.1932844348748538	0.3635256526551193	0.14067115756262	0.5808132844645	0.2125091971753538	0.50478951688159	0.2073575221711787	0.45059481495113	0.2013098378263135	0.17724324328035	0.167483767012169	0.548749025607804	0.1490830396197091
0.1467332661526976	0.49678781037380	0.20799613195458	0.5049301806361891	0.22126035430071	0.457531231685088	0.21474528438538783	0.4582816066736399	0.2214489540077142	0.1486495204273207	0.1799412500415218	0.478245899895218	0.1560243856088281
0.16612193499794538	0.4534703945347576	0.218747654201508	0.4697006217774503	0.256644596881733	0.4486853237367409	0.20267203493699	0.4549881624723207	0.1799412500415218	0.22492669604894	0.25463598585365437	0.1140878151183338	0.1497626369740841
0.160027988625147	0.187027788572482	0.1914270035971592	0.416057305082735	0.25738285636699	0.296423537059862	0.196548347618098	0.331384733387452	0.1950272761922157	0.1420586249892498	0.175760174547678	0.4641757792389461	0.1498055409490683
0.1997320611453871	0.188643736158304	0.188991548921859	0.0993799738380742	0.1425933941300928	0.3954829328493092	0.236456828773435	0.440979861169801	0.22492669604894	0.1700278847877897	0.4728248943016038	0.1507633020115193	0.1584470274096224
0.15080824568239352	0.3224047958724893	0.273343350581406	0.273343350581406	0.273343350581406	0.3792295768220259	0.2037428171251846	0.47823577109645	0.1772998779970121	0.1507633020115193	0.1507633020115193	0.1507633020115193	0.1507633020115193
0.1634034559313753	0.53547410438753224	0.235417632189168	0.528602694694808	0.235320218002867	0.450829323159015	0.185041606919195	0.41853256806989587	0.19550373800520506	0.040078545720267	0.209863880749969	0.4815330934116633	0.1319632741063453
0.1712610390020713	0.443997860014095	0.2281045335470564	0.5232950211581731	0.251897114879390	0.2505243718833147	0.234401886565611	0.5161496671806688	0.2578822247195574	0.575884915554928	0.192753876707827	0.50340532257391	0.1657041590793787
0.1563211463913139	0.4753935202631281	0.208016027490296	0.287330597008006	0.213417091753538	0.500929389911447	0.2334767280129424	0.4866930702825904	0.1773177865258681	0.45093156122309	0.1478715224275771	0.1540542294771	0.137875289231354
0.1752001052608872	0.53437472534913	0.25364404455938	0.61801496179487	0.252633421428391	0.2558961152994653	0.1930499044850949	0.35112053302015302	0.2457009776632020	0.15120583302015302	0.15120583302015302	0.15120583302015302	0.15120583302015302
0.21002483799335	0.359582423158084	0.1915452281150285	0.597786786675794	0.247299368047726	0.49424451657261884	0.23563599152994653	0.5176173379402352	0.172211649894274745	0.458299482299524	0.2358775774250715	0.1577602579236541	0.15397440058612733
0.1695409798472149	0.384094118777597	0.1391418039816495	0.1549808834492423	0.236953876635355	0.47392295768220259	0.1772998779970121	0.4782458924930165	0.150727276192215	0.150727276192215	0.150727276192215	0.150727276192215	0.150727276192215
0.1753271760675438	0.5185560634070586	0.2013610839816495	0.586218820571749	0.205062408697086	0.532163527170604	0.257590061368311	0.504503730265782	0.24320579770825	0.157176186321547	0.141770028737998	0.477789330454023	0.1390835970816427
0.191965598507867	0.47761194538354	0.1867793193125814	0.5286255989857983	0.25939817948911055	0.4537278597389035	0.239388604061787	0.4826367558484804	0.2212453003101751	0.40813325640420404	0.2458638044726023	0.429042610805448	0.1380674742602235
0.18867160242256255	0.38267621237747	0.20649492378523	0.5813786238657983	0.258459815198158	0.4528459815198158	0.2079936015612230	0.4866930702825904	0.1509315612230	0.1509315612230	0.1509315612230	0.1509315612230	0.1509315612230
0.155711492247272	0.483750412524933	0.164433864423826	0.567061447661306	0.2475017763441176	0.507717663202019	0.2174134153187854	0.51270717653349	0.244213074465558	0.1512053302015302	0.1512053302015302	0.1512053302015302	0.1512053302015302
0.143580526493597124	0.45890026493597124	0.167042037416916	0.5075943294438282	0.2436943183510458	0.45218019718104804	0.236953876635355	0.4739224217012796	0.15765746719763617	0.15765746719763617	0.15765746719763617	0.15765746719763617	0.15765746719763617
0.1336195392979341	0.41859519679169308	0.2303993940208506	0.518174267065174	0.2303993940208506	0.45218019718104804	0.2211649894274414	0.4365223572144167	0.18375293715965807	0.4176662529742997	0.1532662877976078	0.1513695387147486	0.1513695387147486
0.1604965665675409	0.46454895648610171	0.2381535027909319	0.5923795709691414	0.2381535027909319	0.45218019718104804	0.202399480163674	0.477899330454023	0.2116927645081692	0.44978748157294	0.1657904849613707	0.4442053302015302	0.159557364351302
0.1569472342276424	0.2965472342276424	0.167042037416916	0.50733907003036	0.213417091753538	0.45218019718104804	0.2078642105616979	0.44573776405211743	0.1772998779970121	0.150727276192215	0.150727276192215	0.150727276192215	0.150727276192215
0.16780442213937	0.4770618870406488	0.2187960336204081	0.5055200634024081	0.2384861794850542	0.4519792321874474	0.2079932321874474	0.4342288559298197	0.1772998779970121	0.150727276192215	0.150727276192215	0.150727276192215	0.150727276192215
0.1554441493940136	0.3910565624384741	0.211773931568684	0.609785428373001	0.230248618885337	0.4588115205403012	0.217452535749982	0.393526754998266205	0.191944516617831	0.1509315612230	0.1509315612230	0.1509315612230	0.1509315612230
0.1676910361693699	0.4445009186310166	0.217109027416916	0.506									

Med. lemniscus L mean	Med. lemniscus L std	Med. lemniscus R mean	Med. lemniscus R std	Middle cerebellar ped. mean	Middle cerebellar ped. std	Pontine crossing tract mean	Pontine crossing tract std	Pontine crossing radiata L mean	Pontine crossing radiata L std	Posterior corona radiata L mean	Posterior corona radiata L std	Posterior corona radiata R mean	Posterior corona radiata R std
0.53433964191052	0.162708267092102	0.559447500293547	0.158430053346454	0.4548981288245107	0.2028263401689684	0.4805780855840935	0.1312998622906505	0.118548375015942	0.381106430981518	0.1125771150264114			
0.5700373516227653	0.1966575354660251	0.5246480307264406	0.186693508347051	0.44074844835999306	0.232707472603436	0.4758951063414007	0.1515150613940297	0.453041461791088	0.1383907337610817	0.4521367992172047	0.1206293589293435		
0.448696982834709	0.1851216097957232	0.482769474255244	0.1870387363530389	0.454260390110291	0.2048714321397782	0.5071845639561126	0.1474334354167497	0.4137858654575648	0.125385434315693	0.4554710628628663	0.1563801792643402		
0.5806721509630346	0.16223437090131	0.585019539643304	0.161813267503223	0.4301661213795335	0.1945425693525833	0.47861647316202446	0.14015277119348788	0.421713196107653	0.1151096785311128	0.4288981507446017	0.113452937368442		
0.5547916653984252	0.1495751728512133	0.5476902118252149	0.1441478324572054	0.4705955315618981	0.176747280589565	0.3925258592238891	0.1191940051438257	0.4613643590893693	0.13588971559880194	0.4924751117245307	0.0972084655662641		
0.3581657088751733	0.2335715812545943	0.497851475075073	0.214287620161452	0.36265784993099389	0.190408253611329	0.464623740769792	0.1537792416565352	0.45498899856493049	0.148734806707658	0.4816202030843053	0.145587678070475		
0.344897117855987	0.1907132011303112	0.5353720174735109	0.1883848631748736	0.4215288262727856	0.1761721701553437	0.4272084907831671	0.14260882345105067	0.43747847452149232	0.127213221673772	0.4584372279131762	0.2269618458727212		
0.3833203520576785	0.18440593392944	0.434485081628587	0.195026723530223	0.4865298637716023	0.1898872091099468	0.382785723567496943	0.12962723567496943	0.2248909434366450	0.1201532994446505	0.18320204463382	0.1201532994446505		
0.4906378751979	0.1564005853718	0.4827422750647273	0.1741485374222172	0.5434058641014	0.213442052909236	0.35639718178376855	0.1337711441875913	0.4684100380381383	0.1306481180404155	0.5163037120011916	0.1157575353806582		
0.565471035716198	0.260832175632079	0.587932290504758	0.2860576295919357	0.44235562820594	0.2587842200797414	0.4819050514981853	0.137585517005235	0.4538300256526029	0.140460419985681	0.4589176757519174	0.149359940455104		
0.5932886984202793	0.1851216097957232	0.482769474255244	0.186950059127929	0.495826391291353	0.19894503725968482	0.3956612596833498	0.14711618994514718	0.432154445643769	0.1339834192959024	0.454215895516162	0.1165259254435424		
0.6059223336481825	0.222920032532987	0.5152682219135293	0.1753794048120405	0.4465637390144875	0.24084762527921092	0.4749847868516186	0.131249932823178	0.5080882605131196	0.130923167968553	0.4991036002303328	0.1433703033018678		
0.479748684808147	0.2747517477612137	0.4938307466540028	0.2829764359658862	0.4566332198795359	0.2916678409605388	0.42832804144973	0.156102901844448	0.485357453046633	0.1535637598153821	0.1565518605171803	0.133638164067211		
0.4722734361995601	0.218161078672027	0.4765300705953388	0.22351945100199041	0.48575091662245057	0.24775091662245057	0.518186184335652	0.18186184335652	0.4412693374203749	0.1208433320392173	0.407795739245208	0.127643612542561		
0.55172501935981	0.184897902032535	0.517764610720246	0.212286353634601	0.44374760896995162	0.21720912320469	0.3295770265632433	0.1426577864048669	0.4637125295804428	0.1052749362891984	0.5085680409152615	0.0992919136628183		
0.5472151351545883	0.231457426968978	0.5182142036603671	0.210970627506472645	0.413755070574683	0.2172544093869935	0.4336916931980933	0.13080144726287683	0.45374223563009774	0.140367988734131	0.44458174742025271	0.12023289882778		
0.5001870647761533	0.2776424786821562	0.476786395311447	0.2245483962369004	0.440523771803013	0.2140984544642877	0.474949478117881263	0.168177168781263	0.4040876268011009	0.1394699562397287	0.50808776783316453	0.130269731335867		
0.538134393841806	0.219393787895208	0.53844051281935	0.26992065835127	0.463023993905313	0.1989130110032827	0.4754297869031357	0.1344861957502077	0.41512352552866693	0.1361024223634984	0.4332950888545949	0.1232757811054938		
0.5164984475093037	0.1946311451769862	0.5073751761748962	0.222920032520223	0.4808704041000201	0.2308747202482452	0.49307430268362452	0.14989639115754764	0.44204793048549694	0.14026593048549694	0.1348410227111434	0.12042800720033059		
0.578787438721428	0.1321627491873454	0.5080505301217103	0.137165151374244	0.482579141840945	0.2108032393511052	0.45186069440512248	0.109309480717922	0.446946370414459	0.132415174757501	0.460226298718449	0.1262998653996		
0.55172501935981	0.184897902032535	0.517764610720246	0.212286353634601	0.44374760896995162	0.21720912320469	0.3295770265632433	0.1426577864048669	0.4637125295804428	0.1052749362891984	0.5085680409152615	0.0992919136628183		
0.5425882152817167	0.180023336491544	0.50781948519094292	0.186950059127929	0.495826391291353	0.19894503725968482	0.3956612596833498	0.14711618994514718	0.432154445643769	0.1339834192959024	0.454215895516162	0.1165259254435424		
0.5001870647761533	0.2776424786821562	0.476786395311447	0.2245483962369004	0.440523771803013	0.2140984544642877	0.474949478117881263	0.168177168781263	0.4040876268011009	0.1394699562397287	0.50808776783316453	0.130269731335867		
0.56059288721617167	0.1916265532103792	0.5080240214750631	0.1787340906745884	0.442654034014821	0.16808639212184	0.3975221916288752	0.152262567550900	0.454403634537968	0.146729929093238	0.5086884792180539	0.134529234118041711		
0.545325303388167	0.222920032532987	0.5152682219135293	0.1753794048120405	0.4465637390144875	0.212280726520932	0.474844798117881263	0.168177168781263	0.4040876268011009	0.1394699562397287	0.50808776783316453	0.130269731335867		
0.5113638865071144	0.1861892396409399	0.5019166488136177	0.16816134282578374	0.4466283634488644	0.20347325723071675	0.4718678409605388	0.1499130110032827	0.43448616957502077	0.				

Posterior limb of int. capsule L mean	Posterior limb of int. capsule L std	Posterior limb of int. capsule R mean	Posterior limb of int. capsule R std	Posterior thalamic radiation L mean	Posterior thalamic radiation L std	Posterior thalamic radiation R mean	Posterior thalamic radiation R std	Retrobulbar part of int. capsule L mean
0.63537739645458	0.133191730512341	0.6096520902596023	0.123315200978531	0.523425851070628	0.1358636908323258	0.503108052847498	0.1472693289970627	0.5419496908045994
0.6166114742707315	0.151935539277938	0.5952173504999737	0.164414728965328	0.5500370321679395	0.1512682708169945	0.54515399090840701	0.1525446113378478	0.585976880902677
0.5502221711505077	0.135657481892232	0.545490228908607	0.1321698043618633	0.567815691041617	0.1439515249862283	0.5374327524808048	0.1456158721962735	0.5542059429404139
0.5720665263631228	0.1332862716731155	0.572267333645403	0.1300110514494889	0.549188437386467	0.1441921574057533	0.5115130601295963	0.1516197501421465	0.5646223167837635
0.5926690591466268	0.149745998256354	0.5795394967199731	0.1532661898363437	0.5628665315427155	0.1750748262371975	0.551689229364085	0.188104799539734	0.5922635804263565
0.516167254922463	0.177947357840759	0.5171490700572138	0.1811390598206124	0.456455484941435	0.1692234079062241	0.5423115251229669	0.1446179962656593	0.5551745482682485
0.439142663872706	0.190935959934349	0.3769911634154811	0.1864890846131746	0.5515779673757527	0.13516568393511687	0.6020754546877585	0.136757199123759	0.588805095726445
0.527987772738204	0.182249399610284	0.39259894571530	0.1660435063307119	0.1188837694886224	0.391106453874681	0.0867186684882021	0.0922213531268813	0.4381373361582707
0.60018280409836	0.155103020873103	0.5675359398097268	0.174776547213239	0.6354057390352018	0.1277517043790066	0.5326595396236719	0.1632770967465163	0.5424307370791664
0.647542220897714	0.1338136422709044	0.604489282633607	0.1289026714741732	0.563377589410209	0.1659459841632381	0.54848172918362663	0.183755639505221	0.5878963309115522
0.61041369951060882	0.140578577263366	0.5834383869877732	0.1559046985408485	0.5749290591045888	0.129268681607742	0.5943868155301211	0.1476678612189214	0.6153846044748137
0.60031893835564	0.1343899578884117	0.512441433995883	0.1216660752383192	0.6077653806196894	0.1520675348539998	0.621578191116951	0.1595961051773498	0.628822707100539
0.613049272663676	0.1598593905492422	0.5788268699658812	0.170326894833535	0.613871111123246	0.1409697383597819	0.6059764575240452	0.1831138925096243	0.6198415792333766
0.56851830052506	0.1294689872221202	0.555572568703577	0.143607389967919	0.60208934493944	0.174377605262024	0.591087173927992	0.164737058400457	0.605912991245882
0.567999780498966	0.121243159719483	0.56770009140583	0.1263461356951912	0.5740648632348967	0.1519917773948974	0.6014104729476587	0.149043790538863	0.5734571006094286
0.6081016136787081	0.1563232424131918	0.5870881163202265	0.1230743698138701	0.5632153209030312	0.1455323116456506	0.5386849557862181	0.1615938132887292	0.56174599633297
0.6135310217797098	0.13864492012229	0.6001195849998439	0.1478253659972	0.563862911552891	0.1428629674010754	0.618602837393754	0.163190405172545	0.6153846044748137
0.588315083701442	0.138534507698109	0.5113935538159	0.1377633229919669	0.544495164382435	0.1409610773526874	0.5504576628031665	0.1511287338402421	0.546387147859248
0.62130079346672734	0.142521103350251	0.5364332217671601	0.146604752058456	0.578222752548481	0.1620211033502517	0.5723887178616767	0.172549276774341	0.5104502207979567
0.6012571925473045	0.1407406154113288	0.535660964153228	0.144476911473919	0.5050982750367588	0.1522554218299659	0.5073489377966363	0.1450528735493987	0.5220111212710753
0.6318877732119612	0.133857389534087	0.6150947033318276	0.1357798464909543	0.53951773841015	0.1447863045940321	0.5564347403585848	0.1531466716302947	0.5699891370400939
0.5529177887281801	0.144978728172956	0.51860122093265018	0.1580186140151533	0.61439824848665	0.1276240220608082	0.53944014458874	0.1601772486915889	0.6017734887248691
0.559799852057263	0.1541441651580325	0.5345835454520445	0.13858546329750536	0.609008675139726	0.156557308633369	0.6244594511671581	0.167769970410783	0.5774471478259767
0.5865192190544437	0.1359494669168683	0.561253999219847	0.1498528522402184	0.5647370144248052	0.17429710221019	0.5608231437513628	0.1670848179719787	0.581337151178397
0.611754876191934	0.127372331464175	0.625490525605647	0.1459590304919087	0.57872227352481	0.1604417740521497	0.5853120001273375	0.172205438767628	0.581661794009301
0.68412548320387698	0.12591081094744	0.6681399320887334	0.122677888707615	0.61214261747309303	0.15711620001273375	0.5740404994042414	0.172205438767628	0.581661794009301
0.56039267269693	0.168872221202	0.592339183916984	0.1447370584721885	0.5091087173927992	0.163776052755505	0.5703489377966363	0.1839700923433199	0.565701672785156
0.567999780498966	0.121243159719483	0.56770009140583	0.1263461356951912	0.5740648632348967	0.1519917773948974	0.6014104729476587	0.149043790538863	0.5734571006094286
0.6081016136787081	0.1563232424131918	0.5870881163202265	0.1230743698138701	0.5632153209030312	0.1455323116456506	0.5386849557862181	0.1615938132887292	0.56174599633297
0.559799852057263	0.1541441651580325	0.5345835454520445	0.13858546329750536	0.609008675139726	0.156557308633369	0.6244594511671581	0.167769970410783	0.5774471478259767
0.5865192190544437	0.1359494669168683	0.561253999219847	0.1498528522402184	0.5647370144248052	0.17429710221019	0.5608231437513628	0.1670848179719787	0.581337151178397
0.611754876191934	0.127372331464175	0.625490525605647	0.1459590304919087	0.57872227352481	0.1604417740521497	0.5853120001273375	0.172205438767628	0.581661794009301
0.68412548320387698	0.12591081094744	0.6681399320887334	0.122677888707615	0.61214261747309303	0.15711620001273375	0.5740404994042414	0.172205438767628	0.581661794009301
0.56039267269693	0.168872221202	0.592339183916984	0.1447370584721885	0.5091087173927992	0.163776052755505	0.5703489377966363	0.1839700923433199	0.565701672785156
0.567999780498966	0.121243159719483	0.56770009140583	0.1263461356951912	0.5740648632348967	0.1519917773948974	0.6014104729476587	0.149043790538863	0.5734571006094286
0.6081016136787081	0.1563232424131918	0.5870881163202265	0.12307436					

Retrobulbar part of int. capsule L std	Retrobulbar part of int. capsule R mean	Retrobulbar part of int. capsule R std	Sag. stratum L mean	Sag. stratum L std	Sag. stratum R mean	Sag. stratum R std	Splenium of CC mean	Splenium of CC std	Sup. cerebellar ped. L mean	Sup. cerebellar ped. L std	Sup. cerebellar ped. R mean	Sup. cerebellar ped. R std
0.1160095077218898	0.5178182588424723	0.0939507809810743	0.5131788551652693	0.14628446961487	0.4649723201987718	0.1223696181982227	0.6343078637149414	0.2121791285265817	0.4816088776091177	0.23385498354406	0.4581808021120194	0.25665080745123
0.1495216184676841	0.5698163430213273	0.140895180816182	0.5086246350673811	0.12760734207458	0.462316183783522	0.177495297315744	0.5981891448917962	0.2602917958586062	0.5402306154185526	0.2830095531199185	0.5637640366487923	0.2608562101624461
0.126720273730368	0.519061701508234	0.121079208487388	0.5032450934399668	0.145626938302008	0.4685387095090413	0.1584675255814847	0.6154240281115926	0.239259032418719	0.5131239719990003	0.24916784784733	0.555497718192618	0.2729614670750395
0.10570833701488	0.5143733220970471	0.1051495183287935	0.4983924819430839	0.160330248133035	0.4475630949569227	0.17353509363560403	0.421155359534453	0.23889282857969	0.541160444366551	0.25566736501498867	0.250287887133245	
0.1042286298947612	0.5604437333458185	0.0891084039954589	0.4708619789475353	0.16093095253745275	0.4829099136130056	0.381082398394557	0.421155359534453	0.23929382857969	0.541160444366551	0.2646907597320573	0.5925660909153949	0.2522946513440334
0.1393375317652042	0.5911659198652052	0.116431204430666	0.493415266607244	0.194401014614548	0.45751618658202774	0.128152657166027	0.50738701491296	0.219522768281986	0.6162844394391234	0.279161056593177	0.493730724207909	0.2663051150035255
0.1132337623269251	0.493415266607244	0.194401014614548	0.45751618658202774	0.128152657166027	0.50738701491296	0.219522768281986	0.6162844394391234	0.279161056593177	0.493730724207909	0.2663051150035255	0.471904374287383	0.2733131050481241
0.228937762191212	0.4393584721921421	0.32779935831487	0.303740159394962	0.19389717982911591	0.33886203283844	0.218429742107491	0.508380363959157	0.5087615402517298	0.23530026459809	0.505532963269975	0.2543843028251556	
0.1493246674725705	0.57579078688002	0.1286842404185	0.555197942333375	0.158831833604128	0.555121240266035	0.142105200104682	0.6242570809742804	0.243008996708974	0.658464733248062	0.197204866832379	0.565117458836135	0.250506574203083
0.1127253679618261	0.5498868839643728	0.1071368152348501	0.576131323704565	0.1387481663024548	0.519190134451753	0.136444248265325	0.254594842214488	0.5256884510183484	0.242345482626162	0.5039647466565277	0.2399128986148938	
0.10063646779572	0.5079934950571624	0.1048105621762936	0.5425586395788668	0.178419781964194	0.5649950862879598	0.15392448369750431	0.490744488444907	0.23309778886837	0.45699927887883	0.210401333972467		
0.128175413661828204	0.6149081291003361	0.1507057505165973	0.587414321136021	0.160851619986768	0.5633912779964102	0.15988229840079	0.616384283940693	0.22139719726883	0.4716402496072096	0.215586756265382	0.4690439320120401	0.219338366536728
0.154375302898277	0.6355608213219419	0.11437338261078	0.5847310113467158	0.156738133961919	0.5814454958462465	0.1495785612731394	0.650565273368555	0.2518468001782771	0.4466376230859175	0.2412370881337101	0.4531109876304399	0.253719897329942
0.101767281201034	0.607161735523756	0.097293409469617	0.53311506012872783	0.1793501752951	0.5454002505492942	0.173840700544929	0.65807762946592	0.2564817609153939	0.2521112089165972	0.2326305296359897	0.4527112089165832	
0.097912915104182	0.604159320372758	0.118544370503819	0.59892868824973	0.139166723664569	0.584666651825281	0.1702021139888	0.746292322202951	0.1855073398770937	0.5147997049132166	0.233867548940913	0.503177643533073	0.2467826377612764
0.1172254947837034	0.574795541841506	0.1068353371386985	0.4805940656671791	0.197673195016822	0.488824285954540	0.168692164300982	0.60220964649843	0.230976518495813	0.406143988134291	0.2094072178874792	0.4208691308446609	0.22165045737821213
0.1023487708754326	0.626550210508588	0.112802045058858	0.514693072318502	0.177182948755447	0.541781984459078	0.164416062685685	0.215925535101105	0.490744488444907	0.23309778886837	0.45699927887883	0.210401333972467	
0.158986883476867	0.541977689172361	0.1091981291003361	0.1507057505165973	0.160851619986768	0.5633912779964102	0.15988229840079	0.616384283940693	0.22139719726883	0.4716402496072096	0.215586756265382	0.4690439320120401	0.219338366536728
0.161289720261516	0.5563135483502323	0.1144285919874501	0.490978954190852	0.167340388071943	0.5489233717236371	0.157987760774019	0.5685575877877339	0.26177339897169193	0.43988244633098	0.2363689231372245	0.52676773831691823	
0.1510826306704989	0.546420359320585	0.109092484006674	0.11437338261078	0.162805210508588	0.53311506012872783	0.132227219917853	0.53539244444308793	0.218657502004961	0.233659028024381	0.443726214466665	0.203996505786153	0.4408535719946876
0.124268728760731	0.6014306651421127	0.1020221165217509	0.555130349136602	0.15835303348929919	0.5607303920916751	0.1224779303305438	0.6936152071874582	0.2122892659379531	0.501930733647456	0.19797671708899	0.4831798627477952	0.197327172304245
0.1091945216154344	0.625345216154344	0.1091945216154344	0.605973004295831	0.17874814630083	0.561953697265931	0.1673404428265325	0.60220964649843	0.230976518793245	0.406143988134291	0.2086345216154344	0.4465056973972455	0.2247544350588316
0.1223467643534526	0.548615179439361	0.1165821242303103	0.457448875854486	0.1754893295389803	0.547708246248323	0.147875134326376	0.5912907226537425	0.2558339930313174	0.3159428765571544	0.2824345744544499	0.3434803730939725	0.1765139457744702
0.1545220036550098	0.5968136975571638	0.110047383778809	0.515240323136607	0.17930937419176	0.51309059901361766	0.1462661343925099	0.5899570151756261	0.273048251342551	0.491044276519455	0.2019587917945894	0.380239402020996	0.2242037900349403
0.1498175735473296	0.5614081735473296	0.109178640906594	0.515273093116302	0.17715665971697895	0.5484947774495204	0.1670132811170497	0.5618304973834981	0.2666240275352093	0.402888339744907	0.2236705135407012	0.397705137700419	0.21980

Sup. corona radiata L mean	Sup. corona radiata L std	Sup. corona radiata R mean	Sup. corona radiata R std	Sup. fronto-occipital fasc. L mean	Sup. fronto-occipital fasc. L std	Sup. fronto-occipital fasc. R mean	Sup. fronto-occipital fasc. R std	Sup. longitudinal fasc. L mean	Sup. longitudinal fasc. L std	Sup. longitudinal fasc. R mean	Sup. longitudinal fasc. R std
0.40444224667002	0.11911465630368611	0.3998671774713338	0.1095838227624745	0.474491040463562	0.1375500214269511	0.5291302766873812	0.1293618963946501	0.460826719856694	0.1342639915512903	0.4571715659663232	0.125782253801541
0.474601861361686	0.133320747650323	0.498648561257565	0.1298596043477307	0.4193270048281162	0.1119000848621121	0.4714787327805195	0.1264986443863301	0.47986499392892626	0.1300495108962691	0.5128755978774554	0.1515249542919379
0.409862770821735	0.1059989014272929	0.4093624639071209	0.0992844954125194	0.3765625791614453	0.1349243169094872	0.430556403565467	0.148373010790895	0.4470323899001904	0.15245188226155	0.4519119297916898	0.137387775578354
0.43679717985242	0.10579985532413	0.45064520252341212	0.1099819057547871	0.41339989357497193	0.12823689518952843	0.4992330591442857	0.1328184664718749	0.46121516764256	0.1393269922499588	0.4666779843980407	0.1399789407010444
0.519398569232697	0.1234820105641962	0.4952100857897266	0.1242559644123722	0.44065778015265	0.1246562239120297	0.471425584697579	0.1200781736256788	0.5163606480764887	0.1484535895479326	0.5167472336783898	0.161717310009998
0.5170065272021755	0.104087488736945	0.477439456713255	0.132541334221638	0.329656157542455	0.1203034251411474	0.283567920455641	0.12102193057997453	0.465931973995253	0.1620474153196438	0.4946654753564337	0.1556495936491492
0.459451958681404	0.157835016358789	0.4920602662845811	0.191153067499866	0.213323645845972	0.1549698660611404	0.297963686058067	0.1558946095767688	0.51511431371235187	0.143041150920462	0.580159026963418	0.140259531172558
0.3365064885393469	0.287739889475886	0.21101875040070473	0.2609276756389	0.110059183877018	0.058484627032372	0.0351904695305657	0.16032466562902	0.1659874567955549	0.16032466562902	0.188388894068782	0.188388894068782
0.50708234922777	0.1196780572347023	0.4953832277446764	0.117536068503851	0.395018762652039	0.175236360121311	0.4076986542551613	0.1499484480195332	0.485820535854857	0.161585217445358	0.552282237651752	0.1620714916882922
0.4865588008729538	0.1155321348972813	0.440556299587244	0.1143879560201233	0.429481094173627	0.128288299806678	0.1443852113390984	0.1120234269813951	0.151773988266939	0.1506693051300882	0.499887548103030	0.124326596684977
0.510140847467670058	0.106177798366060	0.4870039410525944	0.111925542169297	0.4463863670190165	0.150598172617372	0.404121750258866	0.0920536981670913	0.4566891450245401	0.15245188226155	0.4519119297916898	0.13738775578354
0.51911088379173	0.12660517474044768	0.467661340329061	0.11344173737213149	0.3683928101197189	0.14068491931634521	0.3655640357152407	0.1349331970771845	0.493375232526664	0.162971646683059	0.4883369736593674	0.1323032045176168
0.4994351322164686	0.121991688004761	0.443280011321938	0.1433853753037344	0.408660179010054	0.1645944666530854	0.3813638696379181	0.1565001763386651	0.5240936311412507	0.150204038559943	0.167044396665136	0.1556495936491492
0.344653309578141	0.1073245165662989	0.42762805197812	0.107628716563849	0.38037984215596	0.1143259823532171	0.3304584276781276	0.1033700859902	0.460065488572123	0.1351150487415331	0.1258986373258368	0.188388894068782
0.459416653504154	0.09983314037005	0.4519209114686810	0.1009384646865698	0.417802494653925	0.1466644783213514	0.20465574021620620	0.1318964255827691	0.4874594982151351	0.12419511533184	0.151900712761192	0.151900712761192
0.5081022962808264	0.12463278155847	0.4117154043384687	0.10111214245206243	0.478965105219834	0.12228025115271848	0.1753302115326735	0.1472902115326735	0.1502087301901855	0.1492071345681172	0.151900712761192	0.151900712761192
0.456638459422909	0.1155321348972813	0.403314836195995	0.121311001519425	0.419482634524654	0.1463665159185974	0.389288299522290	0.130335642842621	0.4667351120815423	0.1312051520071752	0.1337279521163048	0.1337279521163048
0.460081703509527	0.110394818363030	0.4305640648647168	0.1134170652041471	0.3880928175262562	0.1401162064666077	0.368395348752919	0.1305821503205284	0.4751096481801189	0.14525570971700371	0.14525570971700371	0.14525570971700371
0.47940456379096	0.133678409554040	0.4245035319364236	0.1097009574972549	0.39079872752749	0.117645249147835	0.4157569794020558	0.1349331970771845	0.4667352471636892	0.14026288925311	0.14026288925311	0.14026288925311
0.4486795303277719	0.1021342160556696	0.4245568313070979	0.0959374507494508	0.3785430295295233	0.1130862071675757	0.3168652745622785	0.1224055059975154	0.493193158711571167	0.132320200710822	0.479563812656074	0.141958163267121
0.469953265127554	0.109654515587894	0.4889465693618319	0.096149124878309	0.416965949139396	0.163147791698434	0.399320718052946	0.12792027881532	0.5186779228942586	0.1479368311237868	0.1502683283830131	0.1502683283830131
0.417497889475887	0.0936162376944911	0.41546230972776123	0.10353947276944911	0.3552664277651723	0.167747987277651723	0.40352664277651723	0.1477747987277651723	0.4744275031545004	0.15932730190074889	0.14473230190074889	0.14473230190074889
0.4613188279767213	0.1346393149354331	0.4144142071058007	0.1363053336558864	0.463721365952237	0.12611244736836363	0.470207999309307	0.1299168837207815	0.4592873789739793	0.1506693051300882	0.448563719210325	0.1337279521163048
0.476640415486789	0.118341983467887	0.447407369305404	0.1203252684463344	0.421331423578118	0.13627733636696557	0.41113987055422372	0.140600715259422372	0.4507500517518423	0.1312051520071752	0.4556371454789411	0.1312051520071752
0.51952952029733153	0.11765670211533153	0.490520953319592	0.12520529511533153	0.43252051106710974	0.146941294602113213	0.34225051106710974	0.1501569721169994	0.4592957971201531	0.1515162007170031	0.452223309513331	0.1515162007170031
0.4614337119202327	0.1021332796161596	0.447224651862949	0.112023796161596	0.3707817362752905	0.134915671619962015	0.3072300519322166	0.1303799599487277	0.4505223300519322166	0.149207134533184	0.4556371454789411	0.149207134533184
0.457247052855028	0.12304742058533										

Uncinate fasc. l. mean	Uncinate fasc. l. std	Uncinate fasc. R mean	Uncinate fasc. R std	std FA CSF	std FA GM	std FA WM	std FA mask	xdim
0.41595943514996	0.163091510807129	0.4264332198377514	0.1532650904337668	0.13771697262027	0.093608522313903	0.1725196355106322	0.1722848343846797	2.0
0.239942033757964	0.172516562297069	0.2886646104637189	0.179072050199265	0.112650204259702	0.105713954708408	0.188007315359833	0.1852291403050478	2.0
0.172774024703402	0.1484158126791349	0.3049531733974746	0.158681060548939	0.1374214291389616	0.107108651253786	0.17362163080838326	0.1707663571112138	2.0
0.492970508500902	0.197659508313083	0.46469765304273	0.2121751077927852	0.1340954648453391	0.0950734957375011	0.172387760122447	0.179087357329545	2.0
0.4555460579420589	0.2114530208048047	0.52369630367608843	0.1805775426703049	0.088321552560517	0.0889132395465071	0.19056738166046	0.1860413783465467	1.5
0.245277137841653	0.2584549522705928	0.3668868346472958	0.2506153843621143	0.112917959304436	0.0968093686064878	0.1830317952456377	0.1743086269259608	1.5
0.4417054362503976	0.288021944815754	0.2240694424514376	0.245817392750703	0.118674942653748	0.143703834347981	0.19435260757514	0.18895452231993	1.5
0.0484829338086862	0.0208617952437705	0.0507932332315599	0.0936082609167534	0.20955785789891	0.1950069544624321	0.15208627109548007	0.132973323215599	1.5
0.488427800158847	0.497316182664771	0.1969233295523562	0.09826827140651969	0.0881446814376319	0.194301900305597	0.1838864464047056	0.1838864464047056	1.5
0.5041800729414384	0.2176889047511387	0.479118320006475	0.1616138478441849	0.1359077648715365	0.10531793625653061	0.18207743995898	0.185005788771322	2.0
0.55817293671765247	0.205587941185185	0.4785947510779258	0.1710935741222239	0.15301736400600138	0.1069008265559363	0.1820921680718557	0.1825496864396976	2.0
0.359227304503549	0.1873968850045073	0.49034163064413172	0.1837521510620057	0.1505152803916193	0.16683346981118829	0.1884645703121984	0.191989335390184	2.0
0.477903058612063	0.27237853377782	0.5033523108574093	0.2437932590421916	0.1391768402626202	0.1063188834372179	0.1942062541728052	0.190984671649937	2.0
0.527841054179611	0.2264750644657437	0.15081796213674367	0.15208627109548007	0.132973323215599	0.0936082609167534	0.20955785789891	0.1950069544624321	1.5
0.526970973175968	0.2093031655481741	0.4948166688337702	0.2021608270857454	0.1639359829754243	0.101695233677242	0.1850947497454545	0.1898864464047056	2.0
0.4450653249094905	0.1669140250787037	0.4874852710023971	0.14409336140551186	0.137174833215051	0.09811682277119133	0.1795380902255667	0.1765595833637393	2.0
0.5008972355045073	0.133731401503	0.531315931430396	0.1869515921477118	0.150319350344984	0.111982691932986	0.1857139671751955	0.183616349619962	2.0
0.525257885732368	0.17607416869421	0.509511890381867	0.1837521510620057	0.1505152803916193	0.0950527323292732	0.17059273547437	0.1782374497166993	2.0
0.4742159537105642	0.2584549522705928	0.3668868346472958	0.2506153843621143	0.112917959304436	0.0936082609167534	0.20955785789891	0.1950069544624321	1.5
0.487866641217938	0.1551515156480047	0.50792765119371608	0.1580835727617884	0.1754419008712969	0.10530436464079988	0.196573145361311	0.1699069867937879	2.0
0.4940249234816192	0.203728858516755	0.5704952789249063	0.159363568604289	0.183490483976598	0.099830093321217	0.17939560443947098	0.1837980802430900836	2.0
0.4601821233739593	0.144886192679459	0.3877420266676024	0.16213078052116	0.1605202974074941	0.18170952974074941	0.1826278034530348	0.1826278034530348	2.0
0.44057545095675	0.208527813202685	0.498333492952167	0.139673179405081	0.1543640040958497	0.144384085272868	0.182391579921809	0.174791335473916	2.0
0.4511219681444169	0.172390966670505	0.48791181840106	0.21416920144474791	0.18171795204479	0.102850174693805	0.1811229744891203	0.1812652065777853	2.0
0.48020095610381	0.2020030019545367	0.3005020965190202	0.1600533650091009	0.0983070265594552	0.1856306367510816	0.1875380864396976	0.1875380864396976	2.0
0.4292188001762061	0.1285119042258358	0.34782177207151	0.14940848720183	0.1669930665421903	0.0949068151423903	0.1746491311193674	0.16982323324367	2.0
0.459579135965193	0.2250692671942839	0.443793851205928	0.171144927105928	0.11149261602119284	0.1797410638124033	0.174729960536555	0.174729960536555	2.0
0.50784403050684	0.1922375375450883	0.5739887343872516	0.174592753036769	0.168340691454516	0.130306220983211	0.181537008057568	0.1758008043330105	2.0
0.534576188590049	0.1801728746729165	0.566895944062555	0.1712766514891239	0.1744361361284873	0.11684984005272868	0.1824112078130075	0.1810819071252684	2.0
0.40999730928385	0.19013212211496	0.537398122211496	0.15457398122211496	0.1093087466964799	0.092087746888583	0.1822190576146198	0.1822190576146198	2.0
0.479453118655683	0.2297437755132596	0.4329206688683302	0.1934943752542998	0.145309664165281	0.10149848640931593	0.18605380323324367	0.187500887878239	2.0
0.5172503741469656	0.151315156480047	0.50792765119371608	0.1576508168770662	0.141185445429122	0.1071668408966851	0.1825340363329278	0.180762643754261	2.0
0.383235432381001	0.18194516560001147	0.44740821146988723	0.1621940821146988723	0.159598091190047	0.099059572350265	0.1810925068756986	0.1774042192944483	2.0
0.455332223496615	0.2374146730847495	0.498201813534342	0.20679081832117	0.125295182413021	0.1064124733191945	0.188850081032342	0.188850473450751	2.0
0.5175968243372	0.2017487355148337	0.50473829732470919	0.160399528553342	0.150309852233434	0.10285748174688002	0.17551955688892	0.179003938869637	2.0
0.5800532136726113	0.1282391770823247	0.5137891232470919	0.1634772212222239	0.1343759878449979	0.1082802223227348	0.182391579921809	0.182391579921809	2.0
0.44057545095675	0.208527813202685	0.498333492952167	0.139673179405081	0.15456693446223404	0.102850174489405192	0.174791335473916	0.1824112078130075	2.0
0.4742159537105642	0.17607418188472958	0.443793851205928	0.17109357105642	0.15208574053987	0.0944735202232239	0.1845304363224367	0.18500373095453	2.0
0.4446456202133566	0.1705519537105642	0.443054657464082	0					

```

#!/usr/bin/env python3
# -*- coding: utf-8 -*-
"""
03_TRACTOGRAM
"""

main_dir = '/home/marina/TFG/DATA'
output_file = '/home/marina/TFG/outputs/03_tractograms.csv'

# %% Libraries
import os
import pandas as pd
import nibabel as nib
from dipy.tracking.utils import length
import matplotlib.pyplot as plt
import numpy as np
import seaborn as sns

# %% DF creation

f_dir=[]
s_list=[]
for s in sorted(os.listdir(main_dir)):
    if os.path.isfile(f'{main_dir}/{s}/dwi/{s}_tractogram_CSD_50kseeds.tck'):
        s_list.append(s)
        f_dir.append(f'{main_dir}/{s}/dwi/{s}_tractogram')

for n in ['MARINA', 'SAUL']:
    for p in ['FASTnFURIOUS', 'DIEHARD', 'MORTALKOMBAT', 'SHARKNADO']:
        for v in [15,20]:
            if os.path.isfile(f'{main_dir}/LABIMATGE_{n}/dwi/{v}voxsize_{p}/LABI'):
                f_dir.append(f'{main_dir}/LABIMATGE_{n}/dwi/{v}voxsize_{p}/LABI')
                s_list.append(f'LABIMATGE_{n}_{v}voxsize_{p}')

df = pd.DataFrame()
df['SubjID'] = s_list
df['CSD_lengths'] = None
df['DTI_lengths'] = None
for i,f in enumerate(f_dir):
    for m in ['DTI', 'CSD']:
        f_name=f'{f}_{m}_50kseeds.tck'
        print(f'Working on file {f_name}')
        tractogram = nib.streamlines.load(f_name).tractogram.streamlines
        df.at[i, f'{m}_NOS'] = len(tractogram)
        df.at[i, f'{m}_lengths'] = length(tractogram)

```

03_tractogram

SubjID	CSD_lengths	DTI_lengths	DTI_NOS	CSD_NOS	Dataset
BIOMARCADORES_01	[71.31435496 21.77883969 104.54175674 ... 16.87954311 89.59244858 43.08303698]	[43.49998097 57.99999761 29.0000021 ... 18.4999935 48.49998724 31.4999899]	44628.0	44772.0	BIOMARCADORS
BIOMARCADORES_02	[34.68614441 189.11314124 11.86618472 ... 61.93093278 91.19608691 54.29178799]	[53.00000534 25.49999655 51.49998365 ... 14.4999977 194.5000042 27.99999765]	43295.0	42762.0	BIOMARCADORS
BIOMARCADORES_03	[19.79061103 11.92394029 29.70627317 ... 31.16769018 45.5500856 26.29740806]	[11.00000111 35.49999645 141.49999558 ... 46.99999569 84.50000287 56.50001526]	45012.0	39125.0	BIOMARCADORS
BIOMARCADORES_04	[117.31783329 36.18667118 19.78496209 ... 40.59553395 51.4649926 23.72717233]	[20.99999485 87.99998879 136.4999966 ... 76.5000061 134.49999758 70.000002]	43521.0	44577.0	BIOMARCADORS
CTR_HSA_01	[19.35648905 11.40797521 90.70281621 ... 29.76314032 7.98014725 76.81444556]	[107.4999048 33.49998575 15.5000672 ... 39.99998357 24.4999984 33.50000601]	43582.0	30913.0	BBBHSA
CTR_HSA_02	[10.93216968 21.33243109 11.42179765 ... 29.95625271 47.706975 98.66386954]	[99.999977 40.50000501 56.5000005 ... 20.00000885 66.50000008 202.50000018]	40655.0	30720.0	BBBHSA
CTR_HSA_03	[11.45603179 25.84929194 36.6777625 ... 29.3050536 11.94757763 37.70116118]	[78.4999873 36.49999422 13.00000393 ... 49.49999768 49.49999876 27.9999983]	41653.0	26950.0	BBBHSA
CTR_HSA_04	[37.71755409 30.79973635 10.42200631 ... 54.52871119 12.92381225 28.75045144]	[60.49999613 52.00000313 26.49999816 ... 153.99999592 33.99998229 244.50000717]	44083.0	29743.0	BBBHSA
CTR_HSA_05	[30.83345223 109.55862969 15.35460011 ... 9.9369434 31.79609513 10.46852294]	[33.50000142 196.50000515 115.9999945 ... 125.50001703 63.50000916 94.4999927]	43224.0	31143.0	BBBHSA
EOT_FARA023048	[25.79452911 17.32789276 174.21529362 ... 100.52197407 310.8127354 69.31905664]	[67.00001096 190.49999983 39.50000563 ... 174.00001485 46.50000361 53.00000487]	44760.0	46049.0	EOP
EOT_FARA025000	[26.68809648 79.58419702 14.86842635 ... 115.33412992 27.7280087 86.69693602]	[195.50000041 37.99998735 10.49999534 ... 93.49998911 82.99998054 119.99998838]	44926.0	44972.0	EOP
EOT_FARA027048	[14.36036509 27.69251625 80.64812966 ... 102.38508881 26.73488977 181.66990169]	[76.50001306 83.50000627 38.0000055 ... 113.5000094 103.50000766 133.99999758]	44884.0	46018.0	EOP
EOT_FARA028000	[14.34899834 10.90497403 30.22014847 ... 11.56457124 40.15211568 302.0370105]	[105.49999323 97.49999488 16.99999413 ... 170.49998892 129.00000097 112.999992]	44780.0	42539.0	EOP
EOT_FARA029000	[83.65763685 59.35356025 29.73566453 ... 11.89740151 98.98533029 12.92251364]	[153.99999108 137.50001137 44.99999339 ... 71.49999994 130.4999821 68.99998602]	43099.0	42925.0	EOP
EOT_FARA032000	[28.73939861 54.9829994 10.94275226 ... 12.41156592 60.41462923 158.4725053]	[74.50000178 79.99999359 76.00001716 ... 114.50000073 97.49999519 77.99999548]	45702.0	44076.0	EOP
EOT_FARA034096	[41.99835686 43.71604216 22.72931752 ... 115.35526955 13.38743063 51.06484127]	[43.99999783 89.00000439 101.50000122 ... 54.99999528 56.5000008 100.50000178]	44426.0	46473.0	EOP
EOT_FARA036000	[10.91272025 30.24007965 25.25656181 ... 56.42534465 17.83033617 90.19208188]	[25.00000312 30.00000308 48.50000511 ... 23.49999279 13.50000709 138.99998536]	44826.0	44331.0	EOP
EOT_FARA043048	[23.27562494 81.66200175 73.98577523 ... 69.7402354 38.10946312 207.8260031]	[66.49999248 23.49998983 34.49998318 ... 51.00001048 53.50000696 120.49997808]	44631.0	46871.0	EOP
EOT_FARA046000	[62.94780211 42.57742185 62.31254512 ... 116.34078599 65.80947212 32.23615809]	[123.50000563 53.99999551 138.000003 ... 29.50000152 69.4999998 190.00000676]	46216.0	45979.0	EOP
EOT_FARA048000	[67.38521951 45.08103051 29.74415115 ... 72.20271369 217.197486 104.40885093]	[64.50000358 65.49999509 37.49999641 ... 73.00000232 34.49999522 150.49998754]	46494.0	47141.0	EOP
EOT_FARA048024	[18.30642031 134.74896678 25.26229378 ... 27.7356048 28.75518835 43.53800094]	[87.9999984 28.00000854 179.50001174 ... 16.50000222 64.50000585 124.99998644]	44810.0	46374.0	EOP
EOT_FARA055000	[60.78082726 13.40698169 34.17789828 ... 62.4938202 18.33464727 39.70167325]	[226.50001627 10.9999988 28.00000286 ... 100.00000127 92.99998337 119.50001037]	45015.0	38115.0	EOP
EOT_FARA057024	[173.40690614 17.30479524 38.20139271 ... 50.00245172 163.35909436 161.4052635]	[136.99998819 46.50000146 50.00000856 ... 32.49999608 32.00000513 60.499976]	44891.0	45761.0	EOP
EOT_FARA059000	[34.62140714 106.72939956 32.66860179 ... 175.94937723 98.469996838 36.62397879]	[17.99999795 47.00000656 58.99999414 ... 126.49999179 49.50001958 79.50000126]	45659.0	46481.0	EOP
EOT_FARA059024	[16.34540529 56.36520813 17.82111167 ... 38.62214581 136.67078708 25.24786728]	[18.00000159 88.99999392 40.5000135 ... 73.50001857 45.00000599 109.00000454]	44849.0	46169.0	EOP
EOT_FARA060000	[70.31099915 84.22341083 29.70794035 ... 97.50818094 180.52202605 49.66610514]	[160.00000033 50.00000962 132.4999882 ... 171.50000948 134.00002013 68.50000589]	45905.0	46533.0	EOP
EOT_FARA061000	[27.23240995 46.01045299 77.80736736 ... 27.20913919 145.61293014 18.32721881]	[14.49999289 64.00000329 21.49999767 ... 183.00001325 58.50000126 46.00000749]	44955.0	45500.0	EOP
EOT_FARA062000	[101.0376916 37.17093067 10.3867212 ... 31.19244869 119.7955225 12.88456784]	[65.49998894 38.00000563 149.49998695 ... 73.99999304 62.99999513 105.49998354]	44533.0	39462.0	EOP
EOT_FARA065000	[43.58950194 20.81520415 19.39122194 ... 23.33588599 86.15743485 21.85126084]	[41.99999726 26.99999121 69.00001468 ... 159.00001443 177.99998552 47.50000343]	45833.0	41568.0	EOP
EOT_FARA067000	[146.96462763 104.88345284 71.8104048 ... 15.85195431 69.76376218 228.10594648]	[85.50000892 117.99999799 28.00000804 ... 501.49996774 40.49997794 150.49996355]	45645.0	46821.0	EOP
EOT_FARA069048	[36.63395223 35.10984613 15.38171694 ... 111.86421458 110.37532065 40.58814287]	[171.50000157 43.00000202 38.00001794 ... 11.00000564 75.00000876 63.49998716]	43632.0	44944.0	EOP
EOT_FARA074048	[87.64392752 35.66374728 30.67912294 ... 65.96262044 41.58848687 19.33113638]	[62.99999117 35.00000311 76.49999934 ... 115.9999926 108.4999954 105.00000182]	43900.0	46675.0	EOP
EOT_FARA075000	[104.50576161 41.10555289 48.98124582 ... 137.42507321 248.54655133 31.98547678]	[160.99999751 93.49999919 104.50000815 ... 115.49999475 64.00001578 40.00000356]	45098.0	47529.0	EOP
EOT_FARA084048	[59.38472603 77.62877837 48.52536892 ... 120.11160643 47.00406612 170.20160031]	[16.00000386 39.49999849 88.99999085 ... 79.50001105 71.50000001 131.5000082]	44450.0	47092.0	EOP
EOT_FARA085000	[44.10879657 47.06159306 52.94765267 ... 56.42079084 102.94118036 14.36427698]	[58.50000222 183.99998108 23.49999777 ... 147.99999342 78.00000891 111.50000125]	46694.0	46506.0	EOP
EOT_FARA088048	[13.88492265 21.79241727 166.91280955 ... 26.67531457 18.81366187 114.25272992]	[83.49998698 106.00000504 78.99999775 ... 40.50000331 29.99999544 117.50001026]	43568.0	46	

EOT_FARD088000	[42.47871583 164.20928004 49.44993834 ... 39.21830486 63.7901551 15.24722419]	[54.49998583 55.49998976 121.50001328 ... 112.9999992 89.49999867 53.4999834]	45345.0	47442.0	EOP
EOT_FARe148000	[100.32257033 54.07313806 113.83727877 ... 17.82726879 18.83567431 75.24887471]	[121.00000954 20.99999569 59.00000945 ... 25.50000009 71.00000727 104.00000585]	46146.0	47461.0	EOP
EOT_PERC022000	[39.10235811 60.93504983 38.69112224 ... 44.42455451 68.74177261 42.09437599]	[169.99998209 29.49999934 45.5000046 ... 49.99997564 127.50000324 195.00002047]	46229.0	47305.0	EOP
EOT_PREC007000	[91.12759532 14.36875511 33.6563112 ... 52.46371963 40.13533921 97.9605474]	[71.9999684 121.50000607 35.00000309 ... 53.50000332 29.50000866 33.5000006]	44941.0	46687.0	EOP
EOT_PREC007018	[16.81880433 121.27421326 24.75455487 ... 192.48040112 165.29341448 60.43126146]	[122.49998408 43.49999143 66.50001246 ... 74.49998482 16.99999882 132.49998671]	45057.0	47401.0	EOP
EOT_PREC008018	[64.72221632 20.29983754 20.79622778 ... 84.1491704 31.69038407 98.06025073]	[19.99998981 17.99999514 35.00000496 ... 124.49999329 24.5000063 90.50000472]	43274.0	46820.0	EOP
EOT_PREC011000	[71.80387103 27.72055128 259.8449542 ... 116.29044623 36.1916273 31.73150463]	[33.50000012 36.00000376 63.50002225 ... 28.4999976 19.0000027 125.49999833]	43762.0	47383.0	EOP
EOT_PREC012000	[111.73341924 97.98079283 51.44990028 ... 61.747577 252.85214958 195.84426857]	[76.50001081 62.99999548 36.00001012 ... 12.0000028 160.99998278 60.50001355]	43677.0	47186.0	EOP
EOT_PREC014000	[33.65818656 28.64967601 68.49878183 ... 35.65216758 24.22268527 146.50493464]	[144.9999979 43.99999835 19.99999112 ... 93.50001489 88.00000256 92.00000252]	45415.0	47238.0	EOP
EOT_PREC018000	[89.62043937 11.37328769 66.13939892 ... 147.94274877 209.82465322 46.04474843]	[147.99997538 115.50000245 64.50000476 ... 86.50001406 15.49999668 54.4999801]	46327.0	47925.0	EOP
EOT_PREC019000	[19.2421229 52.42793434 119.63097333 ... 76.18279441 44.99248347 47.99639118]	[11.99999552 45.49999409 123.499996 ... 72.50001111 24.00000167 115.99998007]	44998.0	47828.0	EOP
EOT_PREC020000	[170.76248494 86.12617533 44.5685798 ... 114.27685302 138.10017214 121.76616958]	[102.0000138 126.99999764 95.49999973 ... 24.49999378 21.9999971 48.99999042]	45030.0	47941.0	EOP
EOT_PREC021000	[70.24222848 63.85707001 18.82562158 ... 221.08575717 33.13995367 236.68104459]	[291.4999907 27.50000134 51.00000531 ... 98.50001156 80.49999941 93.00000582]	44419.0	47589.0	EOP
EOT_PREC023000	[95.99453 22.78182618 24.30797724 ... 47.03949086 82.59261737 111.38551532]	[72.49999261 77.0000048 153.49999206 ... 72.00001276 117.50000074 116.99998151]	43837.0	46835.0	EOP
EOT_PREC026000	[11.89351726 146.53365709 153.88647255 ... 152.78835168 114.10994126 158.81660363]	[70.49999651 70.9999804 99.99998975 ... 80.50001144 40.00000612 182.4999874]	43861.0	46498.0	EOP
EOT_PRSC001000	[89.11612894 31.12883126 80.36121228 ... 45.0524968 13.3751378 96.9283216]	[29.50000037 69.49999813 37.00000705 ... 67.00000212 14.50000477 52.49999161]	44852.0	46571.0	EOP
EOT_PRSC003000	[58.86300677 41.34172251 14.32974996 ... 78.88761548 63.33088538 41.11180558]	[92.500000828 99.00001217 36.99999032 ... 29.49999479 70.99999323 113.50000649]	45814.0	46026.0	EOP
EOT_PRSC005000	[50.02052151 95.14075032 11.88898927 ... 71.35396752 50.44427223 85.14148385]	[20.50000462 24.99999641 130.50001544 ... 177.49997781 50.4999945 67.99997173]	45473.0	46179.0	EOP
EOT_PRSC007000	[20.27604795 30.24707954 99.38751922 ... 66.40784226 41.17637297 93.10742214]	[53.50000172 69.99999801 47.50001149 ... 56.99999523 88.49999475 24.00000023]	45737.0	46760.0	EOP
EOT_PRSC008000	[15.32954058 63.34962539 110.38765669 ... 35.20176949 36.61898675 68.85285301]	[79.9999924 54.4999928 34.99999506 ... 113.49999817 223.00000355 141.9999899]	43759.0	45066.0	EOP
EOT_PRSC009000	[114.14820751 19.29142328 19.80103003 ... 71.89653468 132.0762233 45.55585329]	[67.00000255 71.999993 26.00000339 ... 34.99999482 35.49999675 72.00000407]	44822.0	46259.0	EOP
EOT_PRSC011000	[166.30099642 33.18793091 147.44398103 ... 59.38179488 64.27514684 120.79749853]	[77.00000821 46.99999493 48.9999893 ... 41.49999745 38.50001776 86.0000022]	45064.0	47124.0	EOP
EOT_PRSC012000	[35.61339185 27.74000272 16.34736566 ... 156.44808883 263.3059708 61.41054852]	[34.99999967 18.50000229 62.00001458 ... 230.5000022 120.00000305 28.50000354]	43207.0	46093.0	EOP
EOT_PRSC014000	[47.52665993 18.28136365 20.34331298 ... 51.99980576 100.56395852 71.94964187]	[101.49999267 83.00000671 101.00000041 ... 79.49998976 129.499991 45.9999749]	44953.0	43627.0	EOP
EOT_PRSC015000	[24.69602941 76.35619054 69.80369532 ... 75.16172413 75.69930024 35.67655097]	[18.50000388 51.50001205 10.99999159 ... 51.99999506 28.50000808 75.50001043]	43342.0	44967.0	EOP
EOT_PRSC016000	[24.65699939 140.67682384 19.32035596 ... 14.85848735 66.34177781 47.09934642]	[108.49999129 50.49999309 63.50000796 ... 27.00000298 96.00001042 50.49998979]	42279.0	46571.0	EOP
EOT_PRSC017000	[83.40465634 54.30093472 66.25433904 ... 159.88204682 50.96050049 285.4329885]	[21.0000062 31.49999589 25.49999655 ... 61.49999204 128.9999926 92.00000055]	46074.0	47347.0	EOP
EOT_PRSC024000	[65.36712589 153.97176591 192.1248932 ... 16.8809905 63.39120175 49.40833804]	[150.99997826 289.50003721 122.49999438 ... 120.99999025 71.00000366 60.00000263]	45124.0	46554.0	EOP
EOT_PRSC027000	[10.90026372 122.3542323 15.40758691 ... 40.60820005 86.65045572 11.41578926]	[10.49999774 104.99999706 78.00000964 ... 10.99999714 23.00000026 96.9999995]	44288.0	43363.0	EOP
EOT_PRSC029000	[87.6991364 112.85323208 89.6105212 ... 36.09928017 61.32048206 151.39115325]	[101.50000819 147.00000112 117.50000951 ... 241.49999346 28.99999458 57.9999954]	44485.0	46275.0	EOP
EOT_PRSC031000	[34.1731153 11.42927147 40.57563438 ... 24.819747 100.55760605 54.95300659]	[44.9999874 52.9999925 52.50000132 ... 46.50000203 27.50000034 176.49999484]	45622.0	46134.0	EOP
EOT_PRSC033000	[70.81290793 124.25134577 16.32245694 ... 75.27824983 21.21866148 137.53922933]	[64.500001087 55.00000121 129.00000417 ... 41.9999158 66.99998508 86.00000137]	45492.0	46918.0	EOP
EOT_PRSC034000	[92.12203588 19.27937639 184.13121879 ... 70.82787227 13.84063235 15.35034037]	[30.99999555 19.49999664 12.99999524 ... 91.99999281 35.4999907 55.99999315]	44770.0	45615.0	EOP
EOT_PRSC035000	[46.56477171 17.83093833 47.41389511 ... 55.44511292 75.15432121 14.85212869]	[12.00000051 86.00001161 70.99998242 ... 103.50001012 77.99999215 118.99997078]	44399.0	45737.0	EOP
EOT_PRSC039000	[82.64995003 48.52066385 61.90791475 ... 156.94175064 39.1054607 22.24684659]	[106.49999622 34.00000313 131.00000746 ... 110.50000203 11.50000188 73.5000109]	43772.0	45077.0	EOP
EPILENG_C_0000	[30.74815376 13.35078349 22.26762936 ... 45.52546931 151.00514237 59.95053784]	[32.50000152 62.00000017 14.0000			

EPILENG_C_0021	[42.12413821 9.90403845 52.06631407 ... 55.47822984 21.84232917 32.72374016]	[56.49998818 86.9999925 99.00001312 ... 103.50000708 114.49999078 81.99999634]	47404.0	39579.0	EPILENG
S14_R209	[20.8796461 19.34453632 20.28894301 ... 33.90365845 9.41010997 96.1626733]	[101.49999208 51.99999506 47.50000275 ... 63.9999974 99.00001746 19.50000657]	43156.0	38990.0	ALBUCAT
S15_R106	[11.43750183 30.25382747 13.36864535 ... 64.43952507 133.19871752 37.6361507]	[37.49999359 158.99999634 17.00000302 ... 218.50001484 111.49999459 72.4999946]	43425.0	38310.0	ALBUCAT
LABIMATGE_MARINA_20voxsize_FASTnFURIOUS	[39.10536225 24.76150757 30.70516797 ... 55.90596559 48.98898989 173.16693289]	[39.00001036 34.00001523 16.00000408 ... 46.00000309 110.99998781 100.00000252]	43515.0	46097.0	LAB_IMATGE
LABIMATGE_MARINA_15voxsize_DIEHARD	[72.42216624 15.38297047 131.27428244 ... 76.28423889 32.18448562 75.14790118]	[52.50000093 46.50000939 101.50000013 ... 61.99999519 72.0000003 45.99999789]	47414.0	41972.0	LAB_IMATGE
LABIMATGE_MARINA_20voxsize_DIEHARD	[79.20699842 14.39817494 107.45377187 ... 127.33013683 13.33430717 189.19548881]	[30.50000244 44.50001838 42.49999517 ... 74.50000517 166.00000106 63.50000822]	45093.0	41343.0	LAB_IMATGE
LABIMATGE_MARINA_15voxsize_MORTALKOMB	[129.27410099 60.94723927 49.09521832 ... 31.74322407 20.82691692 10.9679178]	[190.49999837 86.00000345 117.00000468 ... 95.49998889 12.49999892 143.99999355]	47002.0	42129.0	LAB_IMATGE
LABIMATGE_MARINA_20voxsize_MORTALKOMB	[49.47030199 11.93199538 100.11710421 ... 74.60135969 76.33204198 12.36849037]	[125.99999505 336.50001157 9.99999965 ... 120.50001103 159.00001327 241.00001465]	44166.0	40445.0	LAB_IMATGE
LABIMATGE_MARINA_15voxsize_SHARKNADO	[11.89729687 53.02838421 18.82151575 ... 50.09813607 38.67894866 19.79573776]	[68.00000035 75.99999195 210.49999252 ... 69.50002136 195.4999814 21.99999424]	46811.0	39396.0	LAB_IMATGE
LABIMATGE_MARINA_20voxsize_SHARKNADO	[74.81889483 99.02266762 47.06766939 ... 72.22407403 12.91840953 82.92112894]	[41.00000238 68.50000747 51.0000045 ... 63.50000962 33.5000059 119.50001208]	44727.0	37953.0	LAB_IMATGE
LABIMATGE_SAUL_15voxsize_FASTnFURIOUS	[10.93804053 9.90885068 55.2610967 ... 12.87010123 135.88178676 73.26853064]	[173.50000519 32.50000742 66.99998404 ... 85.99999213 55.49999375 191.50001587]	46598.0	45215.0	LAB_IMATGE
LABIMATGE_SAUL_20voxsize_FASTnFURIOUS	[65.28227832 29.26322467 91.48066999 ... 144.21229642 214.31234143 86.61556027]	[83.00001018 55.00000575 86.99999136 ... 143.00001457 68.99999436 114.49997897]	42662.0	44351.0	LAB_IMATGE
LABIMATGE_SAUL_15voxsize_DIEHARD	[39.63130669 81.2606411 9.89617061 ... 116.43061647 41.08644436 173.33677561]	[15.99999436 71.50000189 94.50000313 ... 91.99998524 65.49999742 95.9999893]	47436.0	41221.0	LAB_IMATGE
LABIMATGE_SAUL_20voxsize_DIEHARD	[71.24125503 33.66819743 43.0841375 ... 30.2282596 77.26852888 55.40739251]	[42.99999843 66.5000038 60.99999258 ... 120.99995652 15.49999855 48.49998301]	45544.0	39655.0	LAB_IMATGE
LABIMATGE_SAUL_15voxsize_MORTALKOMBAT	[27.2714446 11.8956009 46.05385372 ... 35.11177244 85.69006251 67.83680126]	[42.50000247 34.00000048 122.99996427 ... 9.00000473 18.9999928 77.49998909]	47047.0	41030.0	LAB_IMATGE
LABIMATGE_SAUL_20voxsize_MORTALKOMBAT	[28.33045413 95.98617897 79.25255476 ... 89.61509927 22.31174571 222.07529609]	[15.00000352 202.99999778 199.50002374 ... 120.5000009 32.99998471 275.50000106]	43761.0	40315.0	LAB_IMATGE
LABIMATGE_SAUL_15voxsize_SHARKNADO	[36.17027646 63.42614193 16.84002893 ... 46.99204921 28.74414201 64.44886523]	[66.50001245 63.5000075 18.00000596 ... 11.99999934 94.99999684 159.0000237]	47024.0	38985.0	LAB_IMATGE

```

#!/usr/bin/env python3
# -*- coding: utf-8 -*-
"""
04_STATISTICAL ANALYSIS
"""

#% Libaries

main_dir = '/home/marina/TFG'

import pandas as pd
import seaborn as sns
import matplotlib.pyplot as plt
import numpy as np

#% Upload dataframes

SNR_df = pd.read_csv(f'{main_dir}/outputs/01_SNRs.csv')
SNR_df.set_index('SubjID', inplace = True)

FA_df = pd.read_csv(f'{main_dir}/outputs/02_FAmaps.csv')
FA_df.set_index('SubjID', inplace = True)

dataset_FA = []
for s in FA_df.index:
    if 'CTR_HSA' in s: dataset_FA.append('BBHSA')
    elif 'EOT' in s: dataset_FA.append('EOP')
    elif 'EPILENG' in s: dataset_FA.append('EPILENG')
    elif 'BIOMARCADORES' in s: dataset_FA.append('BIOMARCADORES')
    elif '20voxsize_FASTnFURIOS' in s: dataset_FA.append('20voxsize_FASTnFURIO')
    elif '15voxsize_FASTnFURIOS' in s: dataset_FA.append('15voxsize_FASTnFURIO')
    elif '20voxsize_DIEHARD' in s: dataset_FA.append('20voxsize_DIEHARD')
    elif '15voxsize_DIEHARD' in s: dataset_FA.append('15voxsize_DIEHARD')
    elif '20voxsize_MORTALKOMBAT' in s: dataset_FA.append('20voxsize_MORTALKOMB')
    elif '15voxsize_MORTALKOMBAT' in s: dataset_FA.append('15voxsize_MORTALKOMB')
    elif '20voxsize_SHARKNADO' in s: dataset_FA.append('20voxsize_SHARKNADO')
    elif '15voxsize_SHARKNADO' in s: dataset_FA.append('15voxsize_SHARKNADO')
    else: dataset_FA.append('ALBUCAT')

FA_df['Dataset'] = dataset_FA
FA_df['xdim']=SNR_df['xdim']

#% Figure 1: SNR (for 1.5 mm i 2 mm)

xlabels = ['bvals [0,400]', 'bvals (400,800]', 'bvals (800,1200]',
           'bvals (1200,1600]', 'bvals (1600,2000]', 'bvals (2000,2400]',
           'bvals (2400,2800]', 'bvals (2800,3200]']
sns.set(font_scale=1.2)

fig, axis = plt.subplots(1,2, figsize= (12,5))
fig.suptitle('SNR per each b-value interval and voxel size', fontsize = 20)
a = sns.boxplot(data=SNR_df[SNR_df.xdim==1.5][xlabels], palette='pastel', ax=ax
a.set(ylim=(0,100))

```

```

plt.ylabel('SNR')
axis[0].set_title('voxel size = 1.5mm', fontsize = 20)
a.set_xticklabels(labels= xlabel, rotation=45)

b = sns.boxplot(data=SNR_df[SNR_df.xdim==2][xlabel], palette='pastel', ax=axis
b.set(ylim=(0,100))
axis[1].set_title('voxel size = 2mm', fontsize = 20)
sns.set(rc={"figure.dpi":300, 'savefig.dpi':300})
plt.xticks(rotation=45)
plt.ylabel('SNR')
plt.tight_layout()
plt.show()

# %% Fig 2: FA (1.5 mm)
sns.set(font_scale=1.2)
labels1= ['BBHSA', 'EPILENG', 'ALBUCAT' , '15v_FAST', '15v_DIE','15v_MORT', '15v

fig, axes = plt.subplots(3, 2, figsize=(18, 10))
fig.suptitle('FA per each mask and dataset (voxel size = 1.5mm)', fontsize = 30
a = sns.boxplot(ax=axes[0, 0], data=FA_df[FA_df.xdim==1.5], y='FA GM', x ='Data
a.set(ylim=(0.08,0.188))
a.set_xticklabels(labels = labels1, rotation = 0)

b = sns.boxplot(ax=axes[0, 1], data=FA_df[FA_df.xdim==1.5], y='std FA GM', x =
b.set(ylim=(0.08,0.188))
b.set_xticklabels(labels = labels1, rotation = 0)

c = sns.boxplot(ax=axes[1, 0], data=FA_df[FA_df.xdim==1.5], y='FA WM', x ='Data
c.set(ylim=(0.17,0.45))
c.set_xticklabels(labels = labels1, rotation = 0)

d = sns.boxplot(ax=axes[1, 1], data=FA_df[FA_df.xdim==1.5], y='std FA WM', x =
d.set(ylim=(0.17,0.45))
d.set_xticklabels(labels = labels1, rotation = 0)

e = sns.boxplot(ax=axes[2, 0], data=FA_df[FA_df.xdim==1.5], y='FA CSF', x ='Dat
e.set(ylim=(0.09,0.25))
e.set_xticklabels(labels = labels1, rotation = 0)

f = sns.boxplot(ax=axes[2, 1], data=FA_df[FA_df.xdim==1.5], y='std FA CSF', x =
f.set(ylim=(0.09,0.25))
f.set_xticklabels(labels = labels1, rotation = 0)

plt.tight_layout()

# %% Fig 3: FA (2 mm)
sns.set(font_scale=1.2)

labels2= ['BIOMARCADORES', 'EOP', '20v_FAST', '20_DIE','20v_MORT', '20v_SHAR' ]

fig, axes = plt.subplots(3, 2, figsize=(18, 10))
fig.suptitle('FA per each mask and dataset (voxel size = 2mm)', fontsize = 30
a = sns.boxplot(ax=axes[0, 0], data=FA_df[FA_df.xdim==2], y='FA GM', x ='Dataset

```

```

a.set(ylim=(0.08,0.21))
a.set_xticklabels(labels = labels2, rotation = 0)

b = sns.boxplot(ax=axes[0, 1], data=FA_df[FA_df.xdim==2], y='std FA GM', x='Dataset')
b.set(ylim=(0.08,0.21))
b.set_xticklabels(labels = labels2, rotation = 0)

c = sns.boxplot(ax=axes[1, 0], data=FA_df[FA_df.xdim==2], y='FA WM', x='Dataset')
c.set(ylim=(0.165,0.422))
c.set_xticklabels(labels = labels2, rotation = 0)

d = sns.boxplot(ax=axes[1, 1], data=FA_df[FA_df.xdim==2], y='std FA WM', x='Dataset')
d.set(ylim=(0.165,0.422))
d.set_xticklabels(labels = labels2, rotation = 0)

e = sns.boxplot(ax=axes[2, 0], data=FA_df[FA_df.xdim==2], y='FA CSF', x='Dataset')
e.set(ylim=(0.115,0.248))
e.set_xticklabels(labels = labels2, rotation = 0)

f = sns.boxplot(ax=axes[2, 1], data=FA_df[FA_df.xdim==2], y='std FA CSF', x='Dataset')
f.set(ylim=(0.115,0.248))
f.set_xticklabels(labels = labels2, rotation = 0)

plt.tight_layout()

```

#%%Fig 4: Heatmap FA

```

labels2 = ['Middle cerebellar ped. mean','Pontine crossing tract mean', 'Genu of internal capsule L mean', 'Genu of internal capsule R mean', 'Corticospinal tract L mean', 'Med. lemniscus R mean', 'Med. lemniscus L mean', 'Sup. cerebellar ped. R mean', 'Sup. cerebellar ped. L mean', 'Cerebral pedunculus R mean', 'Ant. limb of int. capsule L mean', 'Posterior limb of int. capsule R mean', 'Retrolenticular part of int. capsule R mean', 'Retrolenticular part of int. capsule L mean', 'Ant. corona radiata L mean', 'Sup. corona radiata R mean', 'Sup. corona radiata L mean', 'Posterior corona radiata L mean', 'Posterior thalamic radiation R mean', 'Posterior thalamic radiation L mean', 'Sag. stratum L mean', 'Ext. capsule R mean', 'Ext. capsule L mean', 'Cingulum (hippocampus) L mean', 'Fornix (cres) / Stria terminalis R mean', 'Fornix (cres) / Stria terminalis L mean', 'Sup. longitudinal fasc. R mean', 'Sup. longitudinal fasc. L mean', 'Sup. fronto-occipital fasc. R mean', 'Sup. fronto-occipital fasc. L mean', 'Inf. fronto-occipital fasc. R mean', 'Inf. fronto-occipital fasc. L mean']

regional_fa=FA_df[labels2].groupby('Dataset').mean()
plt.figure(figsize= (15, 8))
h = sns.heatmap(regional_fa, cmap= 'jet', xticklabels= True) #Mean
plt.title('WM atlas labels mean FA value per each dataset ')
plt.xlabel('Atlas labels')
sns.set(rc={"figure.dpi":300, 'savefig.dpi':300})

```

#%% Read Tractogram df

```

main_dir = '/home/marina/TFG'
df = pd.read_pickle(f'{main_dir}/outputs/03_tractogram_data.pkl')

df.set_index('SubjID', inplace = True)

```

```

dataset = []
for s in df.index:
    if 'CTR_HSA' in s: dataset.append('BBHSA')
    elif 'EOT' in s: dataset.append('EOP')
    elif 'EPILENG' in s: dataset.append('EPILENG')
    elif 'BIOMARCADORES' in s: dataset.append('BIOMARCADORES')
    elif '20voxsize_FASTnFURIOS' in s: dataset.append('20voxsize_FASTnFURIOS')
    elif '15voxsize_FASTnFURIOS' in s: dataset.append('15voxsize_FASTnFURIOS')
    elif '20voxsize_DIEHARD' in s: dataset.append('20voxsize_DIEHARD')
    elif '15voxsize_DIEHARD' in s: dataset.append('15voxsize_DIEHARD')
    elif '20voxsize_MORTALKOMBAT' in s: dataset.append('20voxsize_MORTALKOMBAT')
    elif '15voxsize_MORTALKOMBAT' in s: dataset.append('15voxsize_MORTALKOMBAT')
    elif '20voxsize_SHARKNADO' in s: dataset.append('20voxsize_SHARKNADO')
    elif '15voxsize_SHARKNADO' in s: dataset.append('15voxsize_SHARKNADO')
    else: dataset.append('ALBUCAT')

df['Dataset'] = dataset
df['xdim']=FA_df['xdim']

df.to_csv('/Users/rin/Desktop/spyder/outputs/03_tractogram.csv')

#%%
Extract CSD_lengths per acquisition
for s in df.index:
    print(f'df.loc["{s}"]["CSD_lengths"]')

BIOMARCADORES_s_list = df.loc['BIOMARCADORES_01']['CSD_lengths'], df.loc['BIOMA
EOP_s_list = [df.loc["EOT_FARA023048"]["CSD_lengths"],df.loc["EOT_FARA025000"]]
EPILENG_s_list = [df.loc["EPILENG_C_0000"]["CSD_lengths"],df.loc["EPILENG_C_000
BBBHSA_s_list = [df.loc ['CTR_HSA_01']["CSD_lengths"],df.loc ['CTR_HSA_02']["CS
ALBUCAT_s_list = [df.loc ['S14_R209']["CSD_lengths"],df.loc ['S15_R106']["CSD_l
LABF2_s_list = [df.loc ['LABIMATGE_MARINA_20voxsize_FASTnFURIOS']["CSD_lengths
LABF1_s_list = [df.loc ['LABIMATGE_SAUL_15voxsize_FASTnFURIOS']["CSD_lengths"
LABD1_s_list = [df.loc ['LABIMATGE_MARINA_15voxsize_DIEHARD']["CSD_lengths"], d
LABD2_s_list = [df.loc ['LABIMATGE_MARINA_20voxsize_DIEHARD']["CSD_lengths"], d
LABM1_s_list = [df.loc ['LABIMATGE_MARINA_15voxsize_MORTALKOMBAT']["CSD_lengths
LABM2_s_list = [df.loc ['LABIMATGE_MARINA_20voxsize_MORTALKOMBAT']["CSD_lengths
LABS1_s_list = [df.loc ['LABIMATGE_MARINA_15voxsize_SHARKNADO']["CSD_lengths"], 
LABS2_s_list = [df.loc ['LABIMATGE_MARINA_20voxsize_SHARKNADO']["CSD_lengths"]]

sample_1_csd = np.concatenate((BIOMARCADORES_s_list), axis = 0)
sample_2_csd = np.concatenate((EOP_s_list), axis = 0)
sample_3_csd = np.concatenate((EPILENG_s_list), axis = 0)
sample_4_csd = np.concatenate((BBBHSA_s_list), axis = 0)
sample_5_csd = np.concatenate((LABF2_s_list), axis = 0)
sample_6_csd = np.concatenate((LABF1_s_list), axis = 0)
sample_7_csd = np.concatenate((LABD1_s_list), axis = 0)
sample_8_csd = np.concatenate((LABD2_s_list), axis = 0)
sample_9_csd = np.concatenate((LABM1_s_list), axis = 0)
sample_10_csd = np.concatenate((LABM2_s_list), axis = 0)
sample_11_csd = np.concatenate((LABS1_s_list), axis = 0)
sample_12_csd = np.concatenate((LABS2_s_list), axis = 0)
sample_13_csd = np.concatenate((ALBUCAT_s_list), axis = 0)

```

```
#%% Fig 5,6: 1.5mm CSD
```

```
plt.figure()
sns.histplot(x = sample_13_csd, weights = 1/len(ALBUCAT_s_list), bins = 100, color='red')
sns.histplot(x = sample_4_csd, weights = 1/len(BBBHSA_s_list), bins = 100, color='blue')
sns.histplot(x = sample_3_csd, weights = 1/len(EPILENG_s_list), bins = 100, color='green')
sns.histplot(x = sample_6_csd, weights = 1/len(LABF1_s_list), bins = 100, color='orange')
sns.histplot(x = sample_7_csd, weights = 1/len(LABD1_s_list), bins = 100, color='purple')
sns.histplot(x = sample_9_csd, weights = 1/len(LABM1_s_list), bins = 100, color='brown')
sns.histplot(x = sample_11_csd, weights = 1/len(LABS1_s_list), bins = 100, color='pink')
plt.xlim([0,100])
sns.set(rc={"figure.dpi":300, 'savefig.dpi':300})
plt.title('CSD streamlines length per each dataset (voxel size 1.5mm) ')
plt.tight_layout()
plt.legend()
plt.xlabel('Length')
plt.ylabel('# of streamlines')
```

```
#%% Fig 7,8 2mm CSD
```

```
plt.figure()
sns.histplot(x = sample_1_csd, weights = 1/len(BIOMARCADORES_s_list), bins = 100, color='red')
sns.histplot(x = sample_2_csd, weights = 1/len(EOP_s_list), bins = 100, color='blue')
sns.histplot(x = sample_5_csd, weights = 1/len(LABF2_s_list), bins = 100, color='green')
sns.histplot(x = sample_8_csd, weights = 1/len(LABD2_s_list), bins = 100, color='orange')
sns.histplot(x = sample_10_csd, weights = 1/len(LABM2_s_list), bins = 100, color='purple')
sns.histplot(x = sample_12_csd, weights = 1/len(LABS2_s_list), bins = 100, color='brown')
plt.ylim([0,4000])
sns.set(rc={"figure.dpi":300, 'savefig.dpi':300})
plt.title('CSD streamlines length per each dataset (voxel size 2mm) ')
plt.tight_layout()
plt.legend()
plt.xlabel('Length')
plt.ylabel('# of streamlines')
```

```
#%% Fig 9. NOS
```

```
labelsx= ['BIOM', 'BBHSA', 'EOP', 'EPILENG', 'ALBUCAT' , '20voxsize_FASTnFURIOUS']
labelsx= ['BBHSA', 'EPILENG', 'ALBUCAT' , '15v_FAST', '15v_DIE', '15v_MORT', '15v_SHAR']
labelsx= ['BIOM', 'EOP', '20v_FAST', '20_DIE','20v_MORT', '20v_SHAR' ]

fig, axis = plt.subplots(2,2, figsize= (12,8))
fig.suptitle('Number of streamlines (NOS) per each algorithm, dataset and voxel')
a = sns.boxplot(data = df[df.xdim==1.5], y = 'DTI_NOS', x = 'Dataset', palette='Set1')
axis[0,0].set_title('NOS DTI v=1.5mm')
a.set(ylim=(29000,48000))
a.set_xticklabels(labels = labels1, rotation = 90)

b = sns.boxplot(data =df[df.xdim==1.5], y = 'CSD_NOS', x = 'Dataset', palette='Set1')
axis[0,1].set_title('NOS CSD v=1.5mm')
b.set_xticklabels(labels = labels1, rotation = 90)
b.set(ylim=(29000,48000))
sns.set(rc={"figure.dpi":300, 'savefig.dpi':300})

c = sns.boxplot(data = df[df.xdim==2], y = 'DTI_NOS', x = 'Dataset', palette='Set1')
# a.set(ylim=(0.08,0.21))
```

```

axis[1,0].set_title('NOS DTI v=2mm')
c.set_xticklabels(labels = labels2, rotation = 90)
c.set(ylim=(38000,48000))

d = sns.boxplot(data =df[df.xdim==2], y = 'CSD_NOS', x = 'Dataset', palette='pa
axis[1,1].set_title('NOS CSD v=2mm')
d.set_xticklabels(labels = labels2, rotation = 90)
d.set(ylim=(38000,48000))

plt.tight_layout()

#%% Extract DTI_lengths per acquisition

BIOMARCADORES_s_list = df.loc['BIOMARCADORES_01']['DTI_lengths'], df.loc['BIOMA
EOP_s_list = [df.loc["EOT_FARA023048"]["DTI_lengths"],df.loc["EOT_FARA025000"]][
EPILENG_s_list = [df.loc["EPILENG_C_0000"]["DTI_lengths"],df.loc["EPILENG_C_000
BBBHSA_s_list = [df.loc ['CTR_HSA_01']["DTI_lengths"],df.loc ['CTR_HSA_02']["DT
ALBUCAT_s_list = [df.loc ['S14_R209']["DTI_lengths"],df.loc ['S15_R106']["DTI_l
LABF2_s_list = [df.loc ['LABIMATGE_MARINA_20voxsize_FASTnFURIOS']["DTI_lengths"
LABF1_s_list = [df.loc ['LABIMATGE_SAUL_15voxsize_FASTnFURIOS']["DTI_lengths"
LABD1_s_list = [df.loc ['LABIMATGE_MARINA_15voxsize_DIEHARD']["DTI_lengths"], d
LABD2_s_list = [df.loc ['LABIMATGE_MARINA_20voxsize_DIEHARD']["DTI_lengths"], d
LABM1_s_list = [df.loc ['LABIMATGE_MARINA_15voxsize_MORTALKOMBAT']["DTI_lengths"
LABM2_s_list = [df.loc ['LABIMATGE_MARINA_20voxsize_MORTALKOMBAT']["DTI_lengths"
LABS1_s_list = [df.loc ['LABIMATGE_MARINA_15voxsize_SHARKNADO']["DTI_lengths"], l
LABS2_s_list = [df.loc ['LABIMATGE_MARINA_20voxsize_SHARKNADO']["DTI_lengths"]]

sample_1_dti = np.concatenate((BIOMARCADORES_s_list), axis = 0)
sample_2_dti = np.concatenate((EOP_s_list), axis = 0)
sample_3_dti = np.concatenate((EPILENG_s_list), axis = 0)
sample_4_dti = np.concatenate((BBBHSA_s_list), axis = 0)
sample_5_dti = np.concatenate((LABF2_s_list), axis = 0)
sample_6_dti = np.concatenate((LABF1_s_list), axis = 0)
sample_7_dti = np.concatenate((LABD1_s_list), axis = 0)
sample_8_dti = np.concatenate((LABD2_s_list), axis = 0)
sample_9_dti = np.concatenate((LABM1_s_list), axis = 0)
sample_10_dti = np.concatenate((LABM2_s_list), axis = 0)
sample_11_dti = np.concatenate((LABS1_s_list), axis = 0)
sample_12_dti = np.concatenate((LABS2_s_list), axis = 0)
sample_13_dti = np.concatenate((ALBUCAT_s_list), axis = 0)

#% Fig 10,11 1.5mm DTI
plt.figure()
sns.histplot(x = sample_13_dti, weights = 1/len(ALBUCAT_s_list), bins = 100, co
sns.histplot(x = sample_4_dti, weights = 1/len(BBBHSA_s_list), bins = 100, colo
sns.histplot(x = sample_3_dti, weights = 1/len(EPILENG_s_list), bins = 100, co
sns.histplot(x = sample_6_dti, weights = 1/len(LABF1_s_list), bins = 100, colo
sns.histplot(x = sample_7_dti, weights = 1/len(LABD1_s_list), bins = 100, colo
sns.histplot(x = sample_9_dti, weights = 1/len(LABM1_s_list), bins = 100, colo
sns.histplot(x = sample_11_dti, weights = 1/len(LABS1_s_list), bins = 100, col
plt.xlim([0,100])
sns.set(rc={"figure.dpi":300, 'savefig.dpi':300})
plt.title('DTI streamlines length per each dataset (voxel size 1.5mm) ')
plt.tight_layout()
plt.legend()

```

```
plt.xlabel('Length')
plt.ylabel('# of streamlines')

# %% Fig 12,13 2mm DTI
plt.figure()
sns.histplot(x = sample_1_dti, weights = 1/len(BIOMARCADORES_s_list), bins = 10)
sns.histplot(x = sample_2_dti, weights = 1/len(EOP_s_list), bins = 100, color='red')
sns.histplot(x = sample_5_dti, weights = 1/len(LABF2_s_list), bins = 100, color='blue')
sns.histplot(x = sample_8_dti, weights = 1/len(LABD2_s_list), bins = 100, color='green')
sns.histplot(x = sample_10_dti, weights = 1/len(LABM2_s_list), bins = 100, color='orange')
sns.histplot(x = sample_12_dti, weights = 1/len(LABS2_s_list), bins = 100, color='purple')
plt.xlim([0,100])
sns.set(rc={"figure.dpi":300, 'savefig.dpi':300})
plt.title('DTI streamlines length per each dataset (voxel size 2mm) ')
plt.tight_layout()
plt.legend()
plt.xlabel('Length')
plt.ylabel('# of streamlines')
```